

Diss. ETH No. 22047

**Effects of climate change on redox processes during riverbank  
filtration: Field studies and column experiments**

A dissertation submitted to

ETH ZÜRICH

for the degree of

Doctor of Sciences

presented by

MATTHIAS RUDOLF VON ROHR

MSc ETH Environ. Sc. ETH Zürich

born on December 18, 1983

citizen of Kestenholz (SO), Switzerland

accepted on the recommendation of

Prof. Dr. Urs von Gunten, examiner

Prof. Dr. Janet G. Hering, co-examiner

Dr. Hans-Peter E. Kohler, co-examiner

Prof. Dr. Rizlan Bernier-Latmani, co-examiner

2014







---

## Danksagung

Zuerst möchte ich mich ganz herzlich bei Urs von Gunten bedanken, der mein Hauptbetreuer und Gruppenleiter während dieser Arbeit war. Er hat mir die Möglichkeit gegeben, in dieses grosse Projekt einzusteigen und es zu vervollständigen. Zudem hat er mich überzeugt, dass es eine einmalige Chance ist, eine Dissertation zu beginnen und so ein Themengebiet zu vertiefen. Dank seiner fachlichen Unterstützung und der hilfreichen Vorschläge wusste ich, wo ich stehe und wie es weiter geht mit dem nächsten Experiment oder mit der Verfassung der Publikationen. Ganz herzlich möchte ich mich auch bei Hans-Peter Kohler und Janet Hering bedanken, die meine weiteren Betreuer während der Dissertation waren. Sie haben mir stets geholfen, wenn ich Fragen hatte und haben wertvolle Rückmeldungen bei der Verfassung der Publikationen gemacht. Ein grosser Dank geht auch an Laurent Grasset und an seine „Équipe de géochimie organique“ der Universität von Poitiers für die herzliche Gastfreundschaft und Betreuung in Poitiers, sowie für die Hilfe bei der Auswertung danach. Vielen Dank auch an Rizlan Bernier-Latmani für die Übernahme des Koreferats und an Ulrike Lohmann für den Vorsitz bei der Prüfung.

Mein Dank geht auch an Elisabeth Salhi und Hans-Ueli Laubscher, die mich in technischen Fragen grossartig unterstützt haben und immer eine gute Lösung für jedes mögliche Problem hatten. Ich möchte mich auch bei allen Mitarbeitern des AuA-Labors für die unzähligen Messungen der Proben und stets freundliche Hilfsbereitschaft bedanken. Der Eawag Werkstatt, insbesondere Peter Gäumann und Andreas Raffainer möchte ich auch ein grosses Dankeschön aussprechen für die Konstruktion der Labor-Säulen und weitere Labor-Anfertigungen. Bei Daniel Pellanda möchte ich mich für die hervorragende IT-Unterstützung bedanken und bei Claire Wedema und Ariane Eberhardt für die Administration. Ich möchte auch Thomas Fleischmann, Hans-Ueli Weilenmann und Stefan Koetzsch für die Hilfsbereitschaft in mikrobiologischen Fragen im Labor danken, Irene Brunner, Jaqueline Traber und die BMG Engineering AG für zahlreiche Messungen. Vielen Dank auch an Andreas Voegelin, Marc Boehler und Frederik Hammes für hilfreiche Diskussionen.

Selbstverständlich geht ein grosses Dankeschön an die derzeitigen und ehemaligen Mitarbeiter und Kollegen, sowie Gäste der „von Gunten-Gruppe“. Es war immer ein angenehmes Klima in der Gruppe und im Labor. Ich möchte meinem Labor-Kollegen Fabian Soltermann für

---

die fachlichen und sportlichen Diskussionen sehr herzlich danken und erinnere mich gerne an die Labor- und Büro-Tage bei guten „Sounds!“ und hoffe, dass wir uns wieder mal an einem Derby treffen. Dann danke ich ganz herzlich Sabrina Bahn Müller für ein stets offenes Ohr wenn es nicht immer rund lief und für die vielen fachlichen und nicht-fachlichen Gesprächen über Laborsäulen und Freizeitaktivitäten. Samuel Diem möchte ich für die schönen Momente draussen auf dem Feld danken und für die Hilfe bei Laborarbeiten. Im Weiteren danke ich Silvio Canonica, Frank Leresche, Amisha Shah, Tony Merle, Zhengqian Liu, Yael Schindler, Paul Borer, Hana Mestankova, Philippe Stolz, Thomas Ruettimann, Ursula Schoenenberger, Caroline Stengel, Kangmin Chon, Minju Lee, Yunho Lee, Saskia Zimmermann, Jannis Wenk, Maaïke Ramseier, Tobias Widler, Clara Loi, Angel Borgeat, Melissa Huguet, Justine Criquet und das Unihockeyteam.

Ein grosses Dankeschön geht natürlich auch an Dorothee Zimmermann, die mich unterstützt und auch motiviert hat während der Dissertation bei gemütlichen gemeinsamen Abenden zuhause und auch an meine Eltern für die stets vorhandene Unterstützung. Schliesslich, möchte ich dem Schweizer Nationalfond für die finanzielle Unterstützung im Rahmen des NFP 61 über nachhaltige Wassernutzung herzlich danken.

---

## Table of Contents

Danksagung	i
Table of Contents	iii
Summary	v
Zusammenfassung	viii
<b>1 General Introduction</b>	<b>1</b>
1.1 Groundwater as a drinking water resource: Relevance, protection measures and requirements	2
1.2 Managed aquifer recharge systems: Riverbank filtration	3
1.3 Subsurface microbiology and kinetics of enzymatic reactions	4
1.4 Biogeochemical processes during riverbank filtration	6
1.5 Climate change and its effects on groundwater quality	8
1.6 Role of NOM in the aquatic environment and characterization methods	11
1.7 Pyrolysis-GC-MS methods for the characterization and source identification of NOM	16
1.8 Thesis outline	18
1.9 References	21
<b>2 NOM degradation during river infiltration: Effects of the climate variables     temperature and discharge</b>	<b>29</b>
2.1 Introduction	32
2.2 Materials and Methods	34
2.3 Results and Discussion	39
2.4 Conclusion	49
2.5 References	51
<b>Supporting Information for Chapter 2</b>	<b>55</b>

---

<b>3 Column studies to assess the effects of climate variables on redox processes during riverbank filtration</b>	<b>59</b>
3.1 Introduction	62
3.2 Materials and Methods	64
3.3 Results and Discussion	69
3.4 Conclusion	83
3.5 References	85
<b>Supporting Information for Chapter 3</b>	<b>91</b>
<b>4 Characterization and source identification of particulate organic matter by preparative thermochemolysis-GC-MS</b>	<b>97</b>
4.1 Introduction	99
4.2 Materials and Methods	101
4.3 Results and Discussion	106
4.4 Conclusion	117
4.5 References	119
<b>Supporting Information for Chapter 4</b>	<b>123</b>
<b>5 General Conclusions and Outlook</b>	<b>129</b>
Curriculum Vitae	135



---

## Summary

Riverbank filtration has been practiced in Europe since more than hundred years to produce clean drinking water. Because of its simplicity in operation, cost-effectiveness and efficiency in removing particles, microorganisms and partially removing natural organic matter (NOM) and micropollutants, riverbank filtration has advanced to an established technique for drinking water production. However, past heat waves (especially in 2003) have revealed some limitations of this approach, as anoxic and Mn(III/IV)- and Fe(III)-reducing conditions were observed at some riverbank filtration sites in Switzerland. As a consequence of climate change, such heat waves are predicted to occur more frequently in Switzerland in future and their effects on groundwater quality are largely unknown. So far, researchers have mainly focused on studying the effects of climate change on groundwater quantity and only a few on groundwater quality. The aim of this thesis was to systematically investigate the effects of climate-related variables (temperature, discharge, infiltration rate, proportion of wastewater effluent in river water) on redox processes and on the quality of drinking water derived from riverbank filtration. It is hypothesized that during future heat waves higher temperatures, together with lower river discharges and increasing proportions of wastewater effluents in rivers may lead to the occurrence of anoxic conditions at riverbank filtration sites. To test this hypothesis and further elucidate the biogeochemical processes occurring during riverbank filtration, field investigations and laboratory column experiments were conducted. The field investigations were carried out at the peri-alpine Thur River infiltration site in Niederneunforn (NE-Switzerland). This field site was already equipped with 80 piezometers, most of which were fully screened over the whole thickness of the gravel and sand aquifer. Two sampling campaigns were conducted during the summer and winter 2011 to cover different temperature ranges by sampling Thur River water and groundwater from four selected piezometers situated in a specific transect. The column experiments were carried out in a Plexiglas column packed with fractionated sand (0.125-0.250 mm) from a gravel bar taken at the Thur River field site and using filtered (0.45  $\mu$ m) Thur River water as feed water.

In the second part of this thesis (Chapter 2), the effects of the climate-related variables temperature and discharge on the redox processes (aerobic respiration, denitrification) were assessed by comparing field data with results from column experiments. The oxygen

---

consumption rates at the river-sediment interface showed a strong temperature dependence, with the development of anoxic conditions during summer (without denitrification), but consistently oxic conditions during winter. According to an electron balance for summer conditions, the discrepancy between the consumption of dissolved organic matter (DOM) and oxygen indicates that particulate organic matter (POM) associated with riverbed sediments is the predominant electron donor for aerobic respiration. These observations in the field could be successfully reproduced by column experiments, which were conducted under summer (20°C) and winter (5°C) conditions. The analysis of periodic field data showed that the oxygen consumption increased with increasing discharge, possibly because of an additional POM input into the riverbed sediments during high-discharge conditions.

In the third part of this thesis (Chapter 3), column experiments were carried out to systematically study the effects of temperature, flow rate and proportions of wastewater effluent in the feed water on the redox processes (aerobic respiration, denitrification, reductive dissolution of Mn(III/IV)- and Fe(III)(hydr)oxides) during the infiltration process. A pronounced temperature dependence of aerobic respiration was found, confirming the results from the field studies. An Arrhenius-type approach was used to quantify this observation for the selected temperatures (5-30°C). At 30°C anoxic conditions developed, with partial denitrification and formation of nitrite and ammonium, which are undesired in drinking water. In an experiment carried out at 20°C, in which oxygen and nitrate were removed from the feed water, Mn(II) was mobilized from the reductive dissolution of Mn(III/IV)(hydr)oxides. The results of this experiment highlight the importance of nitrate acting as a redox-buffer during the infiltration process. Similarly to the field study, POM associated with the sand was found to be the main electron donor for the biogeochemical processes in the column experiments. The addition of treated wastewater effluent mixed with Thur River water did not affect the oxygen consumption rate in the column. By adding a readily available carbon source (acetate), an increased oxygen consumption rate was observed at the column inlet, which stimulated bacterial growth. Lower infiltration rates induced a higher oxygen demand in the column compared to higher flow rates. However, these effects disappeared when accounting for the water residence time, implying that the oxygen consumption rate is independent of the flow rate. Based on the results from the field observations and column experiments, future heat waves might lead to transient anoxic conditions at riverbank filtration sites characterized by a gravelly riverbed with a direct hydraulic

---

connection to the groundwater table. Therefore, it is important to monitor groundwater quality (temperature, oxygen and nitrate) during such situations.

In the fourth part of this thesis (Chapter 4), preparative thermochemolysis coupled to gas chromatography-mass spectrometry (GC-MS) was applied to gain insights into the molecular composition and origin of POM associated with the sand used in the column experiments and various environmental matrices (riverbed sediment, river water, macrophytes, periphyton, soil and wastewater effluent). This technique consists of thermal fragmentation of NOM into smaller and more volatile products that can be detected and assigned by GC-MS. The main biological molecules identified in all samples were fatty acid methyl esters (FAMES) derived from lipids, permethylated deoxy aldonic acids from carbohydrates and methylated lignin monomers from lignins. To assess the origin of POM associated with the sand, specific ratios (e.g., branched/C<sub>16</sub> for FAMES, fucose/glucose for carbohydrates and syringyl/ guaiacyl for lignins) of the sand were compared with those of the possible POM sources (riverbed sediment, river water, macrophytes, periphyton, soil and wastewater effluent). Based on the results, the POM origin of the sand samples could not be attributed to a specific POM source. The POM composition of the sand showed a shift in the carbohydrate and lignin signatures during the column experiments, probably due to bacterial growth and respiration processes under aerobic and anaerobic conditions.

Overall, the findings of the present dissertation contribute to a better understanding of the effects of climate change on the quality of drinking water derived from riverbank filtration by combining results from field observations and laboratory column experiments. Moreover, this study highlights the role of POM associated with riverbed sediments as an important driver for redox processes during riverbank filtration and shows that preparative thermochemolysis can be applied for its molecular characterization. Even though this qualitative method has allowed assessing changes in the POM composition during the column experiments, a distinct origin of POM could only be hypothesized. Therefore, other quantitative techniques or the application of alternative biological markers are needed for further studies in this field.

---

## **Zusammenfassung**

Uferfiltration wird in Europa seit über hundert Jahren erfolgreich zur Trinkwassergewinnung eingesetzt. Aufgrund der einfachen Funktionsweise, Kosteneffizienz und Wirksamkeit bei der Entfernung von Schwebstoffen, Mikroorganismen und teilweise auch natürlichem organischen Material (NOM) und Mikroverunreinigungen, ist die Uferfiltration zu einer etablierten Trinkwasseraufbereitungsmethode avanciert. Frühere Hitzewellen (vor allem 2003) haben jedoch gewisse Einschränkungen dieses Verfahrens aufgezeigt, als sich anoxische und Mn(III/IV)- und Fe(III)-reduzierende Verhältnisse in Schweizer Grundwasserleiter ausgebildet haben. Solche Hitzewellen werden vermutlich in der Schweiz in Zukunft vermehrt auftreten als Folge der Klimaänderung und die Auswirkungen auf die Grundwasserqualität sind weitgehend unbekannt. Bisher wurde vor allem über die Auswirkungen der Klimaänderung auf die Grundwasserquantität geforscht und nur geringfügig über die Auswirkungen auf die Grundwasserqualität. Das Ziel dieser Dissertation war es, den Einfluss von klimabestimmten Variablen (Temperatur, Abfluss, Infiltrationsrate, Anteil von geklärtem Abwasser in Flusswasser) auf die Redoxprozesse und auf die Qualität des durch Uferfiltration gewonnenen Trinkwassers systematisch zu untersuchen. Die Hypothese ist, dass während zukünftigen Hitzewellen erhöhte Temperaturen, sowie tiefere Abflüsse und ein erhöhter Anteil von geklärtem Abwasser in Flüssen zu anoxischen Verhältnissen bei der Uferfiltration führen könnten. Um diese Hypothese zu testen und die zugrundeliegenden biogeochemischen Prozesse zu untersuchen, wurden Felduntersuchungen und Laborsäulenversuche durchgeführt. Die Felduntersuchungen wurden am Uferfiltrationssystem der Thur in Niederneunforn (NO-Schweiz) durchgeführt. Dieser Feldstandort war bereits mit 80 Piezometern instrumentiert, welche über die gesamte Mächtigkeit des Schotter- und Sand-Grundwasserleiters verfiltert waren. Zwei Probennahmekampagnen wurden im Sommer und Winter 2011 durchgeführt, um verschiedene Temperaturbedingungen zu erfassen. Dabei wurde Wasser aus der Thur und Grundwasser aus vier ausgewählten Piezometern entnommen. Die Säulenversuche wurden mittels einer aus Plexiglas angefertigten Säule durchgeführt, die mit Sand der Korngrössenfraktion 0.125-0.250 mm aus einer Kiesbank des Feldstandortes gefüllt und mit filtriertem (0.45 µm) Thurwasser betrieben wurde.

---

Im zweiten Teil dieser Arbeit (Chapter 2) wurde der Einfluss der klimabestimmten Variablen Temperatur und Abfluss auf die Redoxprozesse (aerobe Respiration, Denitrifikation) untersucht, indem Feldresultate mit Säulenergebnissen verglichen wurden. Die Sauerstoffzehrungsraten in der Infiltrationszone zeigten eine ausgeprägte Temperaturabhängigkeit, wobei anoxische Bedingungen während des Sommers (ohne Denitrifikation), aber einheitliche aerobe Bedingungen während des Winters festgestellt wurden. Aufgrund der Elektronenbilanz zwischen der Zehrung von gelöstem organischen Material (DOM) und Sauerstoff wurde aus den Sommerdaten ersichtlich, dass das im Sediment gebundene partikuläre organische Material (POM) den wichtigsten Elektronendonator für die aerobe Respiration darstellt. Die Resultate aus den Feldbeobachtungen konnten erfolgreich durch die Säulenversuche bestätigt werden, die unter Sommer- (20°C) und Winter- (5°C) Bedingungen durchgeführt wurden. Langzeitdaten haben zudem gezeigt, dass die Sauerstoffzehrung mit dem Abfluss positiv korrelierte, wahrscheinlich aufgrund eines zusätzlichen POM-Eintrages in den Flussbettsedimenten bei erhöhten Abflussbedingungen.

Im dritten Teil dieser Arbeit (Chapter 3) wurden ausschliesslich Säulenversuche durchgeführt, um den Einfluss von Temperatur, Infiltrationsrate und Anteil von geklärtem Abwasser auf die Redoxprozesse (aerobe Respiration, Denitrifikation, reduktive Auflösung von Mn(III/IV)- und Fe(III)(hydr)oxiden) während dem Infiltrationsprozess zu untersuchen. Die aerobe Respiration zeigte eine ausgeprägte Temperaturabhängigkeit, was mit den Feldbeobachtungen übereinstimmt. Diese Temperaturabhängigkeit konnte durch einen Arrhenius-Ansatz für den ausgewählten Temperaturbereich (5-30°C) quantifiziert werden. Bei 30°C wurden anoxische Bedingungen festgestellt, sowie partielle Denitrifikation mit der Bildung von Nitrit und Ammonium, die im Trinkwasser unerwünscht sind. In einem Experiment, das unter Sauerstoff- und Nitrat-freien Bedingungen bei 20°C durchgeführt wurde, konnte Mn(II) aus der reduktiven Auflösung von Mn(III/IV)(hydr)oxiden mobilisiert werden. Dies zeigt, dass Nitrat ein wichtiger Redoxpuffer während dem Infiltrationsprozess darstellt. Das im Sand gebundene POM war der wichtigste Elektronendonator für die biogeochemischen Prozesse in den Säulenversuchen, wie schon aus den Feldbeobachtungen ersichtlich war. Die Zugabe von verschiedenen Mischungen von geklärtem Abwasser und Thurwasser hatte keinen Einfluss auf die Sauerstoffzehrungsrate in der Säule. Eine erhöhte Sauerstoffzehrungsrate beim Säuleneinlass wurde jedoch bei der Zugabe einer leicht verfügbaren Kohlenstoffquelle (Acetat) festgestellt,

---

welche das bakterielle Wachstum stimulierte. Tiefe Infiltrationsraten bewirkten einen höheren Sauerstoffbedarf in der Säule als höhere Raten. Diese Effekte verschwanden jedoch unter Berücksichtigung der Aufenthaltszeiten, so dass folglich die Sauerstoffzehrungrate unabhängig von der Infiltrationsrate ist. Aufgrund der Resultate der Felduntersuchungen und Säulenversuche kann geschlossen werden, dass zukünftige Hitzewellen zu vorübergehenden anoxischen Bedingungen in Uferfiltrationssystemen führen können, die durch ein durchlässiges Schotter-Flussbett charakterisiert sind und einen direkten hydraulischen Anschluss ans Grundwasser besitzen. Für solche Systeme ist es wichtig, die Grundwasserqualität (Temperatur, Sauerstoff und Nitrat) während zukünftigen Hitzewellen zu überwachen.

Im vierten Teil dieser Arbeit (Chapter 4) wurde die molekulare Zusammensetzung und Herkunft des im Sand gebundenen POM, das für die Säulenversuche verwendet wurde und von verschiedenen Umweltproben (Flussbettsediment, Flusswasser, Makrophyten, Periphyton, Boden und geklärtes Abwasser) mittels eines pyrolytischen Verfahrens („preparative thermochemolysis-gas chromatography-mass spectrometry (GC-MS)“) untersucht. Mit dieser Methode wird das NOM in kleinere und flüchtigere Moleküle fragmentiert, die mittels GC-MS identifiziert und zugeordnet werden können. Die wichtigsten biologischen Moleküle, die in allen Proben identifiziert wurden, waren methylierte Fettsäurenester (FAMES) aus Lipiden, permethylierte Desoxyaldonsäuren aus Kohlenhydraten und methylierte Ligninmonomere aus Ligninen. Um die Herkunft des im Sand gebundenen POM zu bestimmen, wurden spezifische Verhältnisse für den Sand (z.B. verzweigte zu C<sub>16</sub>-FAMES, Fucose zu Glukose und Syringyl zu Guaiacyl) mit denjenigen von möglichen POM-Quellen (Flussbettsedimente, Flusswasser, Makrophyten, Periphyton, Boden und geklärtes Abwasser) verglichen. Die Ergebnisse haben gezeigt, dass die Herkunft des im Sand gebundenen POM nicht einer eindeutigen POM-Quelle zugeordnet werden konnte. Die POM-Zusammensetzung des Sandes veränderte sich während den Säulenversuchen bezüglich der Kohlenhydrat- und Lignin-Komponenten, wahrscheinlich aufgrund des bakteriellen Wachstums und der Respirationprozesse unter aeroben und anaeroben Bedingungen.

Insgesamt trägt diese Dissertation zum besseren Verständnis des Einflusses der Klimaänderung auf die Qualität des durch Uferfiltration gewonnenen Trinkwassers bei, indem Resultate aus Feldbeobachtungen mit denjenigen aus Säulenversuchen kombiniert betrachtet wurden. Zudem wurde die Rolle des im Sand gebundenen POM als wichtiger Treiber für die

---

Redoxprozesse während der Uferfiltration hervorgehoben und mittels eines pyrolytischen Verfahrens dessen molekulare Zusammensetzung charakterisiert. Obwohl diese qualitative Methode Aufschlüsse über Änderungen der Zusammensetzung des im Sand gebundenen POM während den Säulenversuchen gegeben hat, konnten über die Herkunft des POM nur Vermutungen aufgestellt werden. Darum ist es für weitere Forschungsarbeiten in diesem Gebiet wichtig, quantitative Verfahren, oder die Verwendung von alternativen Biomarker heranzuziehen.





# **Chapter 1**

## **General Introduction**

## **1.1 Groundwater as a drinking water resource: Relevance, protection measures and requirements**

Groundwater represents the most important source for drinking water in Europe (about 75% of total drinking water production) and contributes substantially to the drinking water production also in North America (about 50%), while it is less relevant in the rest of the world ( $< 35\%$ ) (Danielopol et al., 2003). In Switzerland, about 80% of the drinking water is derived from groundwater (pumped groundwater and spring water both ca. 40%) and the remaining 20% is covered by surface water, i.e. mainly lake water (Blanc and Schädler, 2013). According to the quality of the source water, different treatment steps are applied to produce drinking water. Surface water (i.e., lake water) requires a multi-step treatment, whereas for groundwater and spring water, no or only single-step treatment is usually applied (Blanc and Schädler, 2013). About one third of the total precipitation in Switzerland contributes to groundwater recharge, another third to evapotranspiration and another third to surface discharge (Schädler and Weingartner, 2002). The contribution of precipitation to groundwater recharge is highly relevant for the drinking water production and might be affected by climate change during future summer conditions (see Section 1.5).

To protect groundwater resources from surface pollution from e.g., agriculture, industry and urban areas, groundwater protection zones (S1-S3) have been implemented in Switzerland (EDI, 1998). The main purpose of these zones is to prevent microbial contamination of groundwater. The protection zone S1 includes the immediate surroundings of the groundwater well (10 m), where no activities other than for drinking water production are allowed (EDI, 1998). The zone S2 is designed so that the minimum groundwater residence time is 10 days, enabling a good removal of microorganisms, but incomplete removal of persistent micropollutants (EDI, 1998). Finally, the zone S3 should guarantee sufficient intervention time and space in case of a chemical contamination.

Drinking water has to meet microbiological, physical and chemical requirements, which in Switzerland are defined by the ordinance for foodstuffs (EDI, 1995). The ordinance determines tolerance values and maximum contaminant levels for the drinking water parameters. If a tolerance value is exceeded and no health risk is present, the drinking water can still be delivered to the consumers, but measures for improvement have to be taken. However, if a maximum contaminant level is surpassed for a specific groundwater well, drinking water cannot be distributed anymore, which could necessitate the temporary closure of a groundwater well.

## 1.2 Managed aquifer recharge systems: Riverbank filtration

Water supplies of several European countries employ managed aquifer recharge (MAR) systems to enhance groundwater recharge for drinking water production (Eckert and Irmischer, 2006). Examples of MAR systems are aquifer storage and recovery, bank filtration or infiltration pond (Fig. 1.1). During aquifer storage and recovery, treated or untreated water is injected into a well for storage and extracted from the same or a different well for drinking water production (Fig. 1.1, (A)). During bank filtration, the groundwater table is actively lowered by pumping groundwater, which induces infiltration from a nearby surface water (river or lake) (Fig. 1.1, (B)). A similar MAR technique consists of artificial infiltration ponds, in which surface water is allowed to infiltrate into an aquifer with the subsequent extraction of groundwater (Fig. 1.1, (C)). Riverbank filtration is the most common MAR technique in Switzerland, with a contribution to the total drinking water production of about 25% (E. Hoehn, 2013, personal communication), comparable to Germany (16%) (Hiscock and Grischek, 2002). In France, Finland and Hungary, this contribution is higher (50%, 48% and 40%, respectively) (Tufenkji et al., 2002).

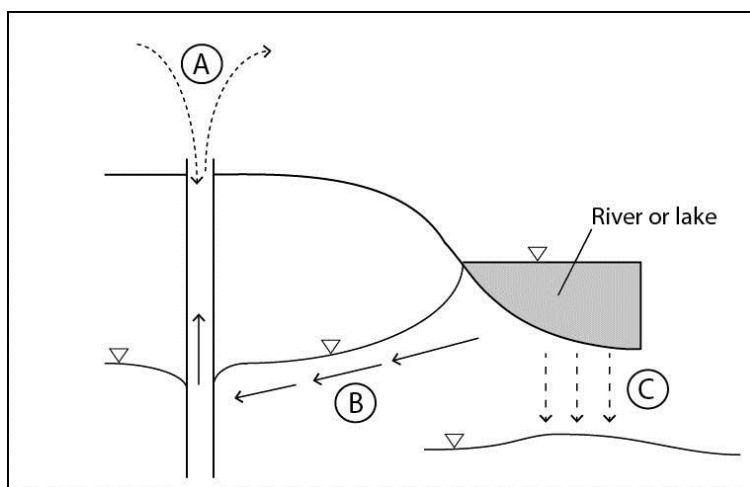


Fig. 1.1. Examples of managed aquifer recharge (MAR) systems. (A) Aquifer storage and recovery, (B) Bank filtration, (C) Infiltration pond. Adapted from Dillon (2005).

Even though riverbank filtration is generally seen as part of a multi-barrier approach to generate drinking water, it is used as the only barrier between surface water and drinking water in Switzerland and in e.g. Berlin (Eckert and Irmischer, 2006; Grünheid et al., 2005; Kuehn and Mueller, 2000). In Switzerland, this is possible because of the high dilution rates of wastewater

effluents in river waters, the high quality standards of the discharged wastewater effluents and the physical, chemical and biological natural attenuation processes occurring during riverbank filtration. The physical processes include filtration, adsorption, dispersion and mixing with groundwater, whereas the biological and chemical processes include biodegradation, reduction/oxidation, precipitation and hydrolysis reactions. All the natural attenuation processes effectively remove particles, bacteria, viruses, parasites and partially remove natural organic matter (NOM) (Grünheid et al., 2005; Hiscock and Grischek, 2002; Kuehn and Mueller, 2000; Sacher and Brauch, 2002). Organic micropollutants are mainly removed by biodegradation and adsorption (Baumgarten et al., 2011; Bertelkamp et al., 2014; Grünheid et al., 2005; Huntscha et al., 2013; Scheurer et al., 2012; Schmidt et al., 2007; Storck et al., 2012), but some polar and persistent compounds, such as pharmaceuticals (e.g., carbamazepine), industrial chemicals (e.g., benzotriazole) or pesticides (e.g., atrazine) are only partially removed by riverbank filtration (Heberer et al., 2004; Reemtsma et al., 2010; Verstraeten et al., 2002).

Two major attenuation zones can be distinguished during riverbank filtration (Hiscock and Grischek, 2002). The first zone consists of the colmation layer situated at the interface between the riverbed and the aquifer, where biodegradation and adsorption take place. The second zone is located underneath the colmation layer along the principal groundwater flow path and is characterized by lower degradation rates. A highly biologically active zone has been observed in the first few meters of infiltration at riverbank filtration systems (Jacobs et al., 1988; Schwarzenbach et al., 1983) and within a few centimeters during column studies (Grünheid et al., 2008; von Gunten and Zobrist, 1993). The biogeochemical processes occurring during riverbank filtration will be explained in detail in Section 1.4.

### **1.3 Subsurface microbiology and kinetics of enzymatic reactions**

Subsurface environments, such as aquifers, are characterized by extreme conditions for life, due to the absence of light and to nutrient constraints (Goldscheider et al., 2006). To survive and grow in such oligotrophic environments, microorganisms use small energy gradients and assimilate nutrients at low concentrations (Goldscheider et al., 2006). Additionally, cell-sizes are much smaller (0.4-0.9  $\mu\text{m}$ ) and growth rates slower than in eutrophic environments. Attached (or benthic) bacteria on solid aquifer materials, such as sediment or mineral surfaces account for most of the biomass and activity of microorganisms in subsurface oligotrophic ecosystems (Goldscheider et al., 2006). The presence of free-living (or planktonic) bacteria is

the result of detachment and attachment processes. Typically, these systems are in a steady state in groundwater (Ahn and Lee, 2003).

The key factors controlling the activity of heterotrophic microorganisms in subsurface ecosystems are temperature, presence of electron acceptors (i.e.,  $O_2$ ,  $NO_3^-$ ,  $Mn(IV)$ ,  $Fe(III)$ ,  $SO_4^{2-}$ ) and electron donors (i.e., biodegradable dissolved organic matter (BDOM)). To gain energy, heterotrophic microorganisms mineralize organic compounds (i.e., BDOM), thereby consuming the available electron acceptor(s). This process is mediated by extracellular enzymes and the kinetics of substrate depletion (either the organic compound or the electron acceptor) and can be described by the Michaelis-Menten equation (Plante and Parton, 2007) (Eq. 1.1):

$$\frac{dS}{dt} = V_m \frac{S}{K_m + S} \quad (1.1)$$

where  $S$  represents the substrate that is consumed,  $V_m$  the maximum reaction rate and  $K_m$  the Michaelis-Menten constant, i.e. the substrate concentration at which the reaction rate equals to  $V_m/2$ . A graphical representation of the Michaelis-Menten equation is shown in Fig. 1.2, with a derivation of  $K_m$ .

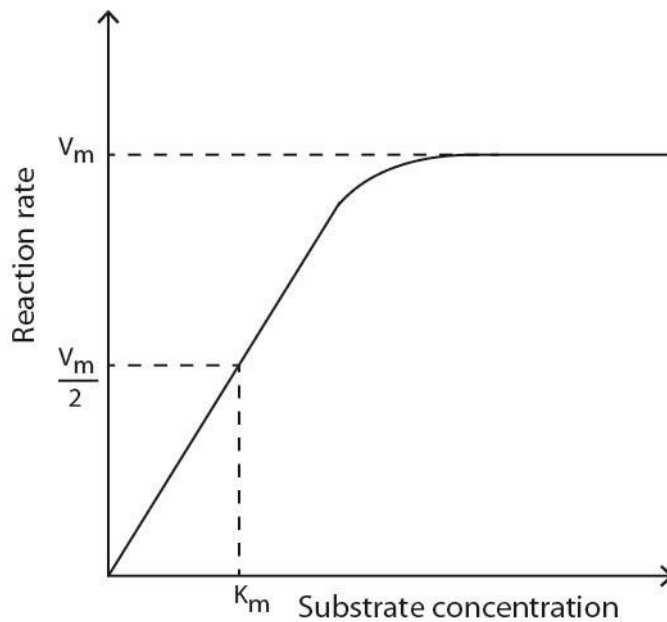


Fig. 1.2. Michaelis-Menten kinetics for an enzyme-substrate reaction.  $V_m$  is the maximum reaction rate and  $K_m$  the Michaelis-Menten constant, which is the substrate concentration at which the reaction rate equals to  $V_m/2$ . Adapted from Plante and Parton (2007).

For substrate concentrations  $\gg K_m$ , the reaction rate  $\frac{dS}{dt}$  is equal to  $V_m$  (Fig. 1.2) and follows a zero-order kinetics (Eq. 1.2):

$$\frac{dS}{dt} = -k_0 \quad (1.2)$$

where  $k_0$  is the zero-order reaction rate constant. Under these conditions, the reaction rate constant does not directly depend on the substrate concentration, but is limited by other factors, such as the enzyme concentration or hydrolytic reactions in case of the degradation of complex polymers (Plante and Parton, 2007). Examples for zero-order kinetics are nitrification reactions at high ammonium concentrations or denitrification at high nitrate concentrations (Plante and Parton, 2007). For substrate concentrations  $\ll K_m$ , the reaction rate depends on the substrate concentration (Fig. 1.2) and follows first-order kinetics (Eq. 1.3), with the first-order reaction rate constant  $k_1$ .

$$\frac{dS}{dt} = -k_1 \cdot S \quad (1.3)$$

Here, an increase of the substrate concentration leads to an enhanced reaction rate (Fig. 1.2), meaning that the consumption of the substrate depends directly on the substrate itself. In this case, the plot of the substrate concentration as a function of time shows an exponential decay.

## 1.4 Biogeochemical processes during riverbank filtration

In subsurface ecosystems, the redox milieu is mainly determined by the biogeochemical processes involving the mineralization of BDOM (Bouwer, 1992). During the microbial mineralization of BDOM, electron acceptors ( $O_2$ ,  $NO_3^-$ ,  $Mn(IV)$ ,  $Fe(III)$ ,  $SO_4^{2-}$ ) are successively consumed and reduced species are produced ( $H_2O$ ,  $N_2$ ,  $Mn^{2+}$ ,  $Fe^{2+}$ ,  $HS^-$ ) in a sequence governed by thermodynamics (Table 1.1). Each process described in Table 1.1 is driven by specific bacterial communities. Depending on the available concentration of BDOM and electron acceptors, distinct redox zones, such as oxic, anoxic ( $< 0.1$  mg/L  $O_2$ ) and strictly anaerobic (absence of oxygen and nitrate) can be observed in subsurface ecosystems (Bradley et al., 2008). These zones are either clearly separated from each other, or overlap, leading to the concurrent occurrence of certain reduced species.

Table 1.1. Mineralization processes of biodegradable dissolved organic matter ( $\text{CH}_2\text{O}$ , representing an “average” organic substrate with carbon in a zero-valent oxidation state). Adapted from Stumm and Morgan (1996).

Microbial process	Electron acceptor	Reaction
Aerobic respiration	$\text{O}_2$	$\text{CH}_2\text{O} + \text{O}_2 (\text{g}) \rightarrow \text{CO}_2 (\text{g}) + \text{H}_2\text{O}$
Denitrification	$\text{NO}_3^-$	$\text{CH}_2\text{O} + 0.8 \text{NO}_3^- + 0.8 \text{H}^+ \rightarrow \text{CO}_2 (\text{g}) + 0.4 \text{N}_2 (\text{g}) + 1.4 \text{H}_2\text{O}$
Mn(IV) reduction	Mn(IV)	$\text{CH}_2\text{O} + 2 \text{MnO}_2 (\text{s}) + 4 \text{H}^+ \rightarrow \text{CO}_2 (\text{g}) + 2 \text{Mn(II)} + 3 \text{H}_2\text{O}$
Fe(III) reduction	Fe(III)	$\text{CH}_2\text{O} + 4 \text{FeOOH} (\text{s}) + 8 \text{H}^+ \rightarrow \text{CO}_2 (\text{g}) + 4 \text{Fe(II)} + 7 \text{H}_2\text{O}$
Sulfate reduction	$\text{SO}_4^{2-}$	$\text{CH}_2\text{O} + 0.5 \text{SO}_4^{2-} + 0.5 \text{H}^+ \rightarrow \text{CO}_2 (\text{g}) + 0.5 \text{HS}^- + \text{H}_2\text{O}$
Methanogenesis	-	$\text{CH}_2\text{O} \rightarrow 0.5 \text{CO}_2 (\text{g}) + 0.5 \text{CH}_4 (\text{g})$

In Switzerland, the prevailing redox conditions at most riverbank filtration sites are aerobic, without any redox zonation. However, seasonal changes of water temperatures can turn the aquifer from oxic to anoxic, leading to the formation of distinct redox zones and reduced species during summer conditions (Greskowiak et al., 2006; Jacobs et al., 1988; Massmann et al., 2006; von Gunten et al., 1994; von Gunten et al., 1991). This situation occurred in the summer of 2003 at the Thur River, NE-Switzerland, when river water temperatures exceeded the 1980-1999 summer average temperature by  $3.5^\circ\text{C}$  (June-August), leading to anoxic and Mn(III/IV)- and Fe(III)-reducing conditions (Hoehn and Scholtis, 2011). In addition to that, nitrite, ammonium and sulfide may be produced under reducing conditions, potentially leading to drinking water problems, which are listed in Table 1.2 (together with guidelines values and treatment options). Nitrite is of health concern and ammonium can lead to the formation of chloramines during chlorine disinfection ( $\text{HOCl} + \text{NH}_3 \rightarrow \text{NH}_2\text{Cl} + \text{H}_2\text{O}$ ), and thus significantly lower the disinfection efficiency (Deborde and von Gunten, 2008). Sulfide is unwanted from an aesthetic point of view (taste and odor concerns), similarly to manganese(II) and iron(II) (taste concerns, rusty water), whereby manganese(II) poses also some health concerns at concentrations above 0.4 mg/L. Because of these adverse effects on drinking water quality, anoxic conditions are undesired during riverbank filtration, even though certain micropollutants, such as sulfamethoxazole, are better removed under these conditions (Heberer et al., 2008).

Table 1.2. Reduced species (nitrite, ammonium, sulfide, Mn(II), Fe(II)) in drinking water: Problems, guideline values and treatment options.

Reduced species	Drinking water problem	Guideline value in drinking water		Treatment
		CH*	WHO**	
NO <sub>2</sub> <sup>-</sup> (mg N/L)	Human toxicology	0.03	0.9	Oxidation (ozonation or chlorination)
NH <sub>4</sub> <sup>+</sup> (mg N/L)	Formation of chloramines	0.4	27	Nitrification, breakpoint chlorination
HS <sup>-</sup> (mg/L)	Taste, odor concerns	-	0.05-0.1	Oxidation (ozonation or chlorination)
Mn(II) (mg/L)	Taste, turbidity	0.05	0.4	Chemical or biological demanganation
Fe(II) (mg/L)	Taste, turbidity	0.3	0.3	Chemical or biological deferrisation

\* Tolerance values according to the Swiss ordinance for foodstuffs (EDI, 1995) \*\* Guideline values according to WHO (2011) (for NH<sub>4</sub><sup>+</sup>, HS<sup>-</sup> and Fe(II), taste/odor threshold values are shown).

## 1.5 Climate change and its effects on groundwater quality

### *Global changes*

Global air temperatures have increased by about 0.85°C from the end of the 19<sup>th</sup> century to now (IPCC, 2013). This increase is attributable to the anthropogenic increase in greenhouse gas concentrations (IPCC, 2013). For short-term scenarios (2016-2035), climate models predict a global warming with mean air temperatures in the range of 0.3°C to 0.7°C relative to the period 1986–2005 (IPCC, 2013). Long-term scenarios (2081-2100) predict a mean increase of > 1°C, which strongly depends on the greenhouse gas emission scenarios (Fig. 1.3).



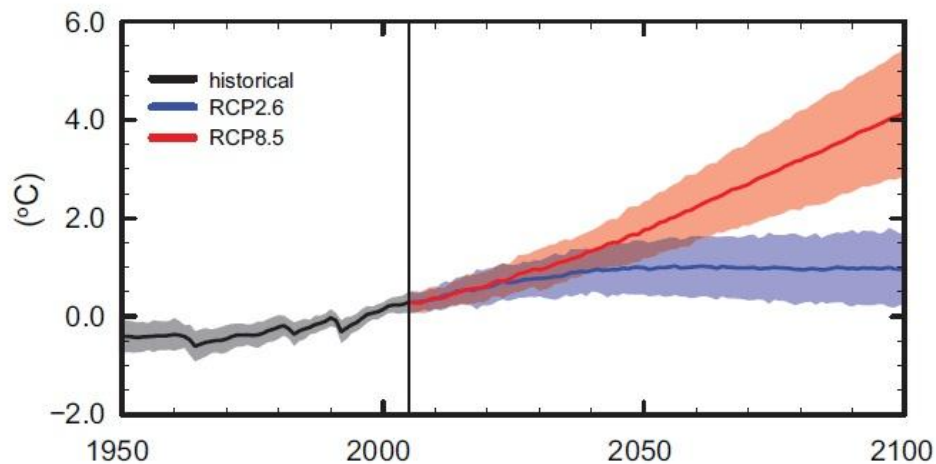


Fig. 1.3. Change in global annual mean air temperature relative to 1986–2005. In the RCP2.6 scenario CO<sub>2</sub> concentrations reach 421 ppm by 2100, in the RCP8.5 936 ppm by 2100. Reprinted with permission, copyright IPCC (2013).

### ***Regional changes***

Climate change affects also Switzerland, where the mean air temperatures have increased by  $> 1.5^{\circ}\text{C}$  in the last hundred years (FOEN, 2012). This warming has accelerated dramatically in the last 30 years (1982–2011), with an increase of up to  $0.5^{\circ}\text{C}$  per decade (FOEN, 2012). The newest short-term (2021–2050) climate change scenario for Switzerland considering the A1B greenhouse gas emission scenario (doubling of the greenhouse gas emissions by 2050 compared to 1990, followed by a stabilization) predicts an increase of the yearly average temperature by  $1.2^{\circ}\text{C} \pm 0.5^{\circ}\text{C}$  relative to the reference period 1980–2009 (FOEN, 2012). On the long-term (2070–2099) scale, yearly average temperatures are predicted to increase by  $3^{\circ}\text{C} \pm 1^{\circ}\text{C}$  and even more during summer ( $4^{\circ}\text{C} \pm 1^{\circ}\text{C}$ ) (FOEN, 2012). The predicted changes in temperature for northeastern Switzerland for winter, spring, summer and autumn are shown in Fig. 1.4. For precipitation, a seasonal pattern is predicted for Switzerland, with a yearly average decrease in summer ( $> 20\%$ ) and a yearly average increase in winter (10–20%) (FOEN, 2012). As a consequence of lower precipitation during summer, river discharges will decrease in catchment areas without glaciers, such as the Thur River catchment. In catchment areas dominated by glaciers, however, river discharges will increase in the near future because of ice melting, but will decrease in the far future (100–150 years), as the glaciers will completely disappear (FOEN, 2012). Lower river discharges will also lead to less dilution and consequently to a higher proportion of effluent organic matter from wastewater treatment plants. The

uncertainties of the predictions mainly depend on the future development of the greenhouse gas emissions and their mitigation strategies.

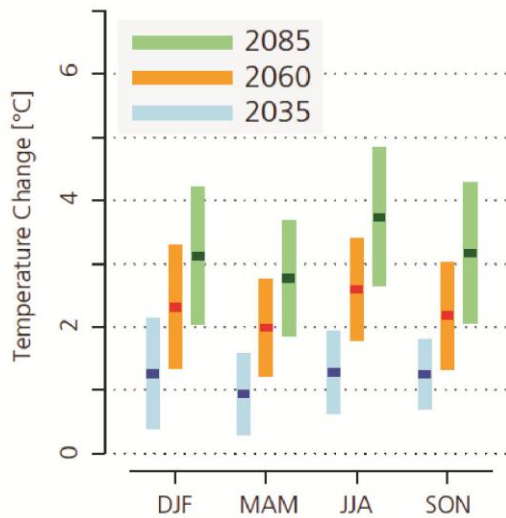


Fig. 1.4. Change in temperature for winter (DJF: December–February), spring (MAM: March–May), summer (JJA: June–August), and autumn (SON: September–November) in northeastern Switzerland under A1B greenhouse gas emission scenario (doubling of emissions by 2050 compared to 1990 and stabilization thereafter). Predictions are for 30-year averages by 2035 (blue), 2060 (orange) and 2085 (green) with respect to the reference period 1980–2009. Lines show medium estimates with model uncertainties. Reprinted with permission, copyright CH2011 (2011).

### ***Effects on groundwater quality***

Over the time period of 1970–2010, river water temperatures in Switzerland have followed the course of the air temperatures quite consistently, showing an increase of up to 1.2°C (FOEN, 2012). Hence, it can be expected that the river water temperatures will keep increasing in future. The extent of this increase is however not clear yet and is currently under investigation (FOEN, 2012). Also for groundwater temperature, the analysis of historical data at selected Swiss riverbank filtration sites has shown increasing values over the last 30–35 years (Figura et al., 2013). At the same time, the oxygen concentration in the groundwater decreased, probably because of the lower oxygen solubility at higher temperatures and because of the enhanced oxygen consumption in the hyporheic zone (Figura et al., 2013). However, changes in the hydrological conditions, i.e. higher groundwater pumping rates and higher river discharges, led to a temporary increase of the oxygen concentration in the groundwater, due to lower groundwater residence times (Figura et al., 2013). It was concluded from this study that climate

change could lead to anoxic conditions at riverbank filtration sites, but that changes in the hydrological conditions (pumping rate, discharge) might attenuate the general effect of decreasing oxygen concentrations in groundwater (Figura et al., 2013). In a review paper, the vulnerability of riverbank filtration systems towards climate change was investigated for two scenarios, drought and flood (Sprenger et al., 2011). A high vulnerability was predicted for the drought scenario, with the occurrence of anaerobic conditions and incomplete DOM removal (Sprenger et al., 2011). For the flood scenario, the highest vulnerability was related to the breakthrough of pathogens, DOM and organic micropollutants (Sprenger et al., 2011). Based on the results of these studies and on past field observations (e.g., summer of 2003), climate change seems to favor anoxic conditions during riverbank filtration. However, more information is needed to assess the effects of climate change variables (temperature and hydrological conditions) on the biogeochemical processes that determine groundwater quality during riverbank filtration.

## **1.6 Role of NOM in the aquatic environment and characterization methods**

### ***Definition of NOM and role in drinking water***

Natural organic matter (NOM) is a heterogeneous assemblage of various organic molecules that originate from the decomposition and transformation of plant, animal and microbial residues (Thurman, 1985). NOM is composed of dissolved organic matter (DOM), which is defined as the fraction smaller than 0.45  $\mu\text{m}$  and particulate organic matter (POM), the fraction larger than 0.45  $\mu\text{m}$  (Leenheer and Croué, 2003; Swift, 1996). In aquatic systems, such as rivers, the source of NOM can be autochthonous, i.e. produced in-situ by algae or allochthonous, i.e. coming from the terrestrial environment (soil) (Leenheer and Croué, 2003; Pusch et al., 1998). Autochthonous NOM is generally more biodegradable than allochthonous NOM (Leenheer and Croué, 2003).

NOM is undesired in drinking water for various reasons (Matilainen et al., 2011). First, aesthetic concerns such as color, taste and odor are very important from a consumer's point of view. Then, NOM can reduce the efficiency of drinking water treatment processes, e.g., by fouling of membranes, adsorption to activated carbon filtration, consumption of disinfectants and lead to undesired compounds such as disinfection byproducts. Moreover, part of the NOM is used as a substrate for bacterial growth in the distribution system, which leads to biologically unstable drinking water and possibly biocorrosion and formation of taste and odor compounds. To counteract these problems, enhanced coagulation followed by sedimentation is the most

accepted and cost-efficient technique used to remove NOM from drinking water (Matilainen et al., 2011). However, also other processes such as removal by adsorption to activated carbon and a combination of ozonation with biological activated carbon can be used. Several analytical techniques can be used for the characterization and quantification of NOM (see Table 1.3) and are shortly described in the following sections.

### ***Bulk parameters***

NOM is usually quantified by the bulk parameters total organic carbon (TOC) and dissolved organic carbon (DOC), as a measure of the total organic matter (POM + DOM) and DOM, respectively. TOC measurements refer to the sum of DOC and POC without 0.45 µm membrane filtration, whereas DOC measurements are preceded by a filtration step. Such bulk parameters are easily and fast measurable, but do not provide any information on NOM composition (see Table 1.3).

### ***Spectroscopic methods***

Spectroscopic methods, such as UV-Vis absorbance and fluorescence, provide information about the presence of aromatic chromophores and fluorophores, respectively, both being associated with the humic fraction of NOM (Leenheer and Croué, 2003). These methods are relatively simple and fast, but can be negatively affected by water quality, such as high nitrate concentrations that interfere with UV-Vis absorbance and pH-effects that lead to a lower fluorescence intensity (Table 1.3). To quantify the aromatic nature of NOM, the specific UV absorbance (SUVA) is commonly used. The SUVA is defined as the ratio of the UV absorbance at 254 nm and the DOC concentration and increases with increasing aromaticity. A more sophisticated and advanced method for NOM characterization is nuclear magnetic resonance (NMR) spectroscopy. This method allows studying the structural and molecular properties (i.e., functional groups) of NOM, often in combination with chromatographic or mass spectrometric techniques (Croué, 2004; Zhong et al., 2011).

### ***Chromatographic methods***

An established chromatographic method for the NOM characterization is size exclusion chromatography coupled to organic carbon or nitrogen detection (SEC-OCD/OND). This technique allows the fractionation of NOM based on its molecular size, with larger molecules eluting first and smaller ones later. In the current literature, the molecular size fractions are

semi-quantitatively divided into biopolymers, humic substances, building blocks, low molecular weight acids and neutrals, in the order of short to long elution times (Huber et al., 2011). The main disadvantage of this method consists of possible interactions between the SEC-column or eluent and NOM (charge effects), which might lead to a retardation of the analyte (Table 1.3). SEC has been widely applied for NOM characterization in the field of water resources, drinking water treatment and wastewater (Baghoth et al., 2008; Chow et al., 2009; Matilainen et al., 2006; Teixeira and Nunes, 2011), since it is a fast and sensitive method (Table 1.3).

### ***Mass spectrometric methods***

Mass spectrometric methods are particularly useful to determine the structural and molecular composition of NOM (Matilainen et al., 2011). Among these methods, pyrolysis techniques followed by gas chromatography-mass spectrometry (GC-MS) have been applied to characterize aquatic NOM (Berwick et al., 2010; Carrie et al., 2009; Frazier et al., 2005; Micić et al., 2011; Steinberg et al., 2009). During pyrolysis-GC-MS, NOM (as a solid phase) is subjected to heat under anoxic conditions and is degraded into smaller low-molecular-weight products, which are subsequently detected by GC-MS (Leenheer and Croué, 2003). This method is sensitive and specific, allowing the identification of NOM constituents (see Section 1.7). Another mass spectrometric method used to gain information about the molecular structure of NOM is liquid chromatography-mass spectrometry (LC-MS), often also coupled to electrospray ionization (ESI) (Mesfioui et al., 2012; Reemtsma and These, 2005). This technique combines physical separation by LC with MS for the identification of the NOM constituents.

### ***Biological methods***

Biological methods for NOM characterization give insights into the biodegradable fraction of NOM (i.e., biodegradable organic matter (BOM)), which is an important parameter to assess the biological stability of drinking water. To quantify BOM, different approaches can be utilized, such as the measurement of (i) bacterial growth (assimilable organic carbon (AOC) assay), (ii) the fraction of DOC consumed by a natural bacterial community (biodegradable dissolved organic carbon (BDOC) method) and (iii) the oxygen consumption (biological oxygen demand (BOD) test) (see Table 1.3).

In an AOC assay, a filtered water sample is inoculated with a natural bacterial community and bacterial growth is measured after a certain time (usually 3 days) (Hammes and

Egli, 2005). The bacterial cell numbers are then converted into an organic carbon concentration (i.e., the AOC concentration) based on a specific conversion factor for carbon assimilation (Hammes et al., 2006). This method is faster compared to the other biological methods and gives insights into the bacterial re-growth potential of water samples, but the assay is highly sensitive to carbon contamination. In the second approach, BOM of a water sample is directly measured in bioreactors or column experiments as difference of the DOC concentration after inoculation with a natural bacterial community (Escobar and Randall, 2001; Søndergaard and Worm, 2001; Volk and LeChevallier, 2000). This difference corresponds to the concentration of biodegradable dissolved organic carbon (BDOC). If bioreactors are used for this method, monitoring of water quality can be easily achieved, but the processing time can be quite long (weeks to months). In a standardized BOD test, such as the closed bottle test (OECD, 1992), a liquid or a solid sample is inoculated in a bottle with a defined microbial sample (e.g. from a secondary effluent), closed and incubated for 5-28 days. The oxygen concentration is recorded at the beginning and at the end of the experiment (after 5-28 days) and the difference corresponds to the BOD value (in mg/L O<sub>2</sub>), which is associated with the degradation of BOM. The main disadvantages of the BOD test are the rather long duration ( $\geq 5$  days) and the relatively high variability of the measurements (up to 20%) (Jouanneau et al., 2013).

Table 1.3. Examples of methods used to characterize NOM. NMR: Nuclear magnetic resonance; SEC-OCD/OND: Size exclusion chromatography-organic carbon detection/organic nitrogen detection; GC-MS: Gas chromatography-mass spectrometry; LC-MS: Liquid chromatography-mass spectrometry; ESI: Electrospray ionization; AOC: Assimilable organic carbon; BDOC: Biodegradable dissolved organic carbon; BOD: Biological oxygen demand. Adapted from Matilainen et al. (2011).

Method	Detected features	Advantages	Disadvantages
<i>Bulk parameters</i>			
TOC	Total organic carbon content	Easy to use, can be used as on-line method	Only quantitative
DOC	Dissolved organic carbon content (0.45 $\mu\text{m}$ filter)	Easy to use, can be used as on-line method	Only quantitative
<i>Spectroscopic</i>			
UV-Vis absorbance	Compounds with aromatic chromophores that absorb UV-Vis light	Simple and fast, can be used as on-line method	Not all compounds detected. Sensitive to interferences, e.g. nitrate
Fluorescence	Compounds with fluorophores that are excited and emit radiation	Simple, fast, sensitive, can be used as on-line method	Sensitive to interferences
NMR	Functional groups	Specific	difficult interpretation of spectra
<i>Chromatographic</i>			
SEC-OCD/OND	Fractions of NOM according to molecular size	Fast, sensitive	Charge effects, only qualitative
<i>Mass spectrometric</i>			
Pyrolysis-GC-MS	Structural and molecular composition of NOM	Sensitive, specific	Unwanted thermal reactions, only qualitative
LC-MS	Structural properties of NOM	Coupling to ESI	Not so sensitive to all NOM species
<i>Biological parameters</i>			
AOC	Assimilable organic carbon	Measurement by bacterial re-growth potential	Sensitive to carbon contamination
BDOC	Biodegradable organic carbon	Bioreactors can be used for	Time for processing

		water quality monitoring	(weeks-months)
BOD	Biological oxygen demand of NOM	Used as standard technique for drinking water and wastewater	Variability of measurements

---

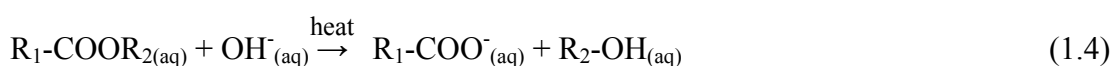
## 1.7 Pyrolysis-GC-MS methods for the characterization and source identification of NOM

### *Thermochemolysis*

As seen in the previous section, pyrolysis-GC-MS methods can be applied for the characterization of the molecular composition of NOM. The basic principle of pyrolysis is thermal fragmentation of complex NOM polymers into low-molecular-weight products by application of high temperatures (400-700°C) under anoxic conditions (Shadkami and Helleur, 2010). The result is the formation of fragmentation products, called pyrolysates, which are mostly volatile and can be detected and assigned by GC-MS.

To achieve a better derivatization of the pyrolysates, thermochemolysis has several advantages. This method operates at lower temperatures ( $\leq 400^{\circ}\text{C}$ ) than conventional pyrolysis (e.g, analytical pyrolysis) and is preceded by a hydrolysis and alkylation step (Shadkami and Helleur, 2010). Specific chemical bonds, such as ester and ether bonds, can be selectively broken (Shadkami and Helleur, 2010). Moreover, the action of the alkylation agent leads to the derivatization of most acidic functional groups. Tetramethylammonium hydroxide (TMAH) is used as a typical alkylating reagent because of its strong alkylating properties and the absence of decarboxylation (Del Rio et al., 1998; Shadkami and Helleur, 2010). However, based on the purpose of derivatization, different alkylating agents can be used (Joll et al., 2004).

The generally accepted reaction mechanism during TMAH-thermochemolysis of NOM involves hydrolysis of specific ester or ether bonds present in NOM by  $\text{OH}^-$  originating from TMAH ( $(\text{CH}_3)_4\text{N}^+\text{OH}^-$ ) (Eq. 1.4) (Challinor, 2001), followed by an alkylating reaction of the hydrolysis products by TMAH (Eq. 1.5) (Shadkami and Helleur, 2010).





In Eq. 1.4, the hydrolysis of an ester is shown ( $R_1\text{-COOR}_{2(aq)}$ ) generating a product ( $R_1\text{-COO}^-_{(aq)}$ ), which is alkylated to an alkyl ester ( $R_1\text{-COOCH}_{3(aq)}$ ) (Eq. 1.5) and analysed by GC-MS thereafter. Heat initiates both the hydrolysis and the alkylating processes, respectively.

Preparative (or off-line) thermochemolysis has been developed to treat a large sample mass (>1 g) without extraction and pre-concentration, which allows analysing samples with a low organic carbon content (Grasset and Amblès, 1998). In contrast to on-line thermochemolysis, preparative thermochemolysis involves several steps, i.e., conditioning with the alkylating reagent, thermochemolysis at  $\leq 400^\circ\text{C}$ , recuperation of the pyrolysates by evaporation, injection of the pyrolysates into a GC-MS and identification of products. Fig. 1.5 shows an example of preparative thermochemolysis, according to Grasset and Amblès (1998). Preparative thermochemolysis has been frequently applied for the characterization of NOM in soils (Grasset et al., 2009; Hatcher et al., 1996), lake sediments (Steinberg et al., 2009) and rivers (Frazier et al., 2005; Frazier et al., 2003) and has shown to be reliable, reproducible and relatively economic since it does not need elaborate laboratory equipment. This method has been mostly applied for qualitative purposes, even though the addition of internal standards and the quantification of single compounds is also possible (Del Rio et al., 1998).

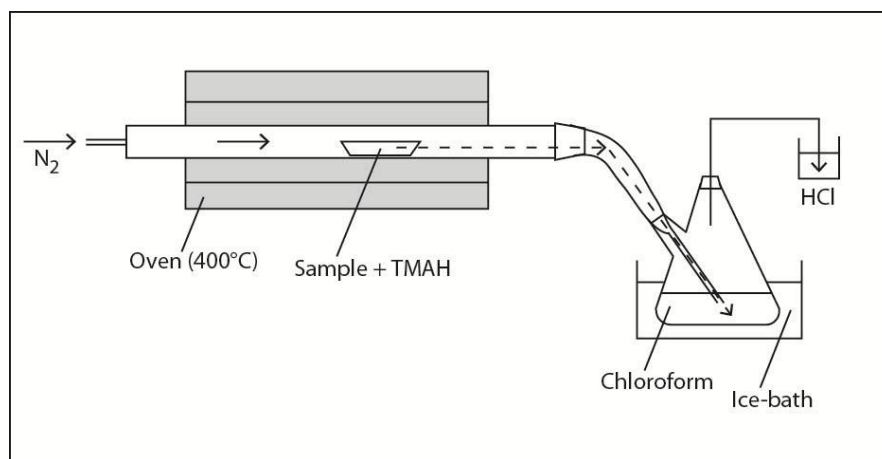


Fig. 1.5. Schematic representation of the thermochemolysis step during preparative thermochemolysis, according to the method of Grasset and Amblès (1998). The thermochemolysis products are swept by nitrogen (dashed arrows) and trapped in a chloroform solution cooled with ice. The remaining TMAH evaporates and is neutralized by its reaction with HCl.

***Biological indicators to assess the source of NOM***

Pyrolysis-GC-MS methods not only provide information about the molecular composition of NOM in environmental samples, they also allow the assessment of the source of NOM by comparing the fingerprints of different classes of biomolecules (Carr et al., 2010; Vancampenhout et al., 2008; White et al., 2004). For lipids, short-chain and branched fatty acids (as methyl ester) are indicative of a bacterial origin (Drenovsky et al., 2004; Zelles, 1999), whereas long-chain fatty acids suggest a vascular plant origin (Kolattukudy et al., 1976). Xylose to glucose and fucose to glucose ratios are generally used for carbohydrates to distinguish between a bacterial and vascular plant origin, respectively (Grasset et al., 2009; Rumpel and Dignac, 2006). Finally, for lignins, different ratios are applied to describe the vegetation type (Harris and Hartley, 1980), the contribution of woody and non-woody tissues (Hedges and Mann, 1979) and the degree of lignin degradation (Hedges and Mann, 1979). These biological indicators are especially used in the field of geochemistry, soil sciences and ecology, whereas they are not so common in the field of water resources and drinking water. An application of pyrolysis-GC-MS techniques could contribute to a better understanding of the source(s) of NOM, which is an important driver for redox processes during riverbank filtration.

**1.8 Thesis outline**

The present doctoral thesis was accomplished within the framework of the National Research Program NRP 61 (2010-2013), which aimed at the elaboration of scientific knowledge, methods and strategies for a sustainable water management in the context of climate change. NRP 61 included 16 projects, investigating various aspects related to water resources and water management. Embedded in the project RIBACLIM (Riverbank filtration under climate change scenarios) there were three PhD theses, (i) investigating photochemical transformation processes of micropollutants, (ii) assessing the effects of climate change on redox processes and on drinking water quality during riverbank filtration by column experiments and field studies and (iii) assessing physical and biogeochemical processes during riverbank filtration at a river-infiltration system in NE-Switzerland in the context of river restoration and climate change.

The objective of the present study (thesis (ii)) was to systematically investigate the effects of climate change on redox processes and on the quality of drinking water derived by riverbank filtration by means of column experiments and field studies in close connection with thesis (iii). The current study is closely related to another NRP 61 project entitled

“Understanding how climate change is affecting groundwater”, which investigated the qualitative aspects of climate change on groundwater by analysis of historical data of oxygen and temperature. In the following, the content of each chapter of the thesis will be discussed briefly.

**Chapter 1** provides a general introduction on the relevance of groundwater as an important drinking water resource and elaborates on managed aquifer recharge systems, such as riverbank filtration. Moreover, the biogeochemical processes occurring during riverbank filtration and the latest climate change scenarios for Switzerland are presented. Finally, an overview on methods for the characterization of NOM is given, with a focus on pyrolysis-GC-MS techniques.

**Chapter 2** shows the results of field sampling campaigns and column experiments under summer and winter conditions. These field studies and column experiments were conducted to assess the effects of temperature and discharge on the redox milieu in a river-infiltration zone characterized by NOM degradation and the consumption of electron acceptors. The field sampling campaigns were carried out at a previously instrumented river-infiltration system in Niederneunforn, NE-Switzerland. The field-based findings revealed a pronounced temperature dependence of the oxygen consumption, which was confirmed by column experiments. Moreover, it was observed that particulate organic matter (POM) acted as the main electron donor under summer conditions in both field and column systems and that flood events could lead to an increased input of POM in riverbed sediments leading to an enhanced oxygen consumption.

**Chapter 3** presents results from a systematic study on the effects of climate variables on biogeochemical processes occurring during riverbank filtration by means of column experiments, in which natural sand from the field site was used as filling material. Temperature, DOM concentration, DOM composition and flow rate were systematically varied to study their effects on the redox conditions, i.e., the consumption of electron acceptors, such as oxygen and nitrate. The previous findings from Chapter 2 could be confirmed by these experiments, showing a strong temperature dependence of the oxygen consumption associated with the degradation of POM. However, DOM concentration and composition of the feed water did not affect the redox conditions. A partial denitrification was observed for the high temperature scenario (30°C), with the formation of nitrite and ammonium. Mn(II) was mobilized under

anaerobic conditions from the dissolution of natural Mn(III/IV)(hydr)oxides, whereas Fe(II) was not formed under the experimental conditions. It was concluded that future heat waves characterized by high temperatures and low flow rates for long-lasting periods could be critical for the development of transient anoxic conditions.

**Chapter 4** focuses on the characterization of the molecular composition of POM associated with the natural sand used in the column experiments (Chapter 3) and possible POM source samples (riverbed sediments, river water, macrophytes, periphyton, soil, wastewater effluent) by preparative thermochemolysis-GC-MS. The goal was to identify the origin of POM of sand samples by comparing selected signatures of biomolecules (lipids, carbohydrates and lignins). This method has shown to be reliable and reproducible to analyze the composition of environmental samples. Although this qualitative method allowed changes in the POM composition during the column experiments to be assessed, a single predominant source of the sand POM could not be identified.

**Chapter 5** provides a general conclusion of the main findings of this thesis and discusses their implications with regard to drinking water quality.

## 1.9 References

- Ahn, I.S., Lee, C.H., 2003. Kinetic studies of attachment and detachment of microbial cells from soil. *Environmental Technology* 24 (4), 411-418.
- Baghoth, S.A., Maeng, S.K., Salinas Rodríguez, S.G., Ronteltap, M., Sharma, S., Kennedy, M., Amy, G.L., 2008. An urban water cycle perspective of natural organic matter (NOM): NOM in drinking water, wastewater effluent, storm water, and seawater. *Water Science and Technology: Water Supply* 8 (6), 701-707.
- Baumgarten, B., Jählig, J., Reemtsma, T., Jekel, M., 2011. Long term laboratory column experiments to simulate bank filtration: Factors controlling removal of sulfamethoxazole. *Water Research* 45 (1), 211-220.
- Bertelkamp, C., Reungoat, J., Cornelissen, E.R., Singhal, N., Reynisson, J., Cabo, A.J., van der Hoek, J.P., Verliefde, A.R.D., 2014. Sorption and biodegradation of organic micropollutants during river bank filtration: A laboratory column study. *Water Research* 52, 231-241.
- Berwick, L., Greenwood, P.F., Smernik, R.J., 2010. The use of MSSV pyrolysis to assist the molecular characterisation of aquatic natural organic matter. *Water Research* 44 (10), 3039-3054.
- Blanc, P., Schädler, B., 2013. Das Wasser in der Schweiz - ein Überblick. Schweizerische Hydrologische Kommission CHy, pp. 27.
- Bouwer, E.J., 1992. Bioremediation of organic contaminants in the subsurface. In: Mitchell, R. (Ed.), *Environmental Microbiology*. Wiley-Liss, pp. 287-318.
- Bradley, P.M., Chapelle, F.H., Löffler, F.E., 2008. Anoxic mineralization: Environmental reality or experimental artifact? *Ground Water Monitoring and Remediation* 28 (1), 47-49.
- Carr, A.S., Boom, A., Chase, B.M., Roberts, D.L., Roberts, Z.E., 2010. Molecular fingerprinting of wetland organic matter using pyrolysis-GC/MS: An example from the southern Cape coastline of South Africa. *Journal of Paleolimnology* 44 (4), 947-961.
- Carrie, J., Sanei, H., Goodarzi, F., Stern, G., Wang, F., 2009. Characterization of organic matter in surface sediments of the Mackenzie River Basin, Canada. *International Journal of Coal Geology* 77 (3-4), 416-423.
- CH2011, 2011. Swiss Climate Change Scenarios CH2011. C2SM, MeteoSwiss, ETH, NCCR Climate and OcCC, Zürich, pp. 88.

- Challinor, J.M., 2001. Review: The development and applications of thermally assisted hydrolysis and methylation reactions. *Journal of Analytical and Applied Pyrolysis* 61 (1-2), 3-34.
- Chow, C.W.K., Kuntke, P., Fabris, R., Drikas, M., 2009. Organic characterisation tools for distribution system management. *Water Science and Technology: Water Supply* 9 (1), 1-8.
- Croué, J.P., 2004. Isolation of humic and non-humic NOM fractions: Structural characterizations. *Environmental Monitoring and Assessment* 92 (1-3), 193-207.
- Danielopol, D.L., Griebler, C., Gunatilaka, A., Notenboom, J., 2003. Present state and future prospects for groundwater ecosystems. *Environmental Conservation* 30 (2), 104-130.
- Deborde, M., von Gunten, U., 2008. Reactions of chlorine with inorganic and organic compounds during water treatment-Kinetics and mechanisms: A critical review. *Water Research* 42 (1-2), 13-51.
- Del Rio, J.C., McKinney, D.E., Knicker, H., Nanny, M.A., Minard, R.D., Hatcher, P.G., 1998. Structural characterization of bio- and geo-macromolecules by off-line thermochemolysis with tetramethylammonium hydroxide. *Journal of Chromatography A* 823 (1-2), 433-448.
- Dillon, P., 2005. Future management of aquifer recharge. *Hydrogeology Journal* 13 (1), 313-316.
- Drenovsky, R.E., Elliott, G.N., Graham, K.J., Scow, K.M., 2004. Comparison of phospholipid fatty acid (PLFA) and total soil fatty acid methyl esters (TSFAME) for characterizing soil microbial communities. *Soil Biology and Biochemistry* 36 (11), 1793-1800.
- Eckert, P., Irmischer, R., 2006. Over 130 years of experience with Riverbank Filtration in Düsseldorf, Germany. *Journal of Water Supply: Research and Technology - AQUA* 55 (4), 283-291.
- EDI, 1995. Verordnung des EDI über Fremd- und Inhaltsstoffe in Lebensmitteln (FIV) no. 817.021.23, 26. Juni 1995, Stand 1. Januar 2014. Eidgenössisches Departement des Innern, EDI. Available at <http://www.admin.ch/opc/de/classified-compilation/19950193/201401010000/817.021.23.pdf> (Last accessed on: 14.04.2014).
- EDI, 1998. Gewässerschutzverordnung no. 814.201, 28. Oktober 1998, Stand 1. Januar 2014. Eidgenössisches Departement des Innern, EDI. Available at <http://www.admin.ch/opc/de/classified-compilation/19983281/index.html#a29> (Last accessed on: 14.04.2014).

- Escobar, I.C., Randall, A.A., 2001. Assimilable organic carbon (AOC) and biodegradable dissolved organic carbon (BDOC): Complementary measurements. *Water Research* 35 (18), 4444-4454.
- Figura, S., Livingstone, D.M., Kipfer, R., 2013. Competing controls on groundwater oxygen concentrations revealed in multidecadal time series from riverbank filtration sites. *Water Resources Research* 49 (11), 7411-7426.
- FOEN, 2012. Effects of Climate Change on Water Resources and Watercourses. Synthesis Report on the "Climate Change and Hydrology in Switzerland" (CCHydro) Project. Federal Office for the Environment FOEN, Bern, pp. 76.
- Frazier, S.W., Kaplan, L.A., Hatcher, P.G., 2005. Molecular characterization of biodegradable dissolved organic matter using bioreactors and [12C/13C] tetramethylammonium hydroxide thermochemolysis GC-MS. *Environmental Science and Technology* 39 (6), 1479-1491.
- Frazier, S.W., Nowack, K.O., Goins, K.M., Cannon, F.S., Kaplan, L.A., Hatcher, P.G., 2003. Characterization of organic matter from natural waters using tetramethylammonium hydroxide thermochemolysis GC-MS. *Journal of Analytical and Applied Pyrolysis* 70 (1), 99-128.
- Goldscheider, N., Hunkeler, D., Rossi, P., 2006. Review: Microbial biocenoses in pristine aquifers and an assessment of investigative methods. *Hydrogeology Journal* 14 (6), 926-941.
- Grasset, L., Amblès, A., 1998. Structural study of soil humic acids and humin using a new preparative thermochemolysis technique. *Journal of Analytical and Applied Pyrolysis* 47 (1), 1-12.
- Grasset, L., Rovira, P., Amblès, A., 2009. TMAH-preparative thermochemolysis for the characterization of organic matter in densimetric fractions of a Mediterranean forest soil. *Journal of Analytical and Applied Pyrolysis* 85 (1-2), 435-441.
- Greskowiak, J., Prommer, H., Massmann, G., Nützmann, G., 2006. Modeling seasonal redox dynamics and the corresponding fate of the pharmaceutical residue phenazone during artificial recharge of groundwater. *Environmental Science and Technology* 40 (21), 6615-6621.
- Grünheid, S., Amy, G., Jekel, M., 2005. Removal of bulk dissolved organic carbon (DOC) and trace organic compounds by bank filtration and artificial recharge. *Water Research* 39 (14), 3219-3228.

- Grünheid, S., Huebner, U., Jekel, M., 2008. Impact of temperature on biodegradation of bulk and trace organics during soil passage in an indirect reuse system. *Water Science and Technology* 57, 987-994.
- Hammes, F.A., Egli, T., 2005. New method for assimilable organic carbon determination using flow-cytometric enumeration and a natural microbial consortium as inoculum. *Environmental Science and Technology* 39 (9), 3289-3294.
- Hammes, F.A., Salhi, E., Köster, O., Kaiser, H.P., Egli, T., von Gunten, U., 2006. Mechanistic and kinetic evaluation of organic disinfection by-product and assimilable organic carbon (AOC) formation during the ozonation of drinking water. *Water Research* 40 (12), 2275-2286.
- Harris, P.J., Hartley, R.D., 1980. Phenolic constituents of the cell-walls of monocotyledons. *Biochemical Systematics and Ecology* 8 (2), 153-160.
- Hatcher, P.G., Nanny, M.A., Minard, R.D., Dible, S.D., Carson, D.M., 1996. Comparison of two thermochemolytic methods for the analysis of lignin in decomposing gymnosperm wood: the CuO oxidation method and the method of thermochemolysis with tetramethylammonium hydroxide (TMAH). *Organic Geochemistry* 23 (10), 881-888.
- Heberer, T., Massmann, G., Fanck, B., Taute, T., Dunnbier, U., 2008. Behaviour and redox sensitivity of antimicrobial residues during bank filtration. *Chemosphere* 73 (4), 451-460.
- Heberer, T., Mechlinski, A., Fanck, B., Knappe, A., Massmann, G., Pekdeger, A., Fritz, B., 2004. Field studies on the fate and transport of pharmaceutical residues in bank filtration. *Ground Water Monitoring and Remediation* 24 (2), 70-77.
- Hedges, J.I., Mann, D.C., 1979. Characterization of plant-tissues by their lignin oxidation-products. *Geochimica et Cosmochimica Acta* 43 (11), 1803-1807.
- Hiscock, K.M., Grischek, T., 2002. Attenuation of groundwater pollution by bank filtration. *Journal of Hydrology* 266 (3-4), 139-144.
- Hoehn, E., Scholtis, A., 2011. Exchange between a river and groundwater, assessed with hydrochemical data. *Hydrology and Earth System Sciences* 15 (3), 983-988.
- Huber, S.A., Balz, A., Abert, M., Pronk, W., 2011. Characterisation of aquatic humic and non-humic matter with size-exclusion chromatography - organic carbon detection - organic nitrogen detection (LC-OCD-OND). *Water Research* 45 (2), 879-885.
- Huntscha, S., Rodriguez Velosa, D.M., Schroth, M.H., Hollender, J., 2013. Degradation of Polar Organic Micropollutants during Riverbank Filtration: Complementary Results



- from Spatiotemporal Sampling and Push–Pull Tests. *Environmental Science and Technology* 47 (20), 11512-11521.
- IPCC, 2013. *Climate Change 2013: The Physical Science Basis*. Ed. T.F. Stocker, D. Qin, G.-K. Plattner, M.M.B. Tignor, S.K. Allen, J. Boschung, A. Nauels, Y. Xia, V. Bex, P.M. Midgley. Intergovernmental Panel on Climate Change IPCC, pp. 27.
- Jacobs, L.A., von Gunten, H.R., Keil, R., Kuslys, M., 1988. Geochemical changes along a river-groundwater infiltration flow path: Glattfelden, Switzerland. *Geochimica et Cosmochimica Acta* 52 (11), 2693-2706.
- Joll, C.A., Couton, D., Heitz, A., Kagi, R.I., 2004. Comparison of reagents for off-line thermochemolysis of natural organic matter. *Organic Geochemistry* 35 (1), 47-59.
- Jouanneau, S., Recoules, L., Durand, M.J., Boukabache, A., Picot, V., Primault, Y., Lakel, A., Sengelin, M., Barillon, B., Thouand, G., 2013. Methods for assessing biochemical oxygen demand (BOD): A review. *Water Research* 49 (1), 62-82.
- Kolattukudy, P.E., Croteau, R., Buckner, J.S., 1976. Biochemistry of plant waxes. In: Kolattukudy, P.E. (Ed.), *Chemistry and Biochemistry of Natural Waxes*. Elsevier, Amsterdam, pp. 289-347.
- Kuehn, W., Mueller, U., 2000. Riverbank filtration: An overview. *Journal / American Water Works Association* 92 (12), 60-69.
- Leenheer, J.A., Croué, J.P., 2003. Characterizing aquatic dissolved organic matter. *Environmental Science and Technology* 37 (1), 18A-26A.
- Massmann, G., Greskowiak, J., Dunnbier, U., Zuehlke, S., Knappe, A., Pekdeger, A., 2006. The impact of variable temperatures on the redox conditions and the behaviour of pharmaceutical residues during artificial recharge. *Journal of Hydrology* 328 (1-2), 141-156.
- Matilainen, A., Gjessing, E.T., Lahtinen, T., Hed, L., Bhatnagar, A., Sillanpää, M., 2011. An overview of the methods used in the characterisation of natural organic matter (NOM) in relation to drinking water treatment. *Chemosphere* 83 (11), 1431-1442.
- Matilainen, A., Iivari, P., Sallanko, J., Heiska, E., Tuhkanen, T., 2006. The role of ozonation and activated carbon filtration in the natural organic matter removal from drinking water. *Environmental Technology* 27 (10), 1171-1180.
- Mesfioui, R., Love, N.G., Bronk, D.A., Mulholland, M.R., Hatcher, P.G., 2012. Reactivity and chemical characterization of effluent organic nitrogen from wastewater treatment plants

- determined by Fourier transform ion cyclotron resonance mass spectrometry. *Water Research* 46 (3), 622-634.
- Micić, V., Kruge, M.A., Köster, J., Hofmann, T., 2011. Natural, anthropogenic and fossil organic matter in river sediments and suspended particulate matter: A multi-molecular marker approach. *Science of the Total Environment* 409 (5), 905-919.
- OECD, 1992. OECD Guideline for Testing of Chemicals, Guideline 301 D. Organisation for Economic Co-operation and Development OECD, pp. 62.
- Plante, A.F., Parton, W.J., 2007. The dynamics of soil organic matter and nutrient cycling. In: Paul, E.A. (Ed.), *Soil microbiology, ecology, and biochemistry*. Academic Press, pp. 433-467.
- Pusch, M., Fiebig, I., Brettar, H., Eisenmann, H., Ellis, B.K., Kaplan, L.A., Lock, M.A., Naegeli, M.W., Traunspurger, W., 1998. The role of micro-organisms in the ecological connectivity of running waters. *Freshwater Biology* 40 (3), 453-495.
- Reemtsma, T., Miehe, U., Duennbier, U., Jekel, M., 2010. Polar pollutants in municipal wastewater and the water cycle: Occurrence and removal of benzotriazoles. *Water Research* 44 (2), 596-604.
- Reemtsma, T., These, A., 2005. Comparative investigation of low-molecular-weight fulvic acids of different origin by SEC-Q-TOF-MS: New insights into structure and formation. *Environmental Science and Technology* 39 (10), 3507-3512.
- Rumpel, C., Dignac, M.F., 2006. Gas chromatographic analysis of monosaccharides in a forest soil profile: Analysis by gas chromatography after trifluoroacetic acid hydrolysis and reduction-acetylation. *Soil Biology and Biochemistry* 38 (6), 1478-1481.
- Sacher, F., Brauch, H.J., 2002. Experiences on the fate of organic micropollutants during riverwater filtration. In: Ray, C. (Ed.), *Riverbank Filtration: Understanding Contaminant Biogeochemistry and Pathogen Removal*. Kluwer Academic Publishers, pp. 135-151.
- Schädler, B., Weingartner, R., 2002. Komponenten des natürlichen Wasserhaushaltes 1961-1990. In: BWG: *Hydrologischer Atlas der Schweiz* (Tafel 6.3), Bern.
- Scheurer, M., Michel, A., Brauch, H.J., Ruck, W., Sacher, F., 2012. Occurrence and fate of the antidiabetic drug metformin and its metabolite guanylurea in the environment and during drinking water treatment. *Water Research* 46 (15), 4790-4802.
- Schmidt, C.K., Lange, F.T., Brauch, H.J., 2007. Characteristics and evaluation of natural attenuation processes for organic micropollutant removal during riverbank filtration. *Water Science and Technology: Water Supply* 7 (3), 1-7.

- Schwarzenbach, R.P., Giger, W., Hoehn, E., Schneider, J.K., 1983. Behavior of organic compounds during infiltration of river water to groundwater. Field studies. *Environmental Science and Technology* 17 (8), 472-479.
- Shadkani, F., Helleur, R., 2010. Recent applications in analytical thermochemolysis. *Journal of Analytical and Applied Pyrolysis* 89 (1), 2-16.
- Søndergaard, M., Worm, J., 2001. Measurement of biodegradable dissolved organic carbon (BDOC) in lake water with a bioreactor. *Water Research* 35 (10), 2505-2513.
- Sprenger, C., Lorenzen, G., Hulshoff, I., Grutmacher, G., Ronghang, M., Pekdeger, A., 2011. Vulnerability of bank filtration systems to climate change. *Science of the Total Environment* 409 (4), 655-663.
- Steinberg, S.M., Nemr, E.L., Rudin, M., 2009. Characterization of the lignin signature in Lake Mead, NV, sediment: Comparison of on-line flash chemopyrolysis (600°C) and off-line chemolysis (250°C). *Environmental Geochemistry and Health* 31 (3), 339-352.
- Storck, F.R., Schmidt, C.K., Wülser, R., Brauch, H.J., 2012. Effects of boundary conditions on the cleaning efficiency of riverbank filtration and artificial groundwater recharge systems regarding bulk parameters and trace pollutants. *Water Science and Technology* 66 (1), 138-144.
- Stumm, W., Morgan, J.J., 1996. *Aquatic Chemistry. Chemical Equilibria and Rates in Natural Waters*, Third Edition. Wiley-interscience.
- Swift, R.S., 1996. Organic Matter Characterization. In: Sparks et al. (Eds.), *Methods of Soil Analysis, Part 3, Chemical Methods*. SSSA Book Series, pp. 1011-1069.
- Teixeira, M.R., Nunes, L.M., 2011. The impact of natural organic matter seasonal variations in drinking water quality. *Desalination and Water Treatment* 36 (1-3), 344-353.
- Thurman, E.M., 1985. *Organic Geochemistry of Natural Waters*. Kluwer Academic Publishers: Dordrecht, The Netherlands.
- Tufenkji, N., Ryan, J.N., Elimelech, M., 2002. Bank filtration. *Environmental Science and Technology* 36 (21), 423-428.
- Vancampenhout, K., Wouters, K., Caus, A., Buurman, P., Swennen, R., Deckers, J., 2008. Fingerprinting of soil organic matter as a proxy for assessing climate and vegetation changes in last interglacial palaeosols (Veldwezelt, Belgium). *Quaternary Research* 69 (1), 145-162.

- Verstraeten, I.M., Thurman, E.M., Lindsey, M.E., Lee, E.C., Smith, R.D., 2002. Changes in concentrations of triazine and acetamide herbicides by bank filtration, ozonation, and chlorination in a public water supply. *Journal of Hydrology* 266 (3-4), 190-208.
- Volk, C.J., LeChevallier, M.W., 2000. Assessing biodegradable organic matter. *Journal / American Water Works Association* 92 (5), 64-76.
- von Gunten, H.R., Karametaxas, G., Kell, R., 1994. Chemical processes in infiltrated riverbed sediments. *Environmental Science and Technology* 28 (12), 2087-2093.
- von Gunten, H.R., Karametaxas, G., Krähenbühl, U., Kuslys, M., Giovanoli, R., Hoehn, E., Keil, R., 1991. Seasonal biogeochemical cycles in riverborne groundwater. *Geochimica et Cosmochimica Acta* 55 (12), 3597-3609.
- von Gunten, U., Zobrist, J., 1993. Biogeochemical changes in groundwater-infiltration systems: Column studies. *Geochimica et Cosmochimica Acta* 57 (16), 3895-3906.
- White, D.M., Garland, D.S., Beyer, L., Yoshikawa, K., 2004. Pyrolysis-GC/MS fingerprinting of environmental samples. *Journal of Analytical and Applied Pyrolysis* 71 (1), 107-118.
- WHO, 2011. *Guidelines for Drinking-water Quality, Fourth Edition*. World Health Organization WHO, pp. 541.
- Zelles, L., 1999. Fatty acid patterns of phospholipids and lipopolysaccharides in the characterisation of microbial communities in soil: A review. *Biology and Fertility of Soils* 29 (2), 111-129.
- Zhong, J., Sleighter, R.L., Salmon, E., McKee, G.A., Hatcher, P.G., 2011. Combining advanced NMR techniques with ultrahigh resolution mass spectrometry: A new strategy for molecular scale characterization of macromolecular components of soil and sedimentary organic matter. *Organic Geochemistry* 42 (8), 903-916.

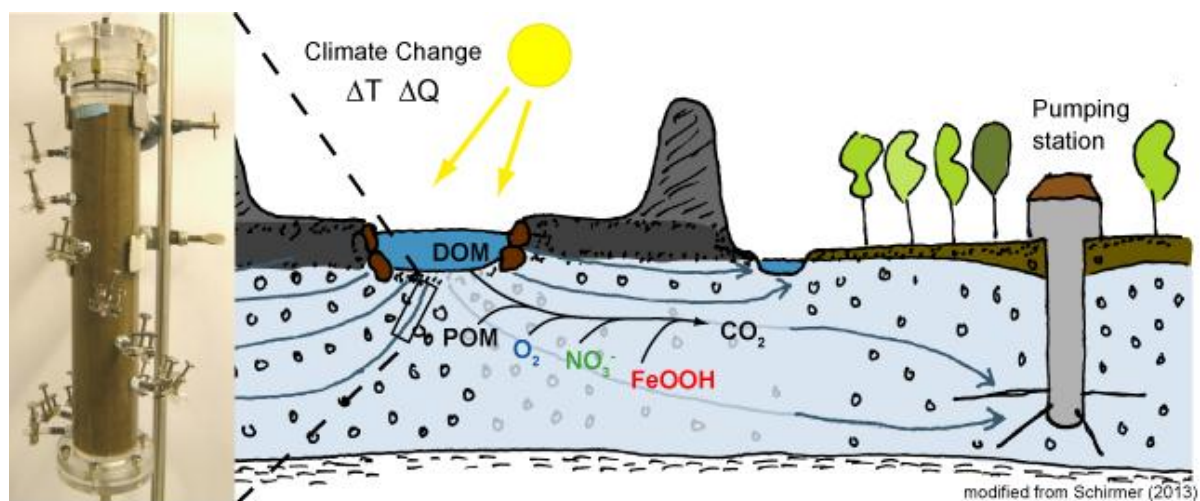
## **Chapter 2**

### **NOM degradation during river infiltration: Effects of the climate variables temperature and discharge**

Reprinted from *Water Research* 47 (17), Diem, S.\*; Rudolf von Rohr, M.\*; Hering, J. G.; Kohler, H.-P. E.; Schirmer, M.; von Gunten, U., NOM degradation during river infiltration: Effects of the climate variables temperature and discharge, 6585–6595. Copyright 2013, with permission from Elsevier.

<http://dx.doi.org/10.1016/j.watres.2013.08.028>

\*Equal contribution of first and second authors



## Graphical Abstract

## Abstract

Most peri-alpine shallow aquifers fed by rivers are oxic and the drinking water derived by riverbank filtration is generally of excellent quality. However, observations during past heat waves suggest that water quality may be affected by climate change due to effects on redox processes such as aerobic respiration, denitrification, reductive dissolution of manganese(III/IV)- and iron(III)(hydr)oxides that occur during river infiltration. To assess the dependence of these redox processes on the climate-related variables temperature and discharge, we performed periodic and targeted (summer and winter) field sampling campaigns at the Thur River, Switzerland, and laboratory column experiments simulating the field conditions. Typical summer and winter field conditions could be successfully simulated by the column experiments. Dissolved organic matter (DOM) was found not to be a major electron donor for aerobic respiration in summer and the DOM consumption did not reveal a significant correlation with temperature and discharge. It is hypothesized that under summer conditions, organic matter associated with the aquifer material (particulate organic matter, POM) is responsible for most of the consumption of dissolved oxygen (DO), which was the most important electron acceptor in both the field and the column system. For typical summer conditions at temperatures  $>20^{\circ}\text{C}$ , complete depletion of DO was observed in the column system and in a piezometer located only a few meters from the river. Both in the field system and the column experiments, nitrate acted as a redox buffer preventing the release of manganese(II) and iron(II). For periodic field observations over five years, DO consumption showed a pronounced temperature dependence (correlation coefficient  $r = 0.74$ ) and therefore a seasonal pattern, which seemed to be mostly explained by the temperature dependence of the calculated POM consumption ( $r = 0.7$ ). The river discharge was found to be highly and positively correlated with DO consumption ( $r = 0.85$ ), suggesting an enhanced POM input during flood events. This high correlation could only be observed for the low-temperature range ( $T < 15^{\circ}\text{C}$ ). For temperatures  $>15^{\circ}\text{C}$ , DO consumption was already high (almost complete) and the impact of discharge could not be resolved. Based on our results, we estimate the risk for similar river-infiltration systems to release manganese(II) and iron(II) to be low during future average summer conditions. However, long-lasting heat waves might lead to a consumption of the nitrate buffer, inducing a mobilization of manganese and iron.

Keywords: riverbank filtration; climate change; DOM; POM; groundwater quality; redox conditions

## 2.1 Introduction

Riverbank filtration is a widely applied technique to produce drinking water and contributes substantially to the overall drinking water production in several European countries (France ~50%, Germany ~16% (Tufenkji et al., 2002), Switzerland ~25%). Natural attenuation processes during river infiltration efficiently remove particles, bacteria, viruses, parasites and, to a lesser extent, organic contaminants, such as pharmaceuticals (Kuehn and Mueller, 2000; Sacher and Brauch, 2002; Grünheid et al., 2005). During river infiltration, biogeochemical processes can alter the composition of the infiltrating water significantly (Jacobs et al., 1988).

The most important biogeochemical process during river infiltration is the biodegradation of natural organic matter (NOM), which occurs within bacterial biofilms in riverbed sediments (Pusch et al., 1998). NOM in river systems originates from both allochthonous (terrestrially-derived) sources and generally more biodegradable autochthonous sources (periphyton) (Pusch et al., 1998; Leenheer and Croue, 2003). NOM is composed of dissolved organic matter (DOM) and particulate organic matter (POM), usually quantified as dissolved organic carbon (DOC) and particulate organic carbon (POC), respectively (Leenheer and Croue, 2003). During infiltration of river water, DOM is transported through the riverbed as a „mobile substrate“, whereas POM is retained in the riverbed sediments as a „stationary substrate“ (Pusch et al., 1998).

The biodegradation of NOM in riverbed sediments leads to a consumption of dissolved or solid terminal electron acceptors, such as oxygen ( $O_2$ ), nitrate ( $NO_3^-$ ), Mn(III/IV)- and Fe(III)(hydr)oxides and sulfate ( $SO_4^{2-}$ ). Redox conditions in riverbank-filtration and artificial-recharge systems were observed to undergo seasonal variations with the formation of anoxic conditions during summer due to the temperature dependence of NOM degradation (Greskowiak et al., 2006; Massmann et al., 2006; Sharma et al., 2012).

In the Swiss context, riverbank filtration is often the only barrier between river water and drinking water. This is possible because of the usually high dilution of wastewater effluents in receiving rivers and the generally oxic conditions of shallow groundwater. However, during the hot summer of 2003, the redox conditions in several riverbank-filtration systems turned anoxic. Hoehn and Scholtis (2011) reported a case at the Thur River, where the redox sequence even proceeded to Mn(IV)- and Fe(III)-reducing conditions. The subsequent re-oxidation of dissolved Mn(II) and Fe(II) at the pumping station led to clogging of the filter screen and to rusty water.

Climate models predict an increase in summer air temperatures (4-5 K) and a decrease in precipitation (25%) inducing lower discharges in rivers during summer months in northern



Switzerland by 2085 (CH2011, 2011; FOEN, 2012). Lower discharges may give rise to less dilution of wastewater effluents and accordingly to higher DOC concentrations. Combined with higher temperatures, the risk for riverbank-filtration systems to become anoxic or even develop Mn(IV)- or Fe(III)-reducing conditions is likely to increase (Sprenger et al., 2011). To assess this risk more accurately, the dynamics of NOM degradation and its dependence on climate variables need to be better understood (Eckert et al., 2008; Green et al., 2011).

Besides the direct influence of temperature and discharge, the biogeochemical processes during river infiltration and hence the redox conditions in the infiltration zone might also be affected by indirect climate-related changes in river water quality. The effect of climate change on river water quality (e.g. dissolved oxygen, nutrients (nitrate, ammonium), DOC and major ions) in relation to hydrologic, terrestrial and resource-use factors has been addressed in many studies (Murdoch et al., 2000; Zwolsman and van Bokhoven, 2007; Park et al., 2010). However, Senhorst and Zwolsman (2005) conclude that the impact of climate change on surface water quality is quite site specific and cannot be generally transferred to other watersheds and hence, should be assessed case by case. Therefore, we focused on the direct effect of the climate-related variables temperature and discharge on NOM degradation and the related consumption of electron acceptors during river infiltration.

The objectives of the present study were to assess the contribution of DOM consumption to the overall consumption of electron acceptors and to examine the effects of the climate-related variables temperature and discharge by means of field investigations and column experiments. To capture different temperature ranges, the field investigations consisted of two detailed sampling campaigns performed during typical summer and winter conditions at the peri-alpine Thur River. The column experiments were performed at temperatures that span the range of typical field conditions. Additionally, the data of periodic field samplings that covered a wide range of temperature and discharge conditions over a period of five years were evaluated.

Firstly, we assessed the temperature dependence of the consumption of dissolved oxygen (DO) and DOM by comparing the data of the field campaigns with those of column experiments and verified the findings by a correlation analysis of the periodic data. Secondly, we investigated the impact of the discharge conditions on DO and DOM consumption using the periodic field data. Finally, we discuss the implications of our findings on the redox-related groundwater quality at riverbank-filtration systems in a changing climate.

## 2.2 Materials and Methods

### 2.2.1 Field site

The field site of our investigation is located in NE-Switzerland (Niederneunforn) at the perialpine Thur River, which drains a catchment of 1700 km<sup>2</sup> (Fig. 2.1a). As no retention basin is located along the whole course of the river, the discharge behaves very dynamically with a range of 3-1100 m<sup>3</sup>/s. During the interdisciplinary RECORD-project (Restored corridor dynamics, <http://www.cces.ethz.ch/projects/nature/Record>, Schneider et al. (2011), Schirmer (2013)), 80 piezometers were installed (Fig. 2.1b). To the northern side of the river, the piezometers are arranged in two transects, the forest transect and the pumping station transect. Most of the piezometers are fully screened, covering the full aquifer thickness (5.3±1.2 m). The gravel-and-sand aquifer, which is underlain by lacustrine clay and overlain by 0.5-3 m alluvial fines, is highly conductive with hydraulic conductivities between 4×10<sup>-3</sup> and 6×10<sup>-2</sup> m/s. The pumping well at the pumping station transect is operated during a daily period of only 3 h extracting a total volume of 36 m<sup>3</sup>.

A groundwater flow and transport model was set up for low-flow conditions (23 m<sup>3</sup>/s) and was calibrated against groundwater heads and experimentally determined travel times (Diem et al., 2012; 2013). According to the resulting groundwater flow field (Fig. 2.1b, c), river water is naturally infiltrating into the aquifer, both at the forest and the pumping station transect. The low abstraction rate of the pumping well was found not to have any significant effect on the infiltration rate or the groundwater flow field. Groundwater flow velocities were in the order of 5-10 m/d at the pumping station transect and ranged between 20-50 m/d at the forest transect.

Neither the pumping station transect nor the forest transect can be considered as a typical riverbank-filtration system with high abstraction rates considerably changing the groundwater flow field. Yet, both transects qualify for studying the microbial degradation processes during river infiltration and their dependencies on the climate-related variables temperature and discharge. Compared to the pumping station transect, the forest transect has the advantage of higher flow velocities and shorter residence times to the closest piezometers, which allows a more detailed assessment of the NOM degradation dynamics. Therefore, in this paper, we focus on results from the forest transect.

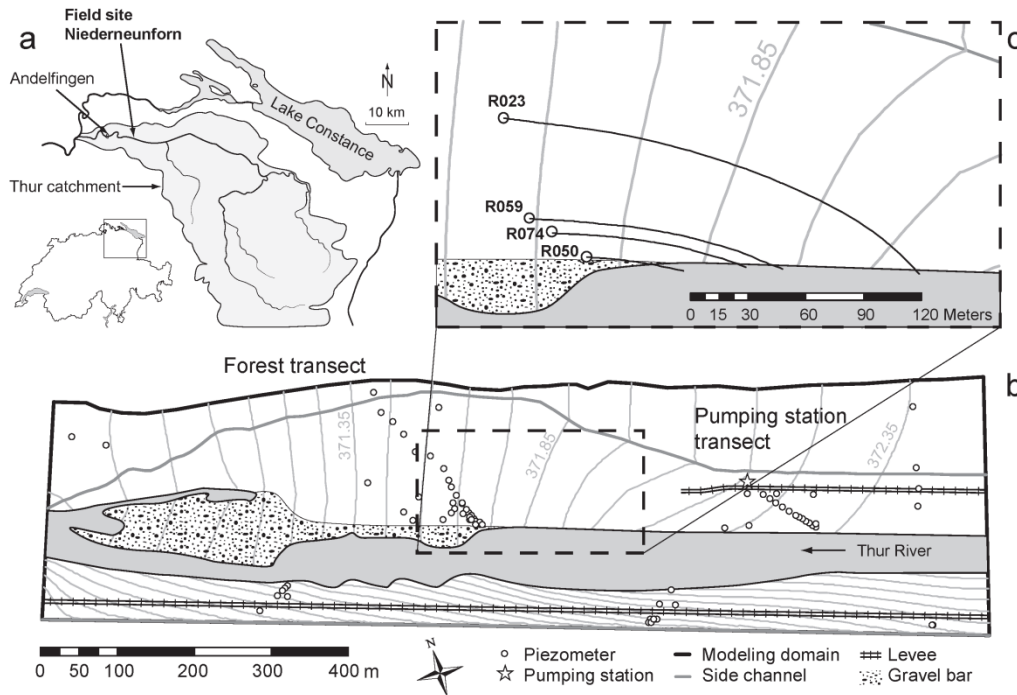


Fig. 2.1. (a) Catchment of the Thur River and location of the Niederneunforn field site, NE-Switzerland. (b) Schematic representation of the Niederneunforn field site. Groundwater head isolines (head equidistance 10 cm, light gray) were extracted from a groundwater flow model (Diem et al., 2013). (c) Enlargement of the area indicated by the dashed rectangle in (b), which contains the locations of the piezometers used in this study. The black lines in (c) indicate the advective flow paths from the river to the piezometers according to the resulting flow field of the groundwater flow model.

## 2.2.2 Sampling campaigns and periodic samplings

To capture different temperature ranges, we conducted two detailed sampling campaigns during summer and winter 2011. We sampled the river and adjacent groundwater on five days between August 19-26, 2011 (summer campaign) and November 23-29, 2011 (winter campaign). The periodic samplings were carried out during a period of five years (2008-2012) and covered a wide temperature and discharge range (supporting information, Fig. S2.1). Samples were taken in different piezometers at the forest transect. For better clarity, we only present results from a representative subset of the sampled piezometers (Fig. 2.1c).

The groundwater samples were pumped by a submersible electric pump (Whale®, Bangor, Northern Ireland) with an average pumping rate of 10 L/min. Before taking the in-situ measurements and the samples, we pumped at least 20 L (twice the piezometer volume) and waited until the electrical conductivity (EC) of the pumped groundwater was stable. We

measured DO concentrations (LDO10115 (optical sensor), Hach Lange GmbH, Berlin, Germany, accuracy  $\pm 0.1$  mg/L), pH and temperature (PHC10115, Hach Lange GmbH, Berlin, Germany, accuracy pH  $\pm 0.1$ , T  $\pm 0.3$  K) and EC (Cond 340i, WTW GmbH, Weilheim, Germany) in a 10 L bottle, which was constantly flushed with groundwater. The small opening on top of the bottle minimized the gas exchange with the atmosphere and thus guaranteed reliable DO measurements at near-zero concentrations. Groundwater and river water was filled into polypropylene bottles (1 L), filtered within 24 h through a 0.45  $\mu$ m cellulose nitrate filter (Sartorius AG, Göttingen, Germany) and stored at 4°C until analysis. Concentrations of DOC (to quantify DOM), nitrate, ammonium and major ions were measured in the river water and groundwater samples (for analytical method see section 2.2.4).

DO, as well as temperature and discharge were continuously measured (10-min intervals) in the Thur River at a gauging station of the Federal Office for the Environment (FOEN), which is located in Andelfingen, 10 km downstream of our field site (Fig. 2.1a). The river DO concentrations in Andelfingen were found to agree well with those at our field site (Hayashi et al., 2012). DO concentrations in the river underwent diurnal fluctuations. Such diurnal DO fluctuations are mainly caused by a combination of photosynthesis of periphyton during daytime and respiration during the night (Hayashi et al., 2012).

We calculated the DO consumption that occurred during infiltration by subtracting the measured DO concentration in groundwater from the daily mean DO concentration in the river. The latter was calculated based on the continuous DO time series measured at the gauging station in Andelfingen to minimize the bias in calculated DO consumption due to diurnal DO fluctuations in the river. As the diurnal fluctuations of the DOC concentrations in the river were not significant, we subtracted the measured DOC concentration in groundwater from the DOC concentration in the river to calculate the DOM consumption.

Eight grab samples were taken from the riverbed at a depth of 0-20 cm close to the first piezometer R050 (Fig. 2.1c). The samples were dried and sieved; the riverbed sediment mainly consists of sandy gravel with little silt and clay. To quantify the POM contained in the riverbed sediment, we measured the POC concentrations for three grain-size fractions  $< 0.25$  mm. The POC concentration was highest for the fraction  $< 0.063$  mm ( $1.4 \pm 0.3\%$  w/w), and lowest for the fraction 0.125-0.25 mm ( $0.5 \pm 0.3\%$  w/w) (for analytical method see section 2.2.4).

### 2.2.3 Column experiments

A schematic representation of the set-up of the column experiments is shown in Fig. 2.2. The column casing consisted of a Plexiglas tube (length 30 cm, inner diameter 5.2 cm) and was packed with fractionated sand (0.125-0.25 mm grain size) from a gravel bar at the field site close to the forest transect. The sand was dried at room temperature and sieved afterwards before being dry-filled into the column in form of a “sand rain” (von Gunten and Zobrist, 1993). The sand was mainly composed of calcite and quartz (40% and 25%, respectively) and the POC concentration was about  $0.3 \pm 0.2\%$  (w/w). The sand fraction 0.125-0.250 mm was chosen because it is well defined and represents the available reactive surfaces with a considerable amount of POM.

Filtered Thur River water (0.45  $\mu\text{m}$ , cellulose nitrate, Sartorius AG, Göttingen, Germany) was stored in a 2 L tank and was used as feed water for the column. It was pumped from the bottom to the top of the column at a flow rate of 0.4 L/d by means of an HPLC pump (Jasco PU-2080, Jasco Corporation, Tokyo, Japan) (Fig. 2.2). Every three days, the storage tank was replenished with fresh Thur River water stored at 5°C. In case of the experiment at 20°C, Thur River water was allowed to equilibrate for about 6 hours before replenishment. No measurable DOM degradation in the storage tank was observed under these conditions. To assess the hydraulics in the column, a tracer test with a 8.55 mM NaCl solution was conducted and the EC was measured at the end of the column. We estimated an effective porosity of 0.32 and a dispersivity of 0.08 cm by inverse modeling with the software CXTFIT (Toride et al., 1995). The corresponding total pore volume of the column was 0.2 L. Hence, the residence time in the column was 0.5 d at a flow rate of 0.4 L/d.

The column was first operated at 20°C in a climatised chamber for 19 days after an equilibration time of about 2 months with Thur River water taken on July 4, 2012 (composition 1, Table S2.1, supporting information). After that, the column was operated at 5°C with the same feed water in an incubator for 26 days including an equilibration time of 20 days. Thereafter, as a control experiment, the column was operated again at 20°C in an incubator for 28 days including an equilibration time of 22 days (water composition 2, Table S2.2, supporting information). This control experiment was conducted to test if any of the column properties relevant for the bacterial degradation processes (sand composition, POM concentration/composition) had changed during the operation period at 5°C.

The column featured 15 sampling ports; one at the inlet, 13 along the column and one at the outlet (Fig. 2.2). DO and temperature were continuously measured at the inlet and at the outlet of the column (LDO101 (optical sensor), Hach Lange GmbH, Berlin, Germany, accuracy

$\pm 0.1$  mg/L,  $T \pm 0.3$  K), while pH was measured after the column (PHC 301, Hach Lange GmbH, Berlin, Germany, accuracy pH  $\pm 0.1$ ) in flow-through cells (Fig. 2.2). For each of the experiments at different temperatures, we measured three DO concentration profiles after an equilibration time of  $\geq 20$  d. DO was measured directly at each sampling port in a flow-through cell. After that, about 40 mL of sample volume was taken at the column inlet (SP0) and outlet (SP14) for the DOC and nitrate analyses by connecting a rinsed regenerated  $0.45 \mu\text{m}$  cellulose filter (National Scientific Company, Rockwood, USA) to the port. The sampling procedure was conducted from the outlet to the inlet of the column, following the opposite direction of the water flow.

The DO consumption in the column was calculated by subtracting the measured DO concentration at sampling port SP14 from the DO concentration at SP0 0.5 d before. The DOM consumption was determined from the difference of DOC concentrations at SP14 and SP0.

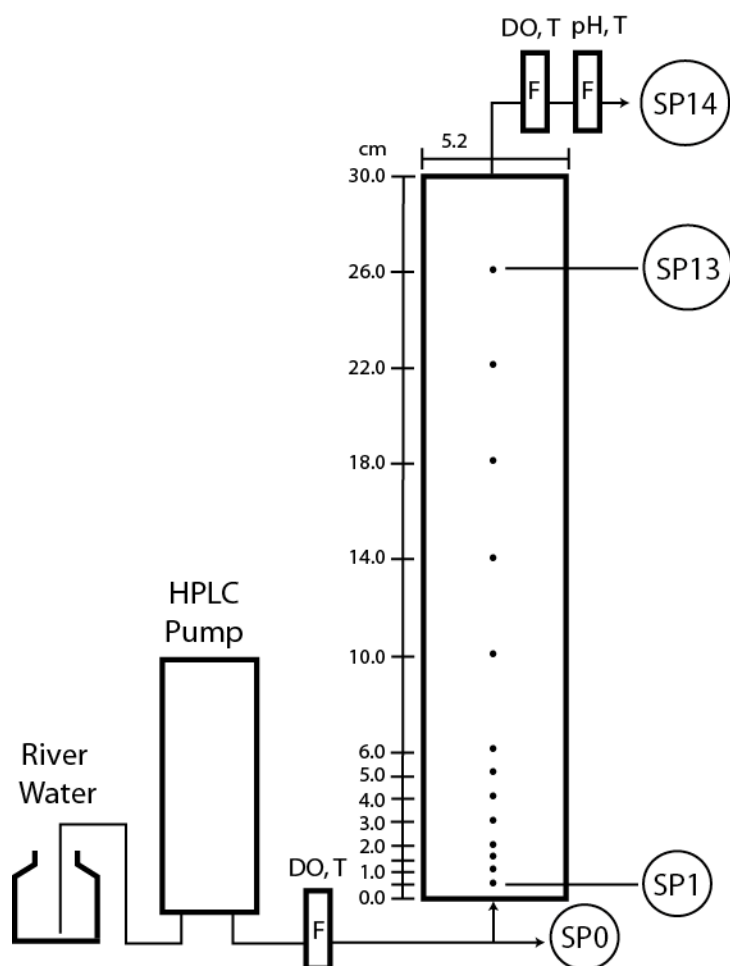


Fig. 2.2. Schematic representation of the set-up of the column experiment with 13 sampling ports along the column (SP1-13) and one at the inlet (SP0) and one at the outlet (SP14). River water was pumped from the bottom to the top of the column. DO, temperature (T) and pH were measured in flow-through cells (F).

### 2.2.4 Analytical methods

DOC concentrations were measured with a Shimadzu TOC-V CPH (Shimadzu Corporation, Kyoto, Japan). Nitrate and the other major ions were analyzed by means of a Metrohm 761 Compact IC (Metrohm Schweiz AG, Zofingen, Switzerland). Ammonium was measured with a Spectrophotometer Varian Cary 50 Bio (Varian BV, Middelburg, The Netherlands). The POC concentrations in sediment samples were determined by subtracting the inorganic carbon fraction, measured with a CO<sub>2</sub> Coulometer CM5015 (UIC Inc., Joilet, USA), from the total carbon fraction, measured with a CNS analyzer Eurovector EA3000 (Hekatech GmbH, Wegberg, Germany).

## 2.3 Results and Discussion

### 2.3.1 Hydraulic conditions and concentration profiles of redox-active compounds

The winter and the summer sampling campaigns were conducted during low-flow conditions. The daily mean discharge of the Thur River during the field sampling campaigns varied between 13.7 and 24.8 m<sup>3</sup>/s in summer and between 5.4 and 6.1 m<sup>3</sup>/s in winter (Fig. 2.3). The daily mean temperatures in the river ranged from 20.9 to 22.9°C in summer and from 5.9 to 6.7°C in winter (Fig. 2.3).

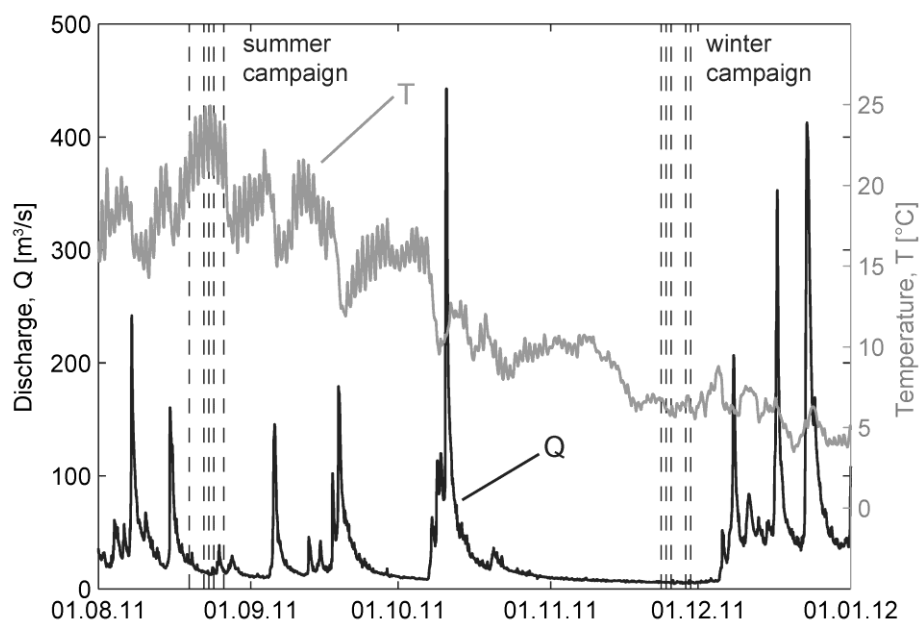


Fig. 2.3. Discharge (black line) and temperature (gray line) time series measured at the FOEN gauging station in Andelfingen covering the two detailed summer and winter sampling

campaigns (August 19-26, 2011 and November 23-29, 2011). Each of the sampling days is shown as a dashed vertical line.

The groundwater residence times between the river and the piezometers were estimated based on a groundwater flow model as well as the analysis of EC time series (Diem et al., 2013) and ranged from 0.5 d at the piezometer closest to the river (R050) to 13 d at the piezometer furthest from the river (R023) (Fig. 2.1c, Fig. 2.4). As the mean residence time in the column was 0.5 d, the column well represented the situation at piezometer R050. The column experiments additionally allowed resolving the microbially-mediated redox processes on a scale that was not accessible in the field system.

The temperature and the concentration profiles of selected redox-active compounds are shown in Fig. 2.4 for the sampling campaigns and in Fig. 2.5 for the column experiments. Most of the DO and DOM consumption in the field occurred between the river and the first piezometer (R050), both during summer and winter conditions. This observation indicates that most of the degradation processes took place within the first meters of the infiltration zone and shows that, in agreement with other studies (Bourg and Bertin, 1993; Brugger et al., 2001a; Sobczak and Findlay, 2002), the microbial activity was highest in this zone. For the piezometers further away from the river, an additional decrease in DO and DOC was observed in winter. However, considering the longer travel times to these piezometers, the corresponding degradation processes occurred much slower.

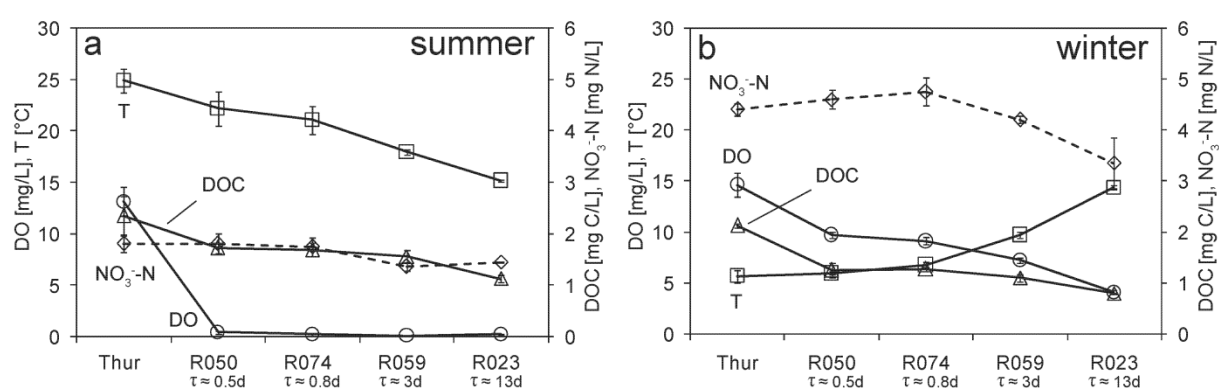


Fig. 2.4. Temperature and concentration profiles of DO, DOC and nitrate during (a) the summer and (b) the winter campaign. Mean and standard deviations are shown as symbols and error bars, respectively ( $n=5$ ). Estimated groundwater residence times ( $\tau$ ) between the river and the piezometers are also indicated.



The DO concentration profiles for the column experiments revealed that the highest DO consumption rate occurred between the first two sampling ports. This is in accordance with other column experiments, for which the highest DO consumption rate was observed within the first centimeter of the column (von Gunten and Zobrist, 1993; von Gunten et al., 1994). At 20°C, the initial decrease of DO was followed by a linear decrease in the column, while at 5°C the DO concentration remained constant after the initial decrease (Fig. 2.5a). The linear decrease at 20°C suggests a zero-order degradation rate, which means that the DO consumption in the column was not limited by the substrates DO and NOM. The DO profile of the control experiment (performed after the 5°C experiment) was almost identical to the DO profile of the first experiment at 20°C (Fig. S2.3, supporting information). This indicates that the column properties decisive for the bacterial degradation processes did not change during the operation period at 5°C.

We consider aerobic respiration of NOM as the only process responsible for the consumption of DO. Based on measured ammonium concentrations in river water, nitrification (oxidation of ammonium) potentially accounted for  $\leq 2\%$  of the DO consumption in the field campaigns and the column experiments, and can therefore be neglected. The removal of DOM during river infiltration might be attributed to both microbial degradation and abiotic sorption processes (Brugger et al., 2001b). However, the summer and winter field sampling campaigns were conducted during relatively stable temperature and discharge conditions. It is therefore reasonable to assume that the sorption processes were in steady state and did not affect the removal of DOM. The same is true for the column system, which was equilibrated for  $\geq 20$  d before the measurements were taken. Therefore, we assume that microbial degradation processes dominated the abiotic sorption processes, which is in agreement with Sobczak and Findlay (2002).

The DO consumption between the river and the first piezometer (R050) was larger in summer than in winter and that between the column inlet and column outlet was larger at 20 than at 5°C. This is a clear indication of the temperature dependence of the microbially mediated degradation of NOM by aerobic respiration. In contrast, the consumption of DOM was similar during summer and winter conditions with about 0.7 mg C/L (Fig. 2.4) during the field sampling campaigns and about 0.3 mg C/L (Fig. 2.5) in the column experiments. Furthermore, the DOM was not consumed completely, both during the field sampling campaigns and in the column experiments. Only a fraction of about 30-50% of the total DOM was degraded, corresponding to the biodegradable DOM (BDOM). Similar values for the

BDOM fraction were reported in several field studies (Sobczak and Findlay, 2002; Sharma et al., 2012). 50-70% of the DOM remained, presumably due to its recalcitrant nature.

During summer conditions, DO was nearly completely consumed at the first piezometer R050 (Fig. 2.4). Similarly, almost anoxic conditions were observed at the column outlet at 20°C (Fig. 2.5). However, denitrification was not observed either in the field, or in the column. Apparently, under summer conditions, there is enough nitrate available to act as a redox buffer preventing Mn(IV)- and Fe(III)-reducing conditions in the infiltration system.

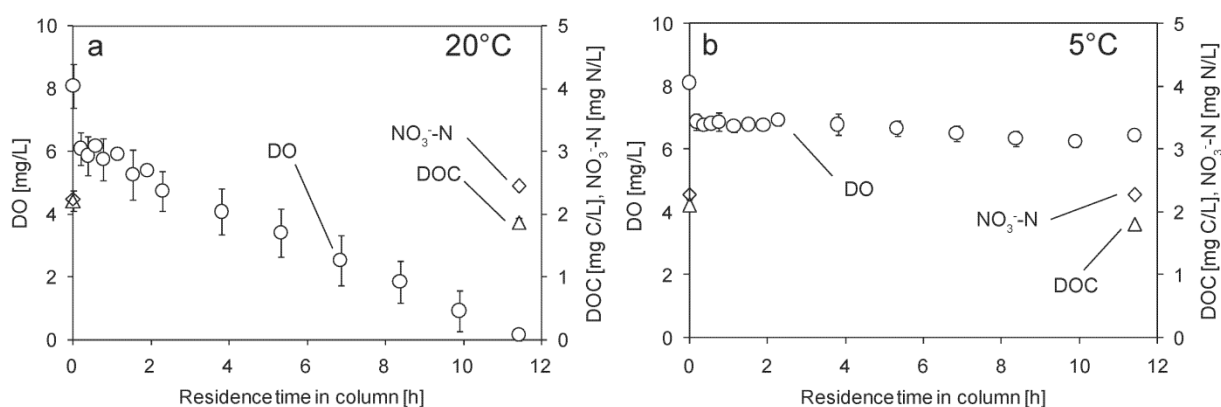


Fig. 2.5. Concentration profiles of DO, DOC and nitrate in the column at (a) 20°C and (b) 5°C. Each symbol represents a sampling port. The first data point corresponds to the sampling port at the inlet of the column (SP0), the last data point to the sampling port at the outlet of the column (SP14). Mean and standard deviations are shown as symbols and error bars, respectively (n=3).

### 2.3.2 Impact of temperature on DO and DOM consumption

#### *Sampling campaigns and column experiments*

To assess the impact of temperature on the aerobic NOM degradation, we compared the DO and DOM consumption between the river and the first piezometer (R050), and between the column inlet and outlet for summer and winter conditions. The resulting mean DO and DOM consumption for the field campaigns and column experiments are shown in Fig. 2.6. For a simplified version of aerobic respiration, one mole of DO (O<sub>2</sub>) is used to oxidize one mole of organic carbon (CH<sub>2</sub>O) (Eq. 2.1):



Accordingly, if DOM consumption would explain the entire DO consumption, the corresponding molar consumptions should be equal (bars in Fig. 2.6). However, during summer conditions (both in the field and in the column), DOM consumption explained only 10-20% of DO consumption (Fig. 2.6). The remaining 80-90% of the reduction capacity to explain the DO consumption must therefore have been provided by other sources. POM in riverbed sediments and the column sand is an obvious source of additional reduction capacity (Brugger et al., 2001b; Sharma et al., 2012).

As mentioned in section 2.3.1, DO consumption in the field and the column system was much smaller for lower than higher temperatures, while the DOM consumption remained at about the same level (Fig. 2.6) and did not seem to be significantly affected by temperature. As a result, DOM consumption accounted for larger fractions of 50% and 100% of the DO consumption at lower temperatures in the column and the field, respectively. Furthermore, the different behavior during summer and winter conditions suggests that the variability and temperature dependence of DO consumption are determined by the POM, rather than the DOM consumption.

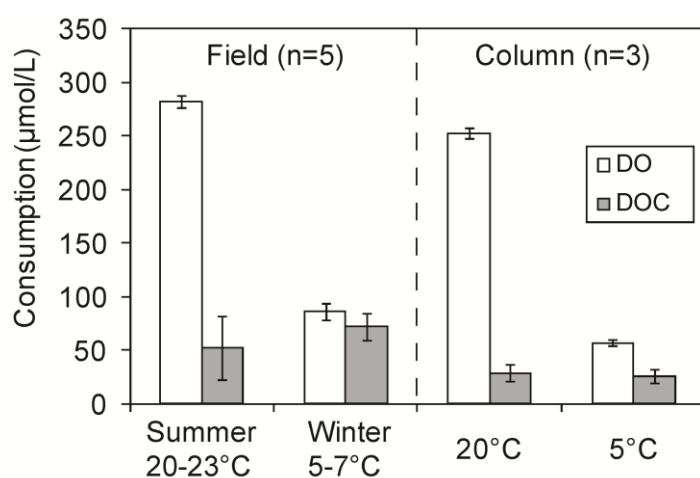


Fig. 2.6. Comparison of DO and DOM (expressed as DOC) consumption for the summer (20-23°C) and winter (5-7°C) field campaigns and for the column experiments at 20 and 5°C, respectively. The consumption refers to the concentration difference between the Thur River and the piezometer R050 in the field and between column inlet and outlet for the column experiments. Standard deviations are shown as error bars.

### *Periodic samplings*

To test the dependence of the DO and DOM consumption on temperature more systematically, we compiled the corresponding data of all the samplings taken between 2008 and 2012 at the

Thur River and the piezometer R050. We additionally calculated the POM consumption according to Eq. 2.2 assuming that the POM consumption corresponds to the difference between DO and DOM consumption:

$$\Delta\text{POC} = \Delta\text{DO} - \Delta\text{DOC} \quad (2.2)$$

Fig. S2.2 (supporting information) shows the DOM and the calculated POM consumption of all the 45 periodic samplings, including the two sampling campaigns of summer and winter 2011. Fig. 2.7 shows a plot of the DO consumption, the DOM consumption and the calculated POM consumption as a function of the daily mean river water temperature in scatter plots together with the calculated correlation coefficients. The DO consumption showed a high and significant correlation ( $r = 0.74$ , Fig. 2.7a) with the daily mean river water temperature. Thus temperature explained the variation in DO consumption to a high degree. However, DOM consumption was not correlated with river water temperature (Fig. 2.7b). This result coincides with the data shown in Fig. 2.6 and is in agreement with findings from Brugger et al. (2001b). Since the calculated POM consumption (Fig. 2.7c) is based on the difference between one highly-correlated parameter (DO consumption) and one uncorrelated parameter (DOM consumption), it is necessarily the case that POM consumption will also be highly correlated with temperature ( $r = 0.7$ ).

This result supports the conjecture that the POM consumption is primarily responsible for the variability and temperature dependence of DO consumption, as stated in section 2.3.2. The divergence between the temperature dependencies observed for DO and DOM consumption also have the consequence that DOM consumption accounts for a larger proportion of DO consumption at lower than at higher temperatures. At lower temperatures ( $<10^{\circ}\text{C}$ ), DOM consumption accounted for 50-100% of DO consumption, while at high temperatures ( $>15^{\circ}\text{C}$ ), DOM consumption accounted for 0-40% of DO consumption (Fig. 2.7). Correspondingly, the calculated POM consumption makes a more important contribution at high temperatures, suggesting that POM is the most important electron donor under these conditions.

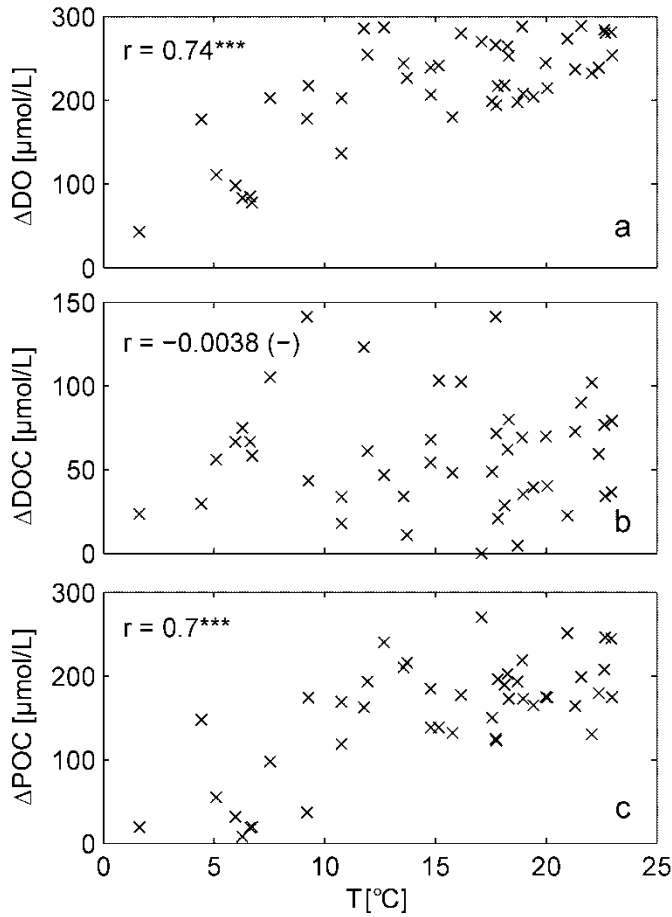


Fig. 2.7. Scatter plots between (a) DO consumption ( $\Delta\text{DO}$ ), (b) DOM consumption ( $\Delta\text{DOC}$ ), (c) calculated POM consumption ( $\Delta\text{POC} = \Delta\text{DO} - \Delta\text{DOC}$ ) at the piezometer R050, and daily mean river water temperature ( $T$ ).  $r$  is the correlation coefficient between two variables with the significance levels:  $*** = p < 0.001$ ,  $** = p < 0.01$ ,  $* = p < 0.05$ ,  $(-) = p > 0.05$ .  $p$  is the probability of two variables being uncorrelated.

### Conceptual explanation

The fact that no correlation was observed between DOM consumption and temperature does not mean that this process is not temperature dependent. One conceptual explanation is based on the fact that consumption of the biodegradable fraction of DOM (BDOM) occurs generally at high degradation rates as it is present in a dissolved and bioavailable form. Even though the BDOM degradation rates might be lower at lower temperatures, bacteria most likely were able to completely consume the full BDOM fraction within the residence times of our field and column systems. Accordingly, on our scales of observation, the DOM consumption was limited by the amount of BDOM rather than by temperature-dependent rates. In contrast, POM consumption involves the cleavage of organic macromolecules into soluble monomers by extracellular hydrolytic enzymes (Egli, 1995; Pusch et al., 1998). Therefore, degradation of

POM generally occurs at lower rates than degradation of BDOM (Greskowiak et al., 2006; Sharma et al., 2012) and the temperature dependence of POM degradation could be resolved on the timescales of our experimental systems (field, column).

This conceptual explanation is based on the assumption that DOM resulting from hydrolysis of POM in bacterial biofilms does not contribute significantly to the DOM pool in the sampled groundwater, and hence did not affect the observed DOM consumption (Fig. 2.7b). In literature, the hydrolysis of POM is considered to be the rate-limiting step in POM degradation, which implies that the DOM resulting from hydrolysis undergoes fast biodegradation (Valentini et al., 1997; Henze et al., 1999; Vavilin et al., 2008). Furthermore, there is evidence that DOM uptake and transformation by bacteria is very efficient in biofilms (Pusch et al., 1998). Bacterial biofilms in sediments act thus as effective sinks of DOM that originated either from the river (as „transported/mobile substrate“) or from the hydrolysis of POM („stationary substrate“).

### **2.3.3 Impact of discharge on DO and DOM consumption**

The temperature dependence of DO consumption might be superimposed by a dependence on hydrologic conditions. High-discharge conditions or flood events are generally not considered to affect the redox conditions in the infiltration zone (Sprenger et al., 2011), but rather to increase the risk of a breakthrough of contaminants or pathogens at the pumping well due to shorter groundwater residence times (Schubert, 2002). However, it is well known that the suspended POM concentration in the river increases with river discharge, as a result of an increased mobilization of allochthonous and autochthonous POM (Meybeck, 1982). The contribution of periphyton (autochthonous POM) to the suspended POM pool in a river was found to positively correlate with discharge, because of the increased abrasive action at the riverbed (Uehlinger, 2006; Akamatsu et al., 2011). Furthermore, it has been observed that the POM import into gravelly riverbed sediments mostly occurred during flood events, which increased the POM concentrations and the microbial respiration rate in the riverbed sediments (Naegeli et al., 1995; Brunke and Gonser, 1997). Hence, the higher POM availability in the riverbed during high-discharge conditions might give rise to an increased DO consumption during river infiltration.

The overall correlation between DO consumption and the daily mean discharge (measured in Andelfingen) was small and not significant (Table S2.3, supporting information). However, DO consumption increased with increasing discharge up to 60 m<sup>3</sup>/s and leveled off at 200-300 µmol/L beyond this point (Fig. 2.8). As the data for discharges below 60 m<sup>3</sup>/s covered

a wide range of temperatures, DO consumption showed only a weak correlation with discharge ( $r = 0.31$ ). To compensate for the temperature dependence, we defined two temperature ranges,  $T < 15^\circ\text{C}$  (circles) and  $T > 15^\circ\text{C}$  (triangles). Following this separation, we found a significant correlation between DO consumption and discharge for the low-temperature range ( $r = 0.85$ ). DOM consumption was not correlated with discharge (Table S2.3, supporting information) suggesting that the increase in DO consumption is probably caused by an enhanced POM consumption, which supports the notion described above.

For the high-temperature range, the correlation between DO consumption and discharge was small and not significant. This result can be explained by the fact that DO consumption for the high-temperature range was already high (200-300  $\mu\text{mol/L}$ ) and nearly complete at low discharges. Hence, an increase in discharge could not lead to a significant increase in DO consumption.

Another process that might explain the increased DO consumption at higher discharges is the leaching of DOM from the soil and vegetation (root zone) at high groundwater tables. At our field site, this effect was found to be restricted to a zone dominated by the pioneer plant *salix viminalis* (willow bush) (Peter et al., 2012). The piezometer R050 was located close to the river, where the gravel-and-sand aquifer is covered by a relatively thin layer of alluvial fines (0.3 m) with no or only little grass vegetation. For this zone, the input of DOM from the soil and vegetation was found to be negligible (Peter et al., 2012).

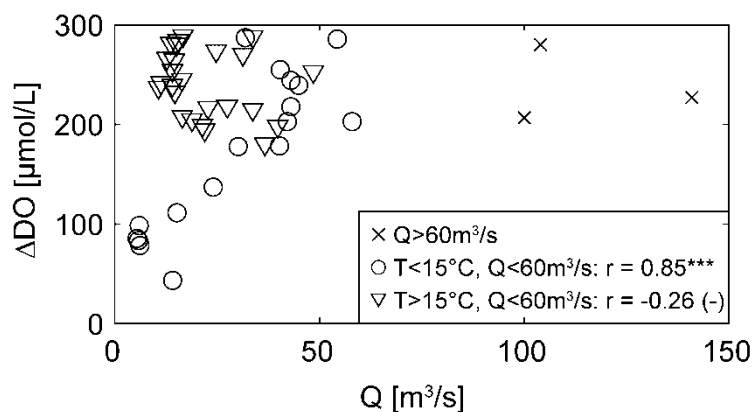


Fig. 2.8. Scatter plot between DO consumption at the piezometer R050 ( $\Delta\text{DO}$ ) and daily mean river discharge ( $Q$ ).  $r$  is the correlation coefficient between the two variables with the significance levels: \*\*\* =  $p < 0.001$ , \*\* =  $p < 0.01$ , \* =  $p < 0.05$ , (-) =  $p > 0.05$ .  $p$  is the probability of two variables being uncorrelated.

Low-discharge conditions are expected to promote the DO consumption as a result of increased groundwater residence times and higher loads of DOM in the river due to less dilution of wastewater effluent (Sprenger et al., 2011). In our observations, however, DO consumption did not reveal a significant increasing trend for decreasing discharges, regardless of the considered temperature range (Fig. 2.8). Furthermore, the DOM consumption did not reveal any significant correlation with discharge, but was positively correlated with DOC concentrations in the river (Table S2.3, supporting information). However, DOC concentrations in the river increased rather than decreased with discharge; the correlation was weak but significant. This suggests DOM sources other than wastewater treatment plants.

### **2.3.4 Implications for groundwater quality at riverbank-filtration systems**

The latest climate change scenarios predict an increase in summer and winter air temperature of 4-5 K for NE-Switzerland by 2085. Furthermore, extreme events, such as summer heat waves, are expected to occur with a higher frequency and intensity (CH2011, 2011). River discharges are expected to decrease in summer and increase in winter. River water temperature, which is decisive for the degradation processes in the riverbed, is likely to increase by the same extent as air temperature, especially during low-flow conditions (FOEN, 2012). During the hot summer of 2003, the mean river water temperature of the Thur River was 22°C for a period of 70-80 d. In the future, we might have to deal more frequently with extreme events of similar or longer duration and even higher mean river water temperatures.

According to our results, the calculated POM consumption showed a pronounced temperature dependence and accounted for most of the DO consumption during summer. Consumption of DO was enhanced during high-flow conditions, probably due to an increased import of POM into the riverbed. On our scales of observation, we could not identify any temperature dependence of the DOM consumption, which was rather limited by the fraction of BDOM. Moreover, the expectation that low-discharge conditions would lead to higher DOC concentrations in the river due to less dilution of wastewater effluents, and hence to an increased DOM and DO consumption during river infiltration, is not supported by our data.

Sprenger et al. (2011) assessed the vulnerability of riverbank-filtration systems to climate change (drought and flood scenarios) with respect to several water quality parameters (DOM, nutrients, pathogens). The vulnerability of a riverbank-filtration system to climate change with respect to the redox milieu in groundwater might depend on three major factors. (1) The hydraulic connection between the river and groundwater. If infiltration occurs through an unsaturated zone, which is aerated, complete DO depletion is not expected (Huggenberger et



al., 1998; Hoehn and Scholtis, 2011). During infiltration in direct hydraulic connection to the groundwater table (saturated), which was the case at our field site, DO is not replenished and might become depleted, as observed during summer. (2) Based on our results, we consider the catchment characteristics as another decisive factor. Rivers in catchments without a retention basin (e.g. a lake) have a more dynamic discharge regime and are likely to have a higher POM load, especially during flood events. (3) The grain-size distribution of the riverbed sediments. In gravelly riverbeds, the import of POM is possible to deeper layers, while in sandy or clogged riverbeds, the import of POM might be physically hindered (Brunke and Gonser, 1997). We therefore anticipate the highest vulnerability to climate change with respect to the redox milieu for riverbank-filtration systems at which infiltration occurs through a gravelly riverbed in direct hydraulic connection to the groundwater table and which are located in catchments without a retention basin.

For such riverbank-filtration systems, we consider future summer heat waves to be critical for the redox-related groundwater quality. A substantial increase in river water temperature during future heat waves will enhance the POM turnover, leading to a complete consumption of DO and potentially nitrate. As a consequence, Mn(II) and Fe(II) could be released, as observed during the hot summer 2003 (Hoehn and Scholtis, 2011). An additional POM input into the riverbed during flood events induces a higher consumption of DO and possibly nitrate, which may enhance the risk for Mn(III/IV)-/Fe(III)-reducing conditions in the infiltration zone.

The subsequent re-oxidation of Mn(II) and Fe(II) and precipitation of Mn(IV)- and Fe(III)(hydr)oxides can lead to clogging problems and deterioration of the drinking water quality (rusty water) at pumping stations of a drinking water supply. For the removal of dissolved Mn(II) and Fe(II), conventional pump-and-treat techniques can be applied, which are based on physical-chemical or biological processes (Mouchet, 1992). Alternatively, in-situ techniques can be used, in which the oxidation processes take place directly in the aquifer (Mettler et al., 2001).

## 2.4 Conclusion

We performed field investigations and laboratory column experiments to investigate the dynamics of redox processes during river infiltration and their dependence on the climate-related variables temperature and discharge. The observations of the summer and winter sampling campaigns in the field could be successfully reproduced by column experiments. Particulate organic matter (POM) was identified as the main electron donor for dissolved

oxygen (DO) consumption during summer conditions and both the DO and the calculated POM consumption revealed a pronounced temperature dependence. The DO consumption was enhanced during flood events, presumably due to an additional POM input into the riverbed.

In our field and column systems, DO was the most important electron acceptor. In summer ( $T > 20^{\circ}\text{C}$ ), DO concentrations in groundwater were close to zero, but denitrification was not observed. Similarly, most of the Swiss aquifers fed by rivers are (sub)oxic under today's summer conditions and nitrate buffers the redox system before it becomes Mn(III/IV)- and Fe(III)-reducing. Therefore, currently there is no need to implement demanganation and deferisation. However, during future summer heat waves, an enhanced availability of POM as electron donor could lead to a full consumption of DO and nitrate, enabling the release of Mn(II) and Fe(II). As the source, quality and quantity of POM and its input into the riverbed are very difficult to assess, it is nearly impossible to find direct intervention strategies.

We recommend long-term monitoring of the redox conditions at riverbank-filtration systems, which are characterized by an infiltration that occurs through a gravelly riverbed in direct hydraulic connection to the groundwater table, and by catchments without a retention basin. Long-term data will allow taking adequate measures in time, while accounting for the site-specific hydrogeological conditions.

## Acknowledgements

This study was accomplished within the National Research Program "Sustainable Water Management" (NRP61) and funded by the Swiss National Science Foundation (SNF, Project No. 406140-125856). We would like to thank Sabrina Bahn Müller, Ryan North, Sebastian Huntscha, Simone Peter and Lena Froyland for their help in the field and the AUA Laboratory, Jacqueline Traber, Sabrina Bahn Müller, Elisabeth Salhi and Irene Brunner for the analytical work. Moreover, we would like to express our gratitude to Eduard Hoehn and Silvio Canonica for helpful discussions. The Federal Office for the Environment (FOEN) provided data of the gauging station in Andelfingen. Additional support was provided by the Competence Center Environment and Sustainability (CCES) of the ETH domain in the framework of the RECORD (Assessment and Modeling of Coupled Ecological and Hydrological Dynamics in the Restored Corridor of a River (Restored Corridor Dynamics)) and RECORD Catchment projects.

## 2.5 References

- Akamatsu, F., Kobayashi, S., Amano, K., Nakanishi, S., Oshima, Y., 2011. Longitudinal and seasonal changes in the origin and quality of transported particulate organic matter along a gravel-bed river. *Hydrobiologia* 669 (1), 183-197.
- Bourg, A.C.M., Bertin, C., 1993. Biogeochemical Processes during the infiltration of River Water into an Alluvial Aquifer. *Environ. Sci. Technol.* 27 (4), 661-666.
- Brugger, A., Reitner, B., Kolar, I., Queric, N., Herndl, G.J., 2001a. Seasonal and spatial distribution of dissolved and particulate organic carbon and bacteria in the bank of an impounding reservoir on the Enns River, Austria. *Freshwater Biol.* 46 (8), 997-1016.
- Brugger, A., Wett, B., Kolar, I., Reitner, B., Herndl, G.J., 2001b. Immobilization and bacterial utilization of dissolved organic carbon entering the riparian zone of the alpine Enns River, Austria. *Aquat. Microb. Ecol.* 24 (2), 129-142.
- Brunke, M., Gonser, T., 1997. The ecological significance of exchange processes between rivers and groundwater. *Freshwater Biol.* 37 (1), 1-33.
- CH2011, 2011. Swiss Climate Change Scenarios CH2011. C2SM, MeteoSwiss, ETH, NCCR Climate and OcCC, Zurich, pp. 88.
- Diem, S., Renard, P., Schirmer, M., 2012. New methods to estimate 2D water level distributions of dynamic rivers. *Ground Water*, doi: 10.1111/gwat.12005.
- Diem, S., Renard, P., Schirmer, M., 2013. Assessing the effect of different river water level interpolation schemes on modeled groundwater residence times. Submitted to *Journal of Hydrology*.
- Eckert, P., Lamberts, R., Wagner, C., 2008. The impact of climate change on drinking water supply by riverbank filtration. *Water Sci. Technol.: Water Supply* 8 (3), 319-324.
- Egli, T., 1995. The ecological and physiological significance of the growth of heterotrophic microorganisms with mixtures of substrates. In: Jones, G.N. (Ed.), *Advances in Microbial Ecology*. Plenum Press, New York, pp. 305-386.
- FOEN, 2012. Effects of climate change on water resources and watercourses. Synthesis report on the “Climate Change and Hydrology in Switzerland” (CCHydro) project. Federal Office for the Environment FOEN, Bern, pp. 76.
- Green, T.R., Taniguchi, M., Kooi, H., Gurdak, J.J., Allen, D.M., Hiscock, K.M., Treidel, H., Aureli, A., 2011. Beneath the surface of global change: Impacts of climate change on groundwater. *J. Hydrol.* 405 (3-4), 532-560.

- Greskowiak, J., Prommer, H., Massmann, G., Nützmann, G., 2006. Modeling seasonal redox dynamics and the corresponding fate of the pharmaceutical residue phenazone during artificial recharge of groundwater. *Environ. Sci. Technol.* 40 (21), 6615-6621.
- Grünheid, S., Amy, G., Jekel, M., 2005. Removal of bulk dissolved organic carbon (DOC) and trace organic compounds by bank filtration and artificial recharge. *Water Res.* 39 (14), 3219-3228.
- Hayashi, M., Vogt, T., Machler, L., Schirmer, M., 2012. Diurnal fluctuations of electrical conductivity in a pre-alpine river: Effects of photosynthesis and groundwater exchange. *J. Hydrol.* 450, 93-104.
- Henze, M., Gujer, W., Mino, T., Matsuo, T., Wentzel, M.C., Marais, G.V.R., Van Loosdrecht, M.C.M., 1999. Activated Sludge Model No.2d, ASM2d. *Water Sci. Technol.* 39 (1), 165-182.
- Hoehn, E., Scholtis, A., 2011. Exchange between a river and groundwater, assessed with hydrochemical data. *Hydrol. Earth Syst. Sc.* 15 (3), 983-988.
- Huggenberger, P., Hoehn, E., Beschta, R., Woessner, W., 1998. Abiotic aspects of channels and floodplains in riparian ecology. *Freshwater Biol.* 40 (3), 407-425.
- Jacobs, L.A., Von Gunten, H.R., Keil, R., Kuslys, M., 1988. Geochemical changes along a river-groundwater infiltration flow path: Glattfelden, Switzerland. *Geochim. Cosmochim. Ac.* 52 (11), 2693-2706.
- Kuehn, W., Mueller, U., 2000. Riverbank filtration - An overview. *J. Am. Water Works Ass.* 92 (12), 60-69.
- Leenheer, J.A., Croue, J.P., 2003. Characterizing aquatic dissolved organic matter. *Environ. Sci. Technol.* 37 (1), 18A-26A.
- Massmann, G., Greskowiak, J., Dünnbier, U., Zuehlke, S., Knappe, A., Pekdeger, A., 2006. The impact of variable temperatures on the redox conditions and the behaviour of pharmaceutical residues during artificial recharge. *J. Hydrol.* 328 (1-2), 141-156.
- Mettler, S., Abdelmoula, M., Hoehn, E., Schoenenberger, R., Weidler, P., von Gunten, U., 2001. Characterization of iron and manganese precipitates from an in situ ground water treatment plant. *Ground Water* 39 (6), 921-930.
- Meybeck, M., 1982. Carbon, nitrogen, and phosphorus transport by world rivers. *Am. J. Sci.* 282 (4), 401-450.
- Mouchet, P., 1992. From conventional to biological removal of iron and manganese in France. *J. Am. Water Works Ass.* 84 (4), 158-167.

- Murdoch, P.S., Baron, J.S., Miller, T.L., 2000. Potential effects of climate change on surface-water quality in North America. *J. Am. Water Resour. As.* 36 (2), 347-366.
- Naegeli, M.W., Hartmann, U., Meyer, E.I., Uehlinger, U., 1995. POM-dynamics and community respiration in the sediments of a floodprone prealpine river (Necker, Switzerland). *Arch. Hydrobiol.* 133 (3), 339-347.
- Park, J.H., Duan, L., Kim, B., Mitchell, M.J., Shibata, H., 2010. Potential effects of climate change and variability on watershed biogeochemical processes and water quality in Northeast Asia. *Environ. Int.* 36 (2), 212-225.
- Peter, S., Koetzsch, S., Traber, J., Bernasconi, S.M., Wehrli, B., Durisch-Kaiser, E., 2012. Intensified organic carbon dynamics in the ground water of a restored riparian zone. *Freshwater Biol.* 57 (8), 1603-1616.
- Pusch, M., Fiebig, D., Brettar, I., Eisenmann, H., Ellis, B.K., Kaplan, L.A., Lock, M.A., Naegeli, M.W., Traunspurger, W., 1998. The role of micro-organisms in the ecological connectivity of running waters. *Freshwater Biol.* 40 (3), 453-495.
- Sacher, F., Brauch, H.J., 2002. Experiences on the fate of organic micropollutants during riverbank filtration. In: Ray, C. (Ed.), *Riverbank filtration: understanding contaminant biogeochemistry and pathogen removal*. Kluwer, Dordrecht, pp. 135-151.
- Schirmer, M., 2013. Das RECORD-Projekt - Flussrevitalisierung, eine ökologische Massnahme in einem komplexen Umfeld. *Aqua und Gas* 3, 22-28.
- Schneider, P., Vogt, T., Schirmer, M., Doetsch, J., Linde, N., Pasquale, N., Perona, P., Cirpka, O.A., 2011. Towards improved instrumentation for assessing river-groundwater interactions in a restored river corridor. *Hydrol. Earth Syst. Sc.* 15 (8), 2531-2549.
- Schubert, J., 2002. Hydraulic aspects of riverbank filtration - Field studies. *J. Hydrol.* 266 (3-4), 145-161.
- Senhorst, H.A.J., Zwolsman, J.J.G., 2005. Climate change and effects on water quality: a first impression. *Water Sci. Technol.* 51 (5), 53-59.
- Sharma, L., Greskowiak, J., Ray, C., Eckert, P., Prommer, H., 2012. Elucidating temperature effects on seasonal variations of biogeochemical turnover rates during riverbank filtration. *J. Hydrol.* 428, 104-115.
- Sobczak, W.V., Findlay, S., 2002. Variation in bioavailability of dissolved organic carbon among stream hyporheic flowpaths. *Ecology* 83 (11), 3194-3209.
- Sprenger, C., Lorenzen, G., Hulshoff, I., Grutmacher, G., Ronghang, M., Pekdeger, A., 2011. Vulnerability of bank filtration systems to climate change. *Sci. Total Environ.* 409 (4), 655-663.

- Toride, N., Leij, F.J., van Genuchten, M.T., 1995. The CXTFIT Code for Estimating Transport Parameters from Laboratory or Field Tracer Experiments, Version 2.0. US Salinity Laboratory, Riverside, CA, pp. 131.
- Tufenkji, N., Ryan, J.N., Elimelech, M., 2002. The promise of bank filtration. *Environ. Sci. Technol.* 36 (21), 422A-428A.
- Uehlinger, U., 2006. Annual cycle and inter-annual variability of gross primary production and ecosystem respiration in a floodprone river during a 15-year period. *Freshwater Biol.* 51 (5), 938-950.
- Valentini, A., Garuti, G., Rozzi, A., Tilche, A., 1997. Anaerobic degradation kinetics of particulate organic matter: A new approach. *Water Sci. Technol.* 36 (6-7), 239-246.
- Vavilin, V.A., Fernandez, B., Palatsi, J., Flotats, X., 2008. Hydrolysis kinetics in anaerobic degradation of particulate organic material: An overview. *Waste Manage.* 28 (6), 939-951.
- von Gunten, H.R., Karametaxas, G., Keil, R., 1994. Chemical Processes in Infiltrated Riverbed Sediments. *Environ. Sci. Technol.* 28 (12), 2087-2093.
- von Gunten, U., Zobrist, J., 1993. Biogeochemical changes in groundwater-infiltration systems: Column studies. *Geochim. Cosmochim. Ac.* 57 (16), 3895-3906.
- Zwolsman, J.J.G., van Bokhoven, A.J., 2007. Impact of summer droughts on water quality of the Rhine River - a preview of climate change? *Water Sci. Technol.* 56 (4), 45-55.

# **Supporting Information for Chapter 2**

## **NOM degradation during river infiltration: Effects of the climate variables temperature and discharge**

3 figures and 3 tables

Reprinted from *Water Research* 47 (17), Diem, S.\*; Rudolf von Rohr, M.\*; Hering, J. G.; Kohler, H.-P. E.; Schirmer, M.; von Gunten, U., NOM degradation during river infiltration: Effects of the climate variables temperature and discharge, 6585–6595. Copyright 2013, with permission from Elsevier.

<http://dx.doi.org/10.1016/j.watres.2013.08.028>

\*Equal contribution of first and second authors

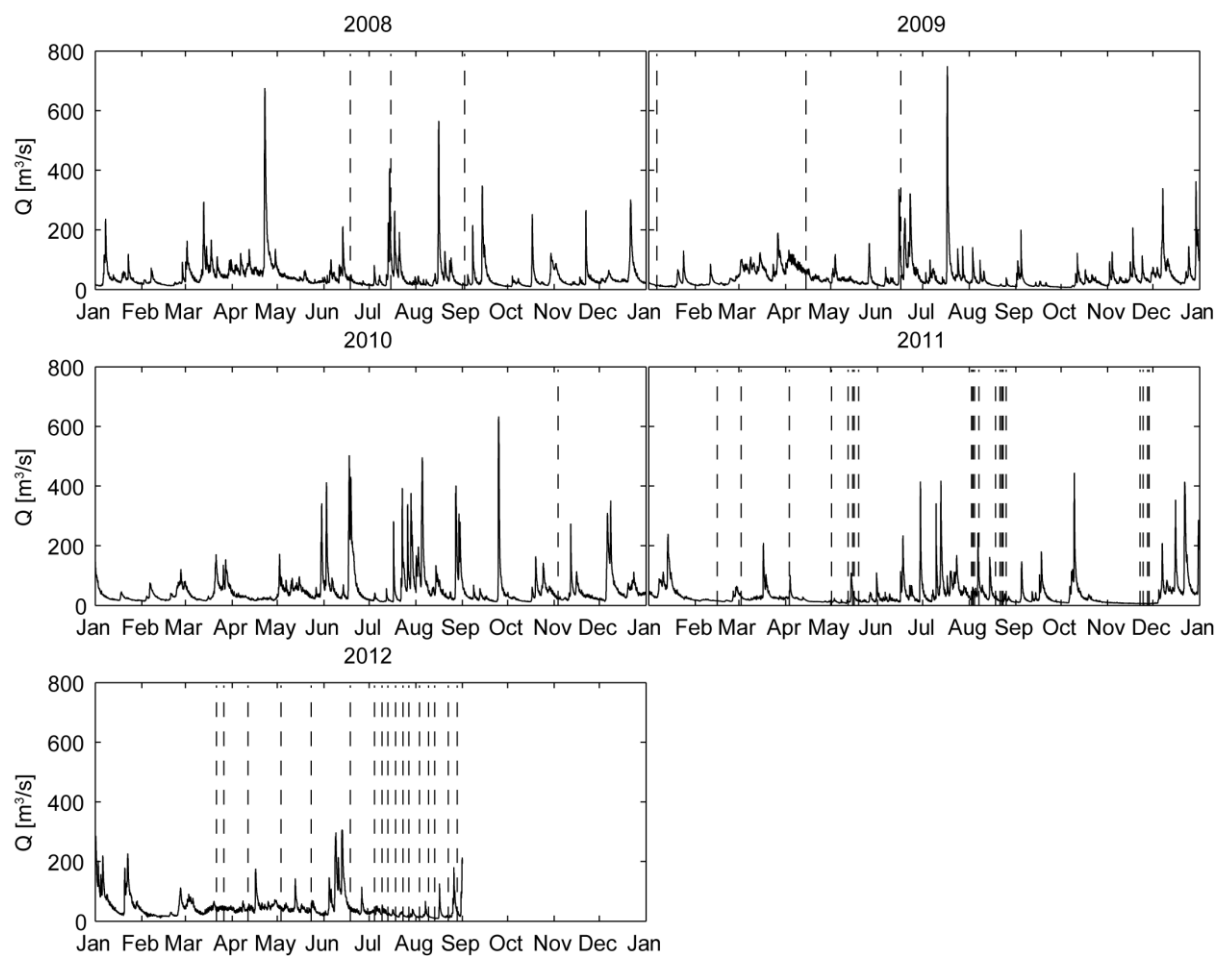


Fig. S2.1. Discharge time series covering all the samples taken at the field site Niederneunforn between 2008 and 2012. Each sampling is shown as vertical dashed line.



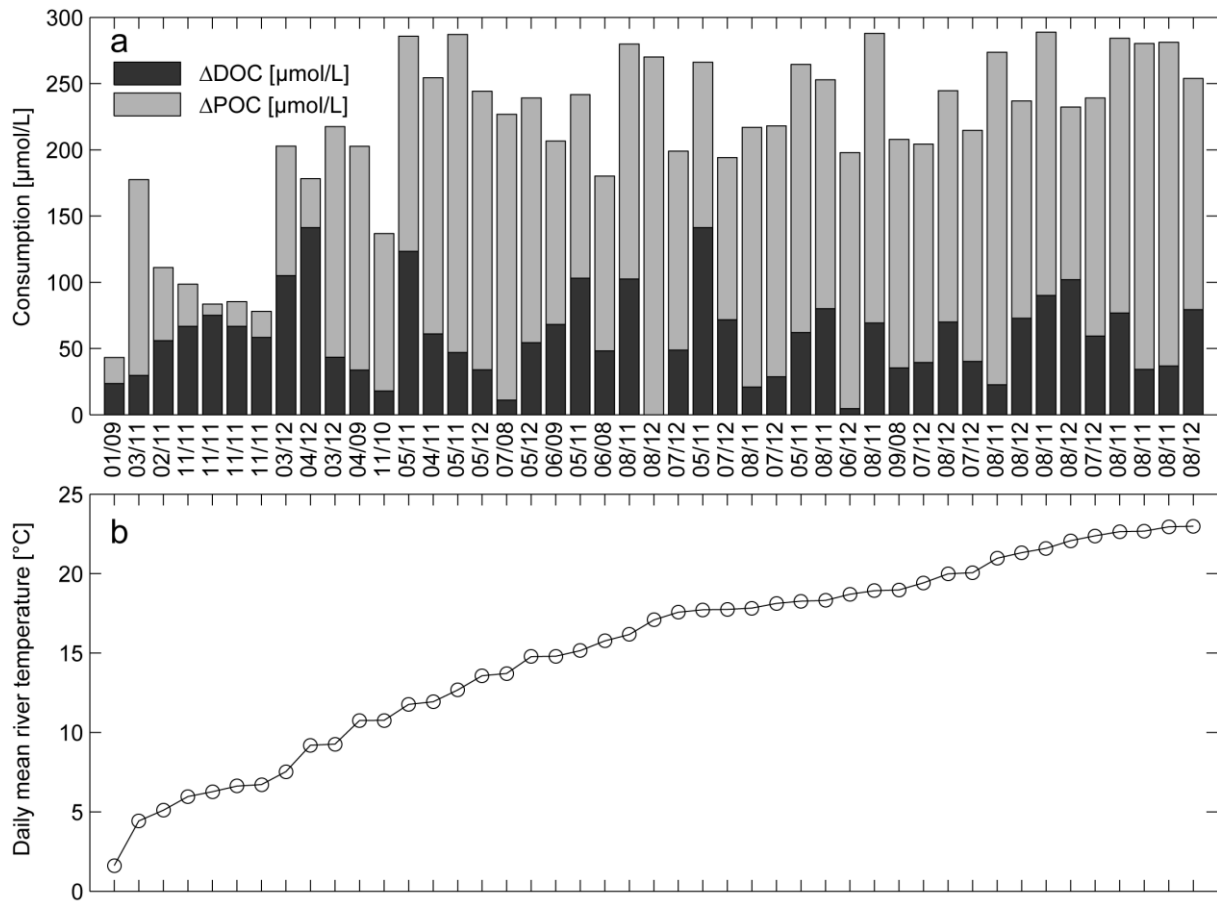


Fig. S2.2. (a) DOM consumption ( $\Delta\text{DOC}$ ) and calculated POM consumption ( $\Delta\text{POC} = \Delta\text{DO} - \Delta\text{DOC}$ ) between the river and the piezometer R050 for the periodic samplings between 2008 and 2012 ( $n=45$ ) including the sampling campaigns of summer and winter 2011. The DO consumption ( $\Delta\text{DO}$ ) corresponds to the sum of the dark and light gray bars. On the x-axis, the month and the year of each sampling are indicated. The data are sorted by increasing daily mean river water temperature, which is shown in (b) for each of the samplings.

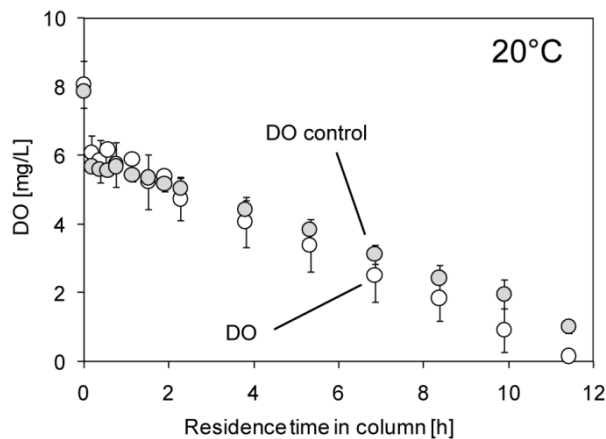


Fig. S2.3. DO concentration profiles in the column measured during the main experiment (white circles) and during the control experiment (gray circles) at 20°C. The control

experiment was conducted after the experiment at 5°C. The mean and the standard deviations are shown as circles and error bars, respectively (n=3).

Table S2.1. Composition 1 of Thur River water used in the column experiments (collected on July 4, 2012).

DOC (mg/L)	pH <sup>a</sup>	El. conductivity <sup>b</sup> (μS/cm)	Alkalinity <sup>c</sup> (mmol/L)	NO <sub>3</sub> <sup>-</sup> (mg N/L)	Na <sup>+</sup> (mg/L)	Ca <sup>2+</sup> (mg/L)	Mg <sup>2+</sup> (mg/L)	PO <sub>4</sub> <sup>2-</sup> <sup>d</sup> (μg P/L)	NH <sub>4</sub> <sup>+</sup> <sup>d</sup> (μg N/L)
2.1	8	407	4.08	2.2	11.9	68.0	12.1	35.5	11.6

<sup>a</sup>measured with a pH meter PHC 301, Hach Lange GmbH, Berlin, Germany

<sup>b</sup>measured with a Metrohm 712 Conductometer, Metrohm Schweiz AG, Zofingen, Switzerland

<sup>c</sup>measured with a Metrohm 809 Titrando, Metrohm Schweiz AG, Zofingen, Switzerland

<sup>d</sup>measured with a Spectrophotometer Varian Cary 50 Bio, Varian BV, Middelburg, The Netherlands

Table S2.2. Composition 2 of Thur River water used in the column experiments (collected on August 13, 2012).

DOC (mg/L)	pH	El. conductivity (μS/cm)	Alkalinity (mmol/L)	NO <sub>3</sub> <sup>-</sup> (mg N/L)	Na <sup>+</sup> (mg/L)	Ca <sup>2+</sup> (mg/L)	Mg <sup>2+</sup> (mg/L)	PO <sub>4</sub> <sup>2-</sup> (μg P/L)	NH <sub>4</sub> <sup>+</sup> (μg N/L)
2.1	8	410	3.83	2.1	18.2	58.9	13.7	14.3	19.0

Table S2.3. Correlation coefficients between the parameters DO consumption ( $\Delta$ DO), DOM consumption ( $\Delta$ DOC), DOC concentration in the river (DOC river), calculated POM consumption ( $\Delta$ POC =  $\Delta$ DO -  $\Delta$ DOC), daily mean river water temperature and daily mean river discharge for the periodic samplings at the piezometer R050 (n=45). Significance levels: \*\*\* =  $p < 0.001$ , \*\* =  $p < 0.01$ , \* =  $p < 0.05$ , (-) =  $p > 0.05$ . p is the probability of two variables being uncorrelated.

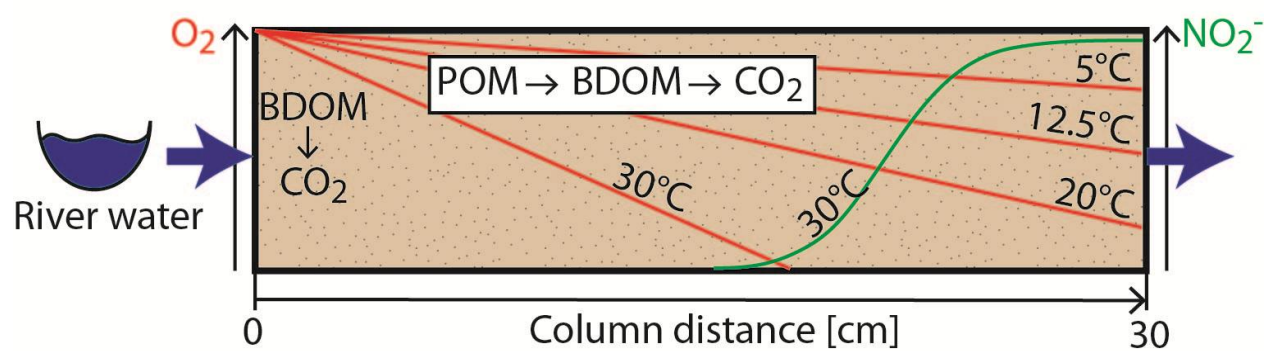
	$\Delta$ DOC	DOC river	$\Delta$ POC	Temperature	Discharge
$\Delta$ DO	0.15 (-)	0.35*	0.87***	0.74***	0.23 (-)
$\Delta$ DOC		0.61***	-0.35*	-0.0038 (-)	-0.066 (-)
DOC river			0.029 (-)	0.14 (-)	0.46**
$\Delta$ POC				0.70***	0.25 (-)

# **Chapter 3**

## **Column studies to assess the effects of climate variables on redox processes during riverbank filtration**

Reprinted from *Water Research* 61, Rudolf von Rohr, M.; Hering, J. G.; Kohler, H.-P. E.; von Gunten, U., Column studies to assess the effects of climate variables on redox processes during riverbank filtration, 263-275. Copyright 2014, with permission from Elsevier.

<http://dx.doi.org/10.1016/j.watres.2014.05.018>



### Graphical Abstract

## Abstract

Riverbank filtration is an established technique used world-wide to produce clean drinking water in a reliable and cost-efficient way. This practice is, however, facing new challenges posed by climate change, as already observed during past heat waves with the local occurrence of anoxic conditions. In this study we investigated the effect of direct (temperature) and indirect (dissolved organic matter (DOM) concentration and composition, flow rate) climate change variables on redox processes (aerobic respiration, denitrification and Mn(III/IV)/Fe(III) reduction) by means of column experiments. Natural river water, modified river water and river water mixed with treated wastewater effluent were used as feed waters for the columns filled with natural sand from a river-infiltration system in Switzerland. Biodegradable dissolved organic matter was mainly removed immediately at the column inlet and particulate organic matter (POM) associated with the natural sand was the main electron donor for aerobic respiration throughout the column. Low infiltration rates ( $\leq 0.01$  m/h) enhanced the oxygen consumption leading to anoxic conditions. DOM consumption did not seem to be sensitive to temperature, although oxygen consumption (i.e., associated with POM degradation) showed a strong temperature dependence with an activation energy of  $\sim 70$  kJmol<sup>-1</sup>. Anoxic conditions developed at 30°C with partial denitrification and formation of nitrite and ammonium. In absence of oxygen and nitrate, Mn(II) was mobilized at 20°C, highlighting the importance of nitrate acting as a redox buffer under anoxic conditions preventing the reductive dissolution of Mn(III/IV)(hydr)oxides. Reductive dissolution of Fe(III)(hydr)oxides was not observed under these conditions.

Keywords: climate change; redox milieu; microbial respiration; effluent; POM; BDOM

### 3.1 Introduction

Several European countries rely on natural or engineered riverbank filtration to produce drinking water, with a contribution of  $< \sim 50\%$  to the total drinking water production in France (Hannappel et al., 2014),  $\sim 16\%$  in Germany (Tufenkji et al., 2002) and  $\sim 25\%$  in Switzerland. During riverbank filtration, river water infiltrates through riverbed sediments into an aquifer, from which it is extracted for drinking water production. The derived groundwater often requires only minimal treatment before distribution, because natural attenuation processes during infiltration efficiently remove particles, microorganisms, natural organic matter (NOM) and partially remove organic contaminants (Kuehn and Mueller, 2000; Grünheid et al., 2005; Schmidt et al., 2007; Scheurer et al., 2012; Storck et al., 2012; Huntscha et al., 2013).

An important criteria for the quality of drinking water derived from riverbank filtration is the redox milieu and the related geochemical processes. The redox milieu is mainly determined by microbial respiration processes (redox processes), in which NOM is the electron donor and oxygen, nitrate, Mn(III/IV)- and Fe(III)(hydr)oxides or sulfate are the electron acceptors. These biogeochemical processes have been extensively studied at riverbank filtration sites (Jacobs et al., 1988; Bourg and Bertin, 1993) and in laboratory column experiments (Matsunaga et al., 1993; von Gunten and Zobrist, 1993). Seasonal changes in the redox milieu, in which anoxic (i.e. oxygen-free) conditions develop and Mn(II) is mobilized in summer and aerobic conditions are maintained in winter, have been ascribed to the temperature dependence of microbial activity (von Gunten et al., 1991; Greskowiak et al., 2006; Massmann et al., 2006).

Besides temperature, the quantity and composition of NOM in river waters also dictate the redox milieu during riverbank filtration, since NOM is an important substrate for microbial respiration (Grünheid et al., 2005; Maeng et al., 2008). Previous studies have focused on dissolved organic matter (DOM) as the main electron donor during riverbank filtration (von Gunten and Zobrist, 1993; Grünheid et al., 2005; Grünheid et al., 2008; Maeng et al., 2008). However, there is evidence that particulate organic matter (POM) in the riverbed sediments may also contribute substantially as a substrate to the consumption of electron acceptors (Grischek et al., 1998; Brugger et al., 2001; Massmann et al., 2006; Diem et al., 2013b).

Furthermore, the hydraulic residence time, which is determined by the infiltration rate, may influence the redox milieu during riverbank filtration. It is assumed that low infiltration rates favor and high infiltration rates inhibit the formation of reducing conditions in the aquifer (Doussan et al., 1997). Drought periods generally tend to bring about anaerobic conditions during summer months as a consequence of long residence times and high temperatures, whereas floods tend to increase the infiltration rate and facilitate the breakthrough of pathogens,

suspended solids and DOM (Sprenger et al., 2011). Moreover, flood events can also lead to an increased oxygen consumption in the infiltration zone, which has been attributed to an increased deposition of POM in this zone under these conditions (Diem et al., 2013b).

All factors that dictate the redox milieu in the riverbank filtration zone may be directly (temperature) or indirectly (NOM quantity and composition in river water, residence time in the infiltration zone) influenced by climate and climate change. By 2085, average summer air temperatures in northern Switzerland are predicted to increase by 4 K and average summer precipitation to decrease by 20% resulting in lower discharges in rivers (CH2011, 2011; FOEN, 2012). The lower river discharges may also lead to lower infiltration rates and thus longer hydraulic residence times in the infiltration zone. In addition, decreasing natural flows will reduce the extent to which effluent organic matter (EfOM) discharged from wastewater treatment plants is diluted and consequently a higher proportion of EfOM in the receiving waters may be expected. Better understanding of the effect of each climate factor on the redox milieu will help to assess future changes in water quality during riverbank filtration.

We hypothesize that the direct and indirect effects of climate change will lead to more frequent occurrence of anoxic conditions in riverbank filtration systems in the future. This could create significant problems for drinking water supplies because of the potentially more frequent occurrence of reduced species, such as nitrite, Mn(II) and Fe(II). Nitrite is a toxic compound for which the WHO guideline is 900 µg N/L (WHO, 2011). When groundwater containing Mn(II) and Fe(II) is exposed to oxygen from the air, the resulting precipitation of Mn(III/IV)- or Fe(III)(hydr)oxides can cause clogging of filter screens and lead to rusty water and aesthetic problems (Mouchet, 1992; Hoehn and Scholtis, 2011).

Here, we assess the effect of direct and indirect climate change variables on redox conditions during riverbank filtration based on column experiments, in which temperature, DOM concentration/composition and flow rate were systematically varied. Moreover, the dynamics of the Mn(II) and Fe(II) mobilization under oxygen- and nitrate-free conditions were investigated.

## 3.2 Materials and Methods

### 3.2.1 Set-up of the column system

Fig. S3.1 shows the set-up of the column system: Filtered Thur River water (0.45  $\mu\text{m}$ , cellulose nitrate, Sartorius AG, Göttingen, Germany) was pumped from the bottom to the top of the column with a HPLC-pump (Jasco PU-2080, Jasco Corporation, Tokyo, Japan). The casing of the column consisted of a Plexiglas tube (length: 30 cm, inner diameter: 5.2 cm). The column was equipped with 13 sampling ports (SP1-13), in addition one was installed before (SP0) and one after (SP14) the column (Fig. S3.1). The column was packed with a dried sand fraction (grain size: 0.125-0.250 mm) sampled at a sand/gravel bar at the Thur River (Diem et al., 2013b). The relatively homogeneous sand fraction 0.125-0.250 mm contained  $0.3 \pm 0.2\%$  (w/w, average of 12 sample aliquots) particulate organic carbon (POC). The filling procedure of the dry sand was conducted in form of a “sand rain”, following von Gunten and Zobrist (1993). X-ray diffraction analysis of the sand showed mainly calcite and quartz (40% and 25%, respectively). Two columns (column I and II) filled with the same sand material were used for the respective experiments under different operational conditions (Section 3.2.2). We assessed the hydraulics in columns I and II by conducting tracer tests with a 8.55 mM NaCl solution. During the tracer tests, the electrical conductivity was measured at the end of the columns and was used for the calculation of the effective porosity and the dispersivity (Table 3.1).

River water was collected at Niederneunforn at a river-infiltration system of the peri-alpine Thur River, NE-Switzerland (Diem et al., 2013b), filtered and used as feed water from a 2 L storage tank (see Table S3.1 for chemical composition of all feed waters). The storage tank was replenished every three days with Thur River water stored at 5°C. For the experiments performed at 12.5°C, 20°C and 30°C, Thur River water was equilibrated to the desired temperature before it was pumped into the columns. No measurable DOM degradation (DOC concentration  $\pm 0.1$  mg C/L) was observed in the storage tank under these conditions.

For varying operational conditions, the profiles of the oxygen concentration were taken for steady-state conditions after an equilibration time of  $\geq 20$  d. Sampling was conducted from the top to the bottom of the column in the opposite direction of the water flow (Fig. S3.1). This procedure enabled sampling of fresh aliquots avoiding sampling from stagnant zones. Oxygen and pH were directly measured at each sampling port in a flow-through cell having a total dead volume of  $\sim 3$  mL (Fig. S3.1). For the analysis of DOC, major cations and anions, a 0.45  $\mu\text{m}$  rinsed regenerated cellulose filter (National Scientific Company, Rockwood, USA) was connected to the port of interest and a  $\sim 40$  mL sample was withdrawn for each sampling event (duration of sampling:  $\sim 40$  minutes at 1 mL/min). Oxygen, pH, DOC and nitrate were measured



between one and three times every 3-5 days (indicated in the figures by “n”, i.e. the number of measurement replicates). For Fe and Mn analysis, a 9 mL sample was acidified to pH 2 with 1 mL of 1 M HCl.

Table 3.1. Hydraulic characteristics of the columns (effective porosity, dispersivity and total pore volume) and sand mass present in the columns. The effective porosity and the dispersivity were calculated with the program CXTFIT (Toride et al., 1995) using the electrical conductivity data.

	Column I	Column II
Effective porosity [-]	0.38	0.32
Dispersivity [cm]	0.1	0.1
Total pore volume [mL]	245	206
Sand mass [g]	885	876

### 3.2.2 Operational conditions of the column experiments

Six different column experiments with varying parameters (feed water, temperature, flow rate) were conducted either with column I or II (Table 3.2). The first experiments for each column (experiment 1.1 for column I and experiment 2.1 for column II, respectively) were initiated after an equilibration time of 2 months feeding Thur River water to reach steady-state conditions for oxygen and DOC.

For experiment 1.1, treated wastewater effluent (herein simply named effluent) from a municipal wastewater treatment plant (Dübendorf Neugut, Switzerland) was first filtered (0.45 µm, cellulose nitrate, Sartorius AG, Göttingen, Germany). The filtered effluent was then electrodialysed (PCCell GmbH, Heusweiler, Germany) to remove nitrate prior to preparing four Thur River water/effluent mixtures to be used as feed waters (Tables S3.1 and S3.2) to study the effect of the type and concentration of DOM on the oxygen consumption.

In experiment 1.2, the effect of the flow rate on the oxygen consumption was investigated. Four flow rates, simulating different infiltration velocities, were chosen: 0.1, 0.2, 0.33 and 1.0 mL/min.

In experiment 2.1, the temperature dependence of the oxygen consumption and NOM degradation was investigated at four temperatures (5, 12.5, 20 and 30°C). While the experiments at 5.0, 12.5 and 20.0°C were carried out with the storage tank at ambient laboratory temperature ( $22 \pm 2^\circ\text{C}$ ), for the 30.0°C experiment the tank had to be placed inside the incubator to prevent outgassing in the HPLC-pump.

In experiment 2.2, unaltered Thur River water was added as feed water and in experiment 2.3, “DOM-free” Thur River water was used as feed water to study the effect of POM on the oxygen consumption. About 96% of the DOM was removed from the Thur River water by addition of 500 mg/L Norit W15 powdered activated carbon (NORIT Deutschland GmbH, Riesbürg, Germany) and filtration through a 0.45 µm filter (cellulose nitrate, Sartorius AG, Göttingen, Germany). DOM removal was achieved without significantly affecting the other water quality parameters (Table S3.3).

In experiment 2.4, a readily available DOM source in form of sodium acetate (6 mg/L or 1.75 mg C/L) was added to the Thur River water inflow immediately before the column inlet (at sampling port SP0) to investigate the effect of easily biodegradable DOM (BDOM) on the oxygen consumption.

In experiment 2.5, the dynamics of the Mn(II) and Fe(II) mobilization under oxygen- and nitrate-free conditions were investigated. Thur River water was electrodialysed to remove nitrate and was re-mineralized thereafter to obtain a similar water composition as the original river water with respect to the alkalinity and the major cations and anions (Table S3.4). To remove oxygen from the feed water, it was continuously purged with a N<sub>2</sub>/CO<sub>2</sub> gas mixture (99.96% N<sub>2</sub> / 0.04% CO<sub>2</sub>) leading to an oxygen concentration below 0.1 mg/L at SP0.

All column experiments except 1.1 and 1.2 were conducted in an incubator ( $\pm 1^\circ\text{C}$ ). Column experiment 1.1 was carried out at ambient laboratory temperature ( $22 \pm 2^\circ\text{C}$ ) and experiment 1.2 in a climatised chamber ( $20 \pm 1^\circ\text{C}$ ). Column I was operated aerobically (experiments 1.1 and 1.2), whereas column II was first operated aerobically for 327 days (experiments 2.1, 2.2, 2.3 and 2.4) and then anaerobically for 66 days (experiment 2.5).

Table 3.2. Operational conditions of all column experiments, which are listed in a chronological order for columns I (1.1, 1.2) and II (2.1-2.5). Experiments 1.2, 2.1 and 2.2 were conducted with unaltered Thur River water as feed water.

Experiment	Flow rate [mL/min] ([m/h])	Residence time [h]	Temperature [°C]	Column
(1.1) Thur River water/effluent mixtures <sup>a</sup>	1.0 (0.07)	4	22	I
(1.2) Variation of flow rate	0.1 (0.007), 0.2 (0.01)	40, 20	20	I
	0.33 (0.02), 1.0 (0.07)	12, 4		
(2.1) Variation of temperature	0.3 (0.03)	11.5	5, 12.5, 20, 30	II
(2.2) Thur River water	0.3 (0.03)	11.5	20	II
(2.3) Addition of “DOM-free” Thur River water	0.3 (0.03)	11.5	20	II
(2.4) Addition of acetate	1.0 (0.09)	3.5	20	II
(2.5) Addition of oxygen- and nitrate-free Thur River water	0.3 (0.03)	11.5	20	II

<sup>a</sup> 90/10, 80/20, 70/30, 60/40%

### 3.2.3 Analytical methods

Oxygen and temperature were measured with an optical sensor LDO101 (Hach Lange GmbH, Berlin, Germany, limit of quantification 0.1 mg/L, accuracy  $\pm 0.1$  mg/L,  $T \pm 0.3$  K), pH was measured with a pH electrode PHC 301 (Hach Lange GmbH, Berlin, Germany, accuracy pH  $\pm 0.1$ ). DOC was taken as a measure for DOM and was determined by catalytic combustion at 720°C with a Shimadzu TOC-V CPH analyzer (Shimadzu Corporation, Kyoto, Japan). The limit of quantification was 0.1 mg C/L and the error of measurement  $\pm 0.1$  mg C/L. The alkalinity was determined with a Metrohm 809 Titrando (Metrohm Schweiz AG, Zofingen, Switzerland).  $\text{NO}_2^-$  and  $\text{NH}_4^+$  were analyzed photometrically with a spectrophotometer Cary 100 Scan Spectrophotometer (Varian AG, Zug, Switzerland) following the norms EN 26777 (DIN, 1993) and DIN 38406 (DIN, 1983a), respectively. The limit of quantification was 0.01 mg N/L and the error of measurement  $\pm 0.002$  mg N/L for both compounds.  $\text{PO}_4^{3-}$  was measured with a spectrophotometer Varian Cary 50 Bio (Varian AG, Zug, Switzerland) according to Vogler (1965).  $\text{NO}_3^-$ ,  $\text{Cl}^-$ ,  $\text{SO}_4^{2-}$ ,  $\text{Na}^+$ ,  $\text{K}^+$ ,  $\text{Ca}^{2+}$  and  $\text{Mg}^{2+}$  were analyzed with a Metrohm 761 Compact IC (Metrohm Schweiz AG, Zofingen, Switzerland) using a “Metrohm Metrosep A Supp 5 100/4 mm” column for the anions and a “Metrohm Cation 1-2 125/4 mm” column for the cations. For  $\text{NO}_3^-$ , the limit of quantification was 0.25 mg N/L and the error of measurement  $\pm 0.1$  mg N/L.  $\text{NO}_3^-$  concentrations  $<0.25$  mg N/L (i.e. for the preparation of the oxygen- and nitrate-free Thur River water, experiment 2.5), were measured with a spectrophotometer Varian

Cary 50 Bio (Varian AG, Zug, Switzerland) according to Müller and Widemann (1955). Here, the limit of quantification was 0.1 mg N/L and the error of measurement  $\pm 0.02$  mg N/L. Fe and Mn were measured with inductively coupled plasma atomic emission spectroscopy (ICP-OES) as total Fe and total Mn concentrations, respectively (SPECTRO Analytical Instruments GmbH, Kleve, Germany). The limit of quantification was 0.1  $\mu\text{g/L}$  and the error of measurement  $\pm 0.1$   $\mu\text{g/L}$ . It could be shown that total Mn corresponded to Mn(II) measured colorimetrically (DIN, 1983b).

The POC concentration of the column sand representing POM was determined by subtracting the content of inorganic carbon, measured with a  $\text{CO}_2$  Coulometer CM5015 (UIC Inc., Joilet, USA), from the total carbon, measured with a CNS analyzer Eurovector EA3000 (Hekatech GmbH, Wegberg, Germany).

A closed bottle biological oxygen demand (BOD) test of the natural sand was conducted by BMG Engineering Ltd., Schlieren, Switzerland as a batch experiment by incubating the sand (3.2 g/L) with an inoculum of a secondary effluent from a municipal wastewater treatment plant at 22°C and measuring the decrease in the oxygen concentration (OECD, 1992). Five batch experiments with different duration were conducted (5, 7, 14, 21 and 28 days). Each batch experiment was done in duplicate (indicated by “n=2”).

The protein content of the pristine sand and of the sand samples from column II was measured according to the bicinchoninic acid method using an assay-kit of Sigma-Aldrich (Smith et al., 1985) after protein extraction with 1 M NaOH at 95°C for 30 minutes (Herbert et al., 1971). Three samples were withdrawn from column II for each sampling port of interest (indicated by “n=3”) after 393 days of operation (i.e., at the end of experiment 2.5). The pristine sand was washed with nanopure water before protein measurements to determine the blank protein content.

The quantification of the reactive pool of Mn(III/IV)(hydr)oxides of the pristine and of the column II sand was conducted at the end of experiment 2.5 with a buffered ascorbate solution according to Hyacinthe et al. (2006). Samples were withdrawn from column II at SP1, SP5, SP8, SP11 and SP13 using a specially designed “sand scoop”. 2.6 g of each sample was mixed with a 150 mL solution consisting of sodium citrate (50 g/L), sodium bicarbonate (50 g/L) and L(+) ascorbic acid (20 g/L) (pH 7.1), which was continuously purged with  $\text{N}_2$ . The experiment was conducted for 2.5 hours and samples were taken after 0.5, 1, and 2.5 hours for ICP-OES analysis.

### 3.2.4 Calculation of manganese concentration in equilibrium with $\text{MnCO}_3$

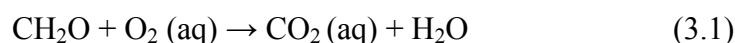
The  $\text{Mn}^{2+}$  concentration in equilibrium with  $\text{MnCO}_3$  was calculated based on the solubility product of rhodochrosite ( $\text{MnCO}_3$ ) ( $\text{Mn}^{2+} + \text{CO}_3^{2-} = \text{MnCO}_3$ ;  $\log K = -10.39$  (Stumm and Morgan, 1996)) and on the  $\text{CO}_3^{2-}$  concentration of  $3.34 \times 10^{-5}$  M. The latter value was calculated from the measured concentration of  $\text{HCO}_3^-$  and pH (8.2) in the column during experiment 2.5. The total Mn(II) concentration was then derived by inserting the calculated  $\text{Mn}^{2+}$  equilibrium concentration, the measured calcium and  $\text{HCO}_3^-$  concentrations and the pH in the chemical equilibrium modeling program ChemEQL V3.0 (Mueller, 2004). The resulting Mn(II) speciation is shown in Table S3.5. The sum of all relevant Mn(II) species is shown as equilibrium concentration (Fig. S3.2 (dashed line)).

## 3.3 Results and Discussion

### 3.3.1 Effect of indirect climate change variables on redox processes

#### *Oxygen and pH profiles*

We investigated the effects of increasing DOC concentration and altered DOM composition on redox processes by utilizing varying mixtures of Thur River water and effluent (experiment 1.1), “DOM-free” Thur River water (experiment 2.3) and Thur River water amended with acetate (experiment 2.4) as feed waters. All oxygen profiles showed a fast initial decrease of the relative oxygen concentration, which is discussed later, followed by a slower decrease between SP1 and SP14 (Fig. 3.1a). The residence times in Fig. 3.1a and 3.1b were calculated by dividing the pore volume at a specific sampling port by the flow rate of the respective experiment. The pH dropped in parallel to the fast initial oxygen drop close to the inlet and showed a slower decrease thereafter (Fig. 3.1b). Both the oxygen and pH profiles can be explained by aerobic respiration (Eq. 3.1). The decrease of the pH, which was caused by formation of  $\text{CO}_2$ , was only partially prevented by the buffering capacity of calcium/magnesium carbonates.



In Eq. 3.1,  $\text{CH}_2\text{O}$  represents DOM with carbon in a zero-valent oxidation state.

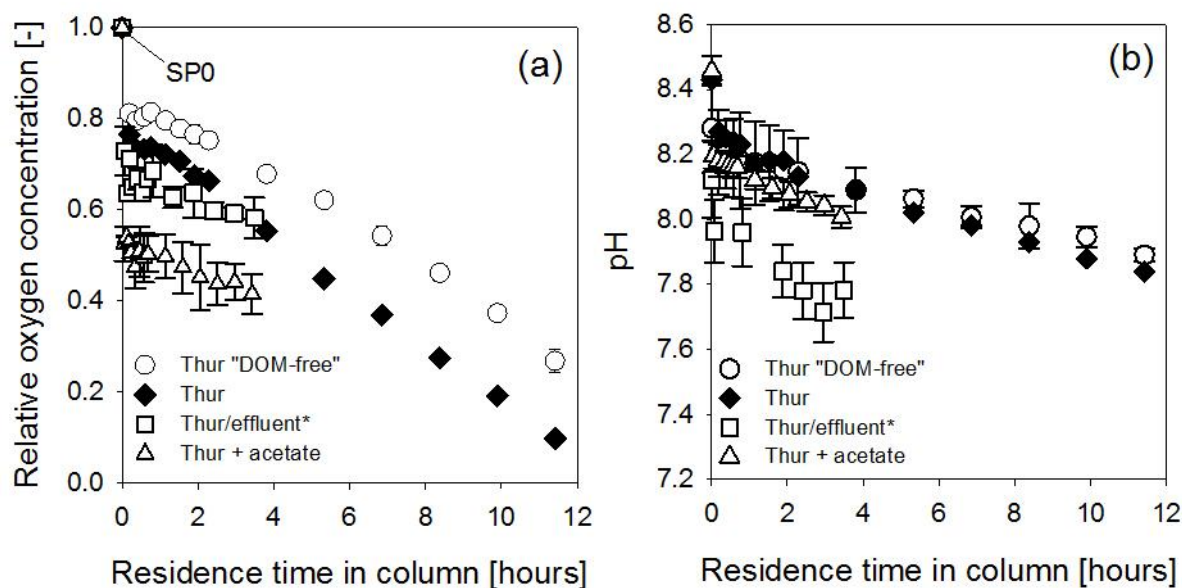


Fig. 3.1. (a) Profiles of the relative oxygen concentration (normalized to the values at SP0) and (b) pH for “DOM-free” Thur River water (n=3) (○), Thur River water (n=1) (◆), Thur River water/effluent mixtures (\*average of four mixtures: 90/10, 80/20, 70/30, 60/40%) (□) and Thur River water amended with 1.75 mg C/L sodium acetate (n=3) (△). The first data point corresponds to the sampling port at the inlet (SP0), the last data point to the sampling port at the outlet of the column (SP14) for each experiment. Mean values and standard deviations are shown as symbols and error bars, respectively.

#### *Role of wastewater effluent and particulate organic matter (POM)*

The addition of effluent of up to 40% (experiment 1.1) did not enhance the oxygen consumption in the column (Fig. 3.1a) even though the DOC concentration was increased by up to 1.4 mg C/L compared with the unamended (experiment 2.2) Thur River water (see Table S3.1). The profile of the relative oxygen concentration of the “DOM-free” Thur River water (experiment 2.3) showed a similar decreasing trend between SP1 and SP14 as the original Thur River water (Fig. 3.1a). This means that the oxygen consumption did not depend on the presence of DOM in the feed water. Thur River water contains mostly humic compounds that are rather persistent (Peter et al., 2012). However, other river waters might contain significantly higher concentrations of biodegradable DOM, which could affect the oxygen consumption during riverbank filtration.

Based on our results, we hypothesize that the electron donor is associated with the sand matrix and consists of particulate organic matter (POM). Our results are in line with previous

column studies conducted with river water (DOC concentration of 15 mg C/L) and a river water/effluent mixture (50% effluent, DOC concentration of 17 mg C/L) showing no enhanced oxygen consumption with the addition of a river water/effluent mixture (Maeng et al., 2008). Furthermore, it has been suggested in field investigations that POM is likely to act as an important electron donor during riverbank filtration (Grischek et al., 1998; Brugger et al., 2001; Massmann et al., 2006; Kedziorek et al., 2008; Diem et al., 2013b). These previous studies have based their conclusions on mass balance calculations of experimental field data. Here, we provide independent evidence from controlled laboratory experiments to support these field observations.

To investigate the role of POM associated with the sand as a support for aerobic respiration in the column, a biological oxygen demand (BOD) test of the pristine sand was conducted. Fig. 3.2 shows the BOD of the sand determined after 5, 7, 14, 21 and 28 days. Even after 28 days, the BOD had not reached a plateau; the maximum observed value was  $\sim 9 \times 10^{-4}$  mg O<sub>2</sub>/mg sand corresponding to a total BOD of at least 800 mg O<sub>2</sub> for the entire sand columns. If we consider that 7 mg/L oxygen was consumed on average in the column with the original Thur River water as feed water based on oxygen saturation conditions at SP0 (Fig. 3.1a), then  $\sim 3$  mg O<sub>2</sub> will be consumed per day. The available POM could therefore sustain aerobic respiration for at least 260 days without being exhausted.

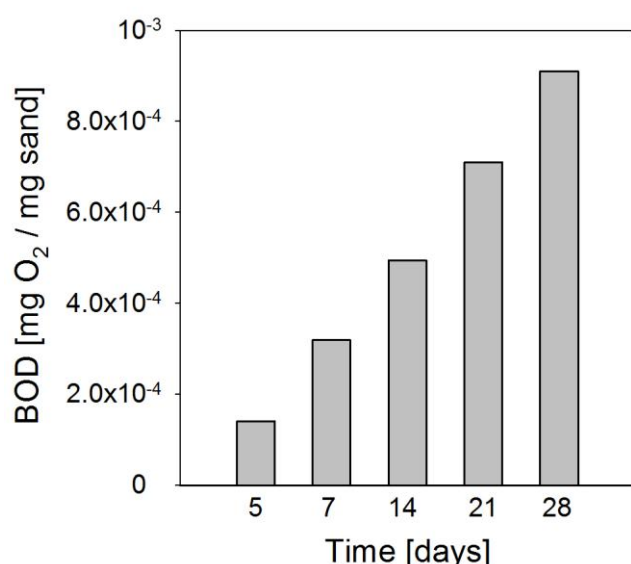


Fig. 3.2. Net biological oxygen demand (BOD) of the pristine sand (mg oxygen/mg sand) determined in individual batch experiments conducted for 5, 7, 14, 21 and 28 days. Mean values (n=2) are shown corrected for the blank associated with oxygen uptake by the inoculum; Error of measurement is  $< 1 \times 10^{-5}$  mg O<sub>2</sub> / mg sand.

*Role of easily biodegradable DOM (BDOM)*

The addition of acetate (1.75 mg C/L, ~0.14 mM C) led to an increased oxygen consumption between the first two sampling ports (Fig. 3.1a). The “theoretical” oxygen consumption assuming complete mineralization of the added acetate and steady-state conditions with respect to DOM sorption and desorption processes (Sobczak and Findlay, 2002), is ~4.7 mg/L O<sub>2</sub> (~0.14 mM) ( $\text{CH}_3\text{COOH} + 2\text{O}_2 \rightarrow 2\text{CO}_2 + 2\text{H}_2\text{O}$ ). This value is in good agreement with the measured oxygen consumption of 4.2 mg/L between the first two sampling ports. Therefore, this suggests that the fast initial oxygen decrease is attributed to the mineralization of acetate, as a model for BDOM, which implies that acetate and not POM was preferentially consumed at the column inlet under these conditions.

Previous results have shown that the addition of a readily available carbon source, such as lactic acid (14 mg C/L), led to a complete consumption of oxygen within the first 1.8 cm of a 30 cm column (von Gunten and Zobrist, 1993). The authors of this study also showed that the highest rate of the oxygen consumption occurred at the column inlet and was attributed to a higher microbial activity in this zone supported by a higher BDOM availability, as also demonstrated by Maeng et al. (2008).

For all experiments except for acetate addition, a similar fast initial decrease of the oxygen concentration between SP0 and SP1 could be observed (Fig. 3.1a). This decrease cannot be totally explained by BDOM degradation, since the differences in DOC concentrations for the Thur River water and Thur/effluent mixtures were small (<0.2 mg C/L) and below the limit of quantification for the “DOM-free” experiment. Small BDOM levels in the Thur River water could however have served as a substrate to stimulate bacterial growth leading to higher bacterial concentrations in this zone (see Section 3.3.2) allowing for a higher oxygen consumption rate associated with POM degradation.

*Effect of flow rate*

To assess the dependence of the oxygen consumption and NOM degradation on the flow rate, four experiments under different flow rate conditions (0.1, 0.2, 0.33 and 1 mL/min, i.e. residence times of 40, 20, 12 and 4 hours, respectively) were conducted at 20°C. The profiles of the relative oxygen concentration depended on the flow rate if plotted as function of the infiltration distance (Fig. 3.3a), please note normalization to SP1). At the highest flow rate of 1 mL/min, oxic conditions persisted through the entire column, whereas at the flow rate of 0.2 mL/min (i.e. 0.01 m/h), anoxic conditions could be observed within 20 cm of the column inlet (Fig. 3.3a). Lower flow rates increased the hydraulic residence time allowing for a



higher oxygen consumption in the same zone of the column and leading to anoxic conditions, which is in agreement with Doussan et al. (1997). Fig. 3.3b shows that the oxygen concentrations curves are superimposable when plotted against the hydraulic residence time, indicating that the differences in the residence times fully account for the observed effects of flow rate.

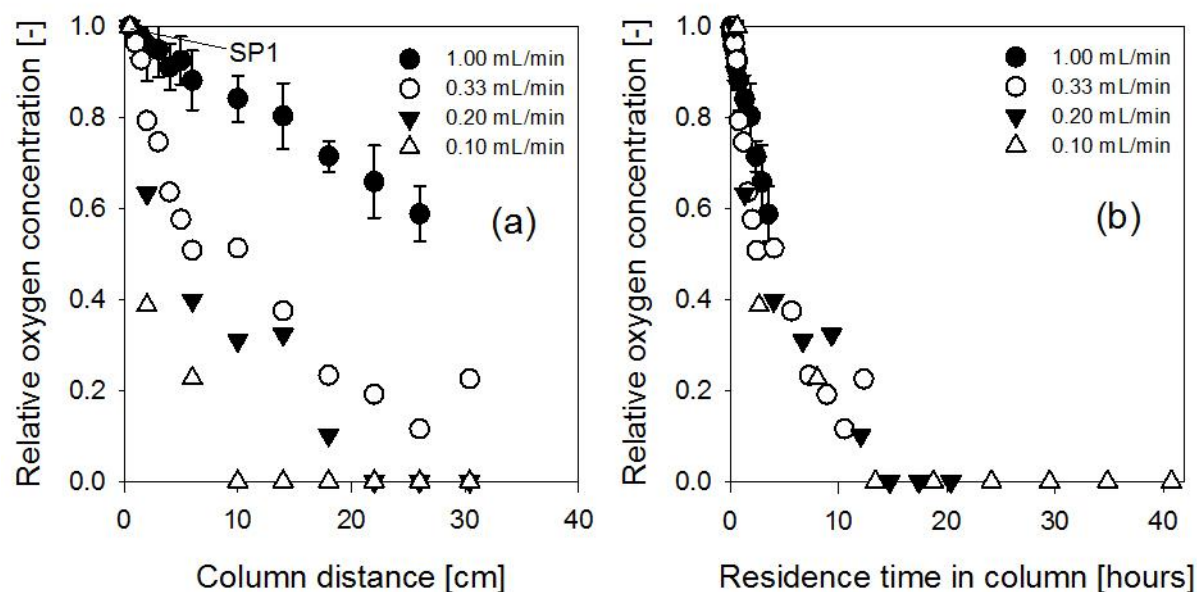


Fig. 3.3. Profiles of the relative oxygen concentration (normalized to the values at SP1) as a function of (a) infiltration distance and (b) residence time at flow rates of 0.10 ( $n=1$ ), 0.20 ( $n=1$ ), 0.33 ( $n=1$ ) and 1.00 ( $n=13$ ) mL/min at 20°C. Mean values and standard deviations (for 1 mL/min) are shown as symbols and error bars, respectively.

### 3.3.2 Effect of direct climate change variable (temperature) on redox processes

#### *Electron balance for oxygen consumption and NOM degradation*

The influence of temperature on the oxygen consumption and on NOM degradation was investigated in four column experiments conducted with Thur River water at 5.0, 12.5, 20.0 and 30.0°C. The oxygen and DOM consumption (measured as difference in DOC concentration) between the column inlet and outlet is shown as a function of temperature in Fig. 3.4. The DOM consumption between the column inlet and outlet explained only ~30% of the oxygen consumption at 5°C and <~7% at 12.5°C-30°C. At 30°C, the DOM consumption was lower than at the other temperatures possibly because of partial DOM degradation (~0.1 mg C/L, i.e. ~8 mM) already in the storage tank. The small contributions of the DOM consumption to the oxygen consumption for each temperature are a further confirmation for the hypothesis that

POM associated with the sand is most likely the electron donor for aerobic respiration (see Section 3.3.1).

A strong temperature dependence of the oxygen consumption could be observed between the column inlet and outlet reaching almost a plateau at 20°C (Fig. 3.4, white bars). Conversely, the DOM consumption between the column inlet and outlet did not seem to depend on temperature, since the values lie within the measurement uncertainty (Fig. 3.4, grey bars).

The small DOM consumption ( $<17 \mu\text{M C}$ , i.e.  $0.2 \text{ mg C/L}$ ) between the column inlet and outlet for all temperatures could be related to the recalcitrant nature of the DOM. Previous results from column studies also did not show any temperature dependence of the DOM consumption after the first sampling point at a retention time of about one day (Grünheid et al., 2008). Moreover, the authors of field studies at river-infiltration systems observed a high correlation between oxygen consumption and temperature, but no correlation between DOM consumption and temperature (Brugger et al., 2001; Diem et al., 2013b).

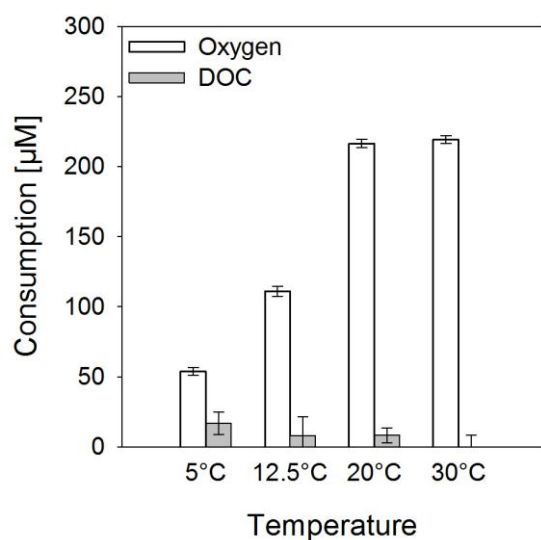


Fig. 3.4. Total average oxygen and DOM (as DOC) consumption in column experiments between SP0 and SP14. Standard deviations are shown as error bars ( $n=3$ ).

#### *Kinetics of oxygen consumption*

The measured oxygen concentration profiles for each temperature (5°C, 12.5°C, 20°C and 30°C) are shown in Fig. 3.5. The oxygen concentration of the feed water was  $7.8 \text{ mg/L}$  at  $5.0^\circ\text{C}$ ,  $12.5^\circ\text{C}$  and  $20.0^\circ\text{C}$  and  $7.0 \text{ mg/L}$  at  $30.0^\circ\text{C}$ . Similarly to the previous experiments (see Section 3.3.1), the highest rates of the oxygen consumption could be observed at the column inlet (i.e., between SP0 and SP1) (Fig. 3.5).

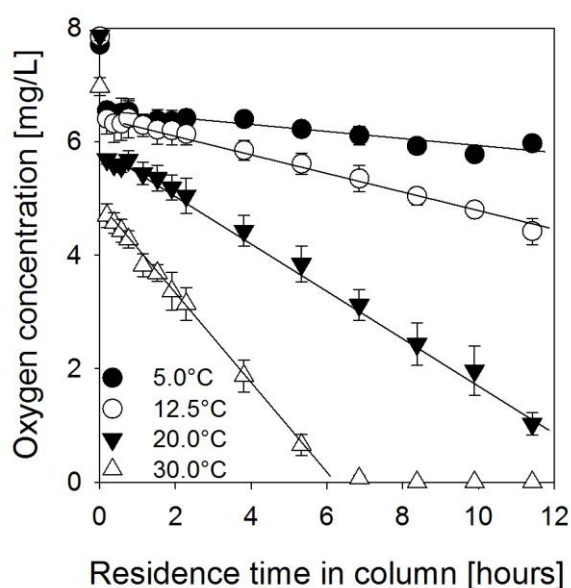


Fig. 3.5. Measured oxygen concentration profiles (symbols) and least-squares linear regression lines at 5.0, 12.5, 20.0 and 30.0°C at a flow rate of 0.3 mL/min. Mean values and standard deviations are shown as symbols and error bars, respectively (n=3).

After the initial phase, the profiles of the oxygen concentration showed a nearly linear behavior, corresponding to zero-order kinetics (Fig. 3.5). This can be normally observed when the rate at which the growth-limiting nutrient becomes available is the rate-limiting step (Alexander, 1999). In our case, POM is assumed to be the primary electron donor for microbial respiration and hence for oxygen consumption. POM degradation involves hydrolytic reactions (Egli, 1995; Pusch et al., 1998) generating BDOM, which is subsequently oxidized to CO<sub>2</sub> by aerobic respiration. Fig. 3.6 shows a schematic representation of the processes involving POM hydrolysis (reaction 1) and BDOM oxidation (reaction 2), respectively. Oxygen and CO<sub>2</sub> in the aqueous solution enter the biofilm through diffusion. The hydrolytic reactions are commonly assumed to be the rate-limiting step for POM degradation (Valentini et al., 1997; Henze et al., 1999; Vavilin et al., 2008). Therefore, we hypothesize that the observed oxygen consumption rates for each temperature were mainly controlled by POM hydrolysis. This, together with the large POM reservoir identified in the column sand through the BOD measurements, explains well the observed pseudo-zero order reaction kinetics for the oxygen consumption in the column.

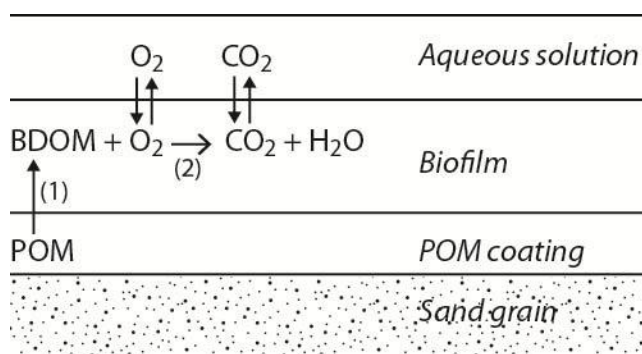


Fig. 3.6. Schematic representation of oxygen consumption associated with degradation of POM on sand grains. Reaction (1) represents POM hydrolysis and reaction (2) BDOM oxidation.

The observed pseudo-zero order behavior also implies that the concentration of bacteria must be fairly constant over the length of the column (between SP1 and SP13). Bacterial densities were estimated indirectly by a protein assay conducted at the end of experiment 2.5 after column II was operated anaerobically for 66 days (see Section 3.2.3 for analytical methods). We expect that the protein content of the sand samples from column II did not vary significantly after having changed the column operation mode from aerobic, which lasted 327 days, to anaerobic (66 days).

The protein content of the pristine sand was lower than the samples from the column, indicating that a significant bacterial growth occurred during the column experiments (Fig. 3.7). Nearly constant protein concentrations were measured in samples SP2-SP13 suggesting a uniform growth and distribution of bacteria through the column (Fig. 3.7). This implies that POM supporting bacterial growth was hydrolyzed at a constant rate throughout the column (i.e., after SP1), which is consistent with the observed pseudo-zero order reaction kinetics for the oxygen consumption. A higher protein concentration in sample SP1 compared with the average of SP2-SP13 ( $p < 0.001$ , Z-test statistics) may reflect bacterial growth by the presence of non-measurable BDOM near the column inlet (see Section 3.3.1).

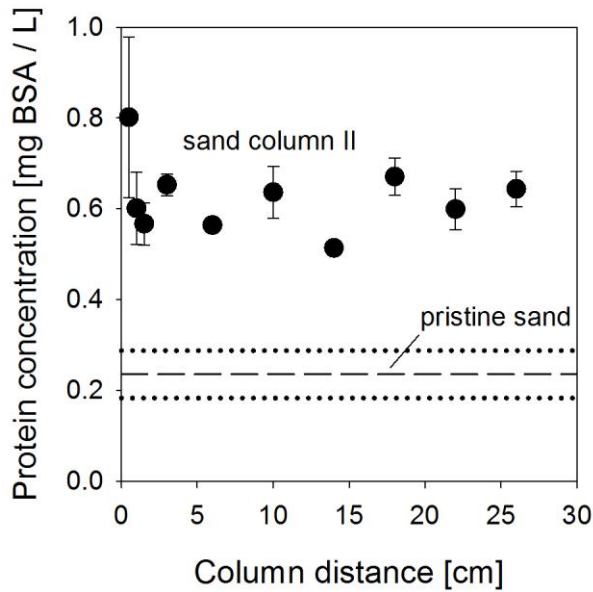


Fig. 3.7. Protein concentration (expressed as bovine serum albumin concentration, BSA) of the sand from column II (SP1, SP2, SP3, SP5, SP8, SP9, SP10, SP11, SP12, SP13) (●) measured after 393 days of operation (Table 3.2, end of experiment 2.5) and of pristine sand (dashed line). The dotted lines represent the errors of measurement for the pristine sand (n=3). Mean values and standard deviations are shown as symbols and error bars, respectively (n=3).

#### *Temperature dependence of aerobic respiration: Activation energy*

The oxygen consumption in the column has been shown to be associated with the degradation of POM present on the sand and to depend on temperature (Fig. 3.5). To quantify the observed temperature dependence, an Arrhenius-type approach, typical for chemical and biological reactions (Middelburg et al., 1996; Weston and Joye, 2005; Burdige, 2011), was applied (Eq. 3.2):

$$\ln(k(T)) = \ln(A) - \frac{E_a}{R} \cdot \frac{1}{T} \quad (3.2)$$

where  $k(T)$  is the temperature-dependent reaction rate constant (in our case the observed pseudo zero-order oxygen consumption rate constant in  $\text{Ms}^{-1}$ ),  $A$  the pre-exponential factor (in  $\text{Ms}^{-1}$ ),  $E_a$  the apparent Arrhenius activation energy (in  $\text{Jmol}^{-1}$ ),  $R$  the universal gas constant (in  $\text{Jmol}^{-1}\text{K}^{-1}$ ) and  $T$  the temperature (in K). Fig. 3.8 shows an Arrhenius-type plot of the data. Based on the good linearity ( $r^2=0.97$ ), the apparent activation energy  $E_a$  can be determined from the slope  $\left(\frac{E_a}{R}\right)$  of the straight line in Fig. 3.8, which results in a value of  $\sim 70 \text{ kJmol}^{-1}$ .

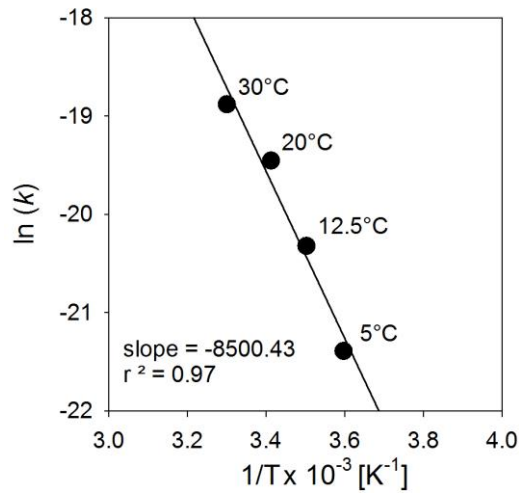


Fig. 3.8. Arrhenius-type correlation between the rate constant ( $\ln(k)$ ) for oxygen consumption and  $\frac{1}{T}$ . The symbols represent the experimental data at 30.0, 20.0, 12.5 and 5.0°C (n=3) (Fig. 3.5), the line shows a least-squares linear regression.

The  $E_a$  value of  $\sim 70 \text{ kJmol}^{-1}$  derived from our column experiments is consistent with a value of  $51 \pm 12 \text{ kJmol}^{-1}$  (n=94) determined from measurements of benthic respiration over the temperature range 5-25°C on stones collected from the Thur River (Acuna et al., 2008). Similar values of 54-125  $\text{kJmol}^{-1}$  (Middelburg et al., 1996) and 46-89  $\text{kJmol}^{-1}$  (Weston and Joye, 2005) were reported in studies of the temperature dependence of organic matter degradation in intertidal and marine sediments, respectively.

The activation energy for oxygen consumption can also be calculated from field observations of oxygen concentrations at, for example, the Thur River infiltration system (Diem et al., 2013a). In this study, the oxygen consumption rates were modeled with a temperature factor defined by a function with a maximum rate at 35°C (O'Connell, 1990) and with a discharge-dependent term. The activation energy for aerobic respiration during infiltration was estimated to be  $\sim 63 \text{ kJmol}^{-1}$  over the temperature range 5-30°C for low river discharges of  $<20 \text{ m}^3/\text{s}$  (Diem et al., 2013a). This activation energy is similar to our experimentally derived activation energy ( $\sim 70 \text{ kJmol}^{-1}$ ), showing a good agreement between the field-based model and our experimentally derived value.

### *Redox processes involving nitrogen species*

The profiles of the oxygen concentration in Fig. 3.5 show that the oxygen consumption rate increased with increasing temperatures, leading to anoxic conditions at 30.0°C for residence times >7 h (i.e., at SP11, after 18 cm). To better characterize the redox milieu under such conditions, nitrate, nitrite and ammonium were measured in the column after an operation time of 18 days (Fig. 3.9). As soon as the oxygen concentration approached  $\leq 0.1$  mg/L, nitrite started to increase, reaching a maximum of 55  $\mu\text{g N/L}$  at a residence time of about 10 h (Fig. 3.9). Ammonium appeared at a residence time of about 8 h and did not reach a maximum. Nitrate showed a decreasing trend for residence times >8 h (i.e., at SP12, after 22 cm). These findings indicate that denitrification proceeded in the same section of the column where nitrite, an intermediate product of denitrification, was formed. This view was corroborated by the fact that ~30% of the nitrate decrease can be explained by the detected nitrite concentration. The remaining 70% of the nitrate lost might be explained by the formation of  $\text{N}_2$ , or other denitrification products (e.g.  $\text{N}_2\text{O}$ ). Formation of ammonium could be related to the anoxic degradation of nitrogen containing organic compounds, or to nitrate ammonification. The maximum detected nitrite concentration (55  $\mu\text{g N/L}$ ) is about one order of magnitude lower than the concentration recommended in the WHO guideline for drinking water (900  $\mu\text{g N/L}$ ) (WHO, 2011) and in a similar range as the value in the European guideline (150  $\mu\text{g N/L}$ ) (EU, 1998). Although the nitrite concentrations given in the WHO and EU guidelines are not exceeded under our experimental conditions, the formation of nitrite represents a potential threat for drinking water quality under such anoxic conditions.

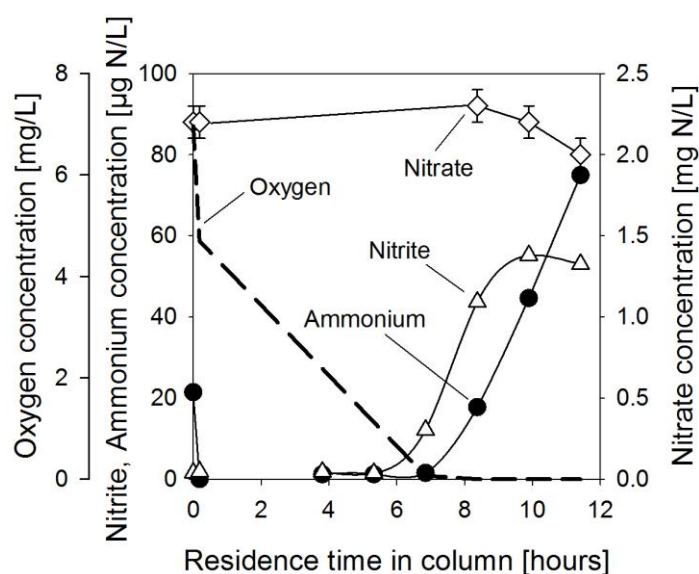


Fig. 3.9. Measured oxygen (---), nitrate (◇), nitrite (△) and ammonium (●) concentrations after 18 days of operation of column II at 30.0°C at a flow rate of 0.3 mL/min (Table 3.2, experiment

2.1). Mean values and standard deviations (for nitrate) are shown as symbols and error bars, respectively (n=3). For nitrate, nitrite and ammonium, lines help to guide the reader's eye.

### **3.3.3 Mobilization of Mn(II) under oxygen- and nitrate-free conditions**

Nitrate-free Thur River water stripped of oxygen was added as feed water to test whether Mn(III/IV)- and Fe(III)-reducing conditions could develop under this scenario. No Fe(II) could be measured in the entire column during this experiment, whereas Mn was mobilized as Mn(II) (Fig. 3.10a), suggesting that in the absence of oxygen and nitrate, Mn(III/IV)(hydr)oxides became terminal electron acceptors for the microorganisms.

According to the homogeneous POM distribution throughout the column and in analogy to aerobic respiration, we would have expected a constant reductive dissolution rate of Mn(III/IV)(hydr)oxides throughout the column leading to a steady Mn(II) increase between SP1-SP14, only limited by  $\text{MnCO}_3$  solubility (for calculations, see Section 3.2.4). However, we observed a fast increase of Mn(II) near the column inlet (SP1-SP5) after 9, 16 and 27 days, followed by a decrease beyond SP8 (Fig. S3.2). This can also be observed in Fig. 3.10a, which shows the Mn(II) concentration as a function of the column operation time for each sampling port. Here, the Mn(II) concentration increased quickly for all sampling ports and peaked after ~7, ~14 and ~21 days for SP1, SP5 and SP8, respectively, approaching zero after that, whereas it reached  $\text{MnCO}_3$  equilibrium for SP11 and SP14 (Fig. 3.10a).

We hypothesize that the fast Mn increase near the column inlet could be associated with a higher biological activity in this zone (see Section 3.3.2) and hence to a higher POM hydrolysis rate. From the experiments under aerobic conditions at 20°C (Fig. 3.1a and Fig. 3.5), we already observed a fast oxygen consumption at the column inlet (SP0-SP1) related to POM hydrolysis generating BDOM. In absence of oxygen and nitrate, part of this BDOM could propagate into the column and be available for Mn(III/IV) reduction. The decrease of the Mn(II) concentration beyond SP8 (Fig. S3.2) could be due to adsorption processes of Mn(II) on e.g., Mn(III/IV)(hydr)oxide surfaces.

Furthermore, the Mn(II) concentration profiles in Fig. S3.2 are shifted towards the outlet with increasing operation time, possibly because of a depletion of Mn(III/IV)(hydr)oxides in the zone between SP1-SP8. To test this hypothesis, the reactive pools of Mn(III/IV)(hydr)oxides of the pristine and the column sand were quantified at the end of the experiment (after 66 days) with a buffered ascorbate solution at pH 7.1, according to Hyacinthe et al. (2006) (see Section 3.2.3). The amount of Mn(II) reduced by ascorbate in the pristine sand (~23 µg/g sand) was significantly higher than that in the column sand for all sampling ports,



showing that a considerable part of the reactive Mn pool was consumed during the experiment (Fig. 3.10b). Lower Mn(II) sand concentrations were found at SP1 and SP5 compared to SP8, SP11 and SP14 (Fig. 3.10b). This is a confirmation of a partial depletion of the reactive pool of Mn(III/IV)(hydr)oxides at SP1 and SP5.

As a consequence of the initial depletion of the Mn pool, the extent of reductive dissolution rate of Mn(III/IV)(hydr)oxides decreased in the first section of the column (SP1-SP5) with increasing column operation time. This led to lower Mn(II) concentrations at SP1, SP5 and possibly SP8 (the Mn(II) concentration at SP8 reflects the accumulation of Mn(II) between SP1-SP8). For the sampling ports further in the column (SP8, SP11 and SP14), higher manganese concentrations in the sand were found (Fig. 3.10b), giving sufficient potential for a further increase of Mn(II) at SP11 and SP14. However, the Mn(II) concentrations at these sampling points were limited by the solubility of  $\text{MnCO}_3$ .

Even though  $\sim 75 \mu\text{g Fe/g}$  sand could be measured in the pristine sand by the ascorbate method (data not shown), Fe(II) could not be detected during the experiment. This suggests that conditions favorable for the reductive dissolution of Fe(III)(hydr)oxides did not occur in our experimental system, but cannot be excluded at actual riverbank filtrations sites.

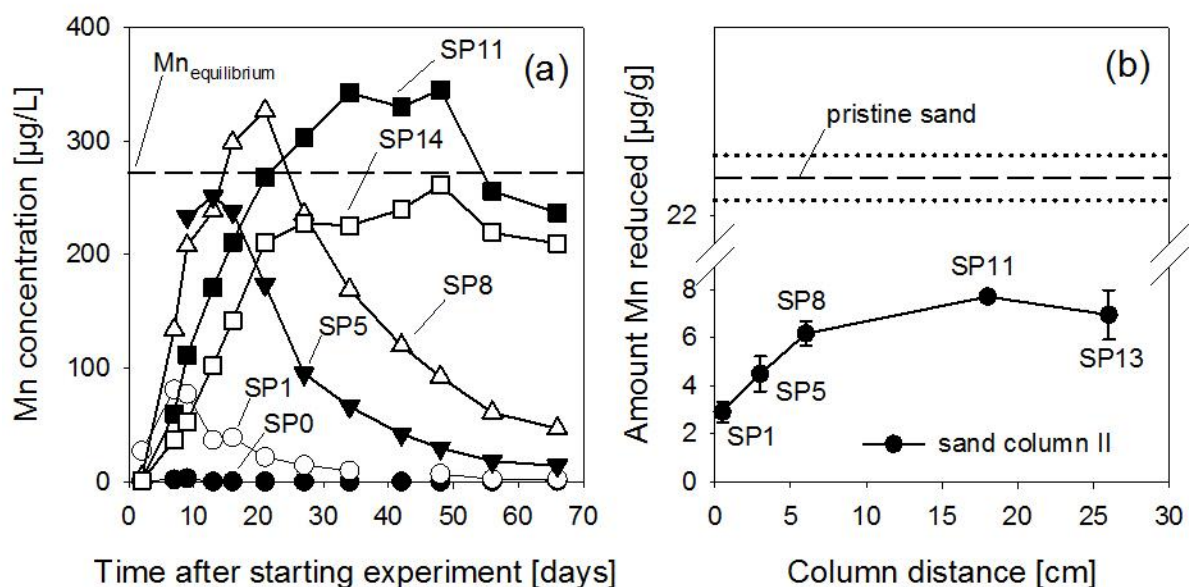


Fig. 3.10. (a) Mn(II) concentration at SP0 (●), SP1 (○), SP5 (▼), SP8 (△), SP11 (■) and SP14 (□) as a function of the column operation time at 20°C and at a flow rate of 0.3 mL/min. The Mn(II) concentration in equilibrium with rhodochrosite ( $\text{MnCO}_3$ ) is shown by the dashed line (for calculations, see Section 3.2.4). (b) Average amount of Mn reduced [ $\mu\text{g/g}$  sand] by ascorbate in the pristine (dashed line) and in the sand from column II (circles) (SP1, SP5, SP8, SP11 and SP13) after 66 days of operation. For the pristine sand, an average of three samples

after 0.5, 1, and 2.5 hours equilibration with the ascorbate solution is shown with the errors of measurement (dotted lines), for the column II samples, an average of samples after 0.5, 1, and 2.5 hours equilibration is shown together with the corresponding standard deviations.

### **3.3.4 Practical implications**

Several studies have investigated the impact of climate change on groundwater quantity, but only a few have focused on processes affecting groundwater quality (Green et al., 2011). A recent review by Sprenger et al. (2011) evaluated the vulnerability of riverbank filtration systems to climate change considering two scenarios, drought and flood. Overall, increasing surface water temperatures are expected to favor anoxic/anaerobic conditions in the future (Sprenger et al., 2011), which is in line with our results (see Section 3.3.2). High vulnerability for the drought scenario is projected for the DOM removal because of higher DOC concentrations in the source water and incomplete degradation under anaerobic conditions (Sprenger et al., 2011). The effects of the presumed increased DOC concentrations and altered DOM composition on the redox processes are however still unknown.

Currently, an upgrade of wastewater treatment plant effluents in Switzerland with ozonation (Joss et al., 2008; Zimmermann et al., 2011) or powdered activated carbon (Nowotny et al., 2007) is planned to reduce the discharge of organic micropollutants to the water bodies. Ozonation is usually followed by a sand filtration step, which effectively removes BDOM formed during ozonation (Zimmermann et al., 2011). Powdered activated carbon treatment reduces DOM by adsorption processes (Nowotny et al., 2007; Worch, 2010). Therefore, DOM loads from upgraded wastewater treatment plants into the receiving rivers are expected to be reduced in the future, counteracting the smaller dilution, which would lead to higher DOC concentrations. In addition to that, our results showed that increasing DOC concentrations from wastewater effluent did not affect the redox processes in our experimental system (see Section 3.3.1). Based on the lower DOM input in rivers by polishing treatment of wastewater plant effluents and its subordinate role as an electron donor, only a minor effect of DOM on the development of anoxic conditions is expected during future summer conditions.

In the column experiments, a significant effect of the hydraulic residence time on the oxygen consumption and on the development of anoxic conditions was observed (see Section 3.3.1). At the same time, however, high hydraulic residence times are beneficial for the removal of microorganisms and pathogens (Sprenger et al., 2011). Since infectious diseases represent the most important health risks with respect to drinking water, removal of microorganisms and pathogens has absolute priority (WHO, 2011). The Swiss regulation for groundwater protection

defines a minimum groundwater travel time of 10 days before abstraction, which allows for an adequate inactivation of microorganisms (Kunz et al., 2009). To determine the optimal residence time, which allows for good pathogen removal without the formation of anoxic conditions, site-specific information about the hydrogeological conditions and the redox parameters are needed, as also suggested by Schoenheinz and Grischek (2011).

Today, groundwater derived from riverbank filtration in Switzerland is generally oxic and denitrification is rarely observed. During future summer conditions, however, the effect of high temperatures ( $\geq 20^{\circ}\text{C}$ ) over several weeks/months could lead to transient anoxic conditions. Complete denitrification was not observed in the present study, but cannot be excluded at actual riverbank filtration systems during future heat waves. Therefore, it will be essential to monitor oxygen and nitrogen species (nitrate, nitrite and ammonium) at riverbank filtration systems especially during future heat waves.

The formation of ammonium could be problematic in the context of drinking water disinfection, since it can quickly react with chlorine leading to the formation of chloramines ( $\text{HOCl} + \text{NH}_3 \rightarrow \text{NH}_2\text{Cl} + \text{H}_2\text{O}$ ), which lower the disinfection efficiency (Deborde and von Gunten, 2008). At Swiss riverbank filtration systems, such as the Thur River, disinfection is not practiced, but in cases where low chlorine doses are applied (e.g.  $7 \mu\text{M Cl}_2$  or  $0.5 \text{ mg/L Cl}_2$ ), the formation of ammonium in moderate concentrations ( $< 7 \mu\text{M NH}_4^+$ ) can substantially reduce the disinfection efficiency of chlorine.

### 3.4 Conclusion

Laboratory column experiments carried out with filtered river water were conducted to simulate the effect of temperature, DOM concentration/composition and flow rate on redox processes during riverbank filtration. The following conclusions can be drawn from our results:

1. Biodegradable dissolved organic matter (BDOM) was mainly removed immediately at the column inlet by aerobic respiration. This might lead to higher microbial concentrations near the infiltration zone at actual riverbank filtration systems even if BDOM is not measurable. DOM from wastewater treatment plant effluents did not enhance aerobic respiration and did not promote anoxic conditions in our laboratory columns.
2. Particulate organic matter (POM) associated with natural sand appears to be the main terminal electron donor in the infiltration process and can sustain aerobic respiration for long periods. A POM limitation was not observed in the laboratory column system.

3. Low infiltration rates induce a higher oxygen consumption than higher rates for a certain infiltration distance, which could lead to anoxic conditions.
4. The aerobic respiration associated with POM degradation strongly depends on temperature with an activation energy of  $\sim 70 \text{ kJmol}^{-1}$ . Only a small fraction of the riverine DOM is easily degradable (i.e., BDOM) and its consumption does not seem to be sensitive to temperature.
5. At high temperatures ( $30^\circ\text{C}$ ), fully anoxic conditions were observed, with partial denitrification ( $\sim 30\%$ ) and formation of nitrite and ammonium. Although nitrite concentrations were below WHO and EU drinking water guidelines in our experiments, this parameter should be monitored at actual riverbank filtration sites during future heat waves. If the produced water is chlorinated, the presence of ammonium could lead to a reduction in disinfection efficiency due to chloramine formation.
6. The combined action of high temperatures ( $\geq 20^\circ\text{C}$ ) and low infiltration rates ( $\leq 0.01 \text{ m/h}$ ) could lead to transient anoxic conditions during future summer conditions. Even under fully anoxic conditions, no complete denitrification was observed, so that nitrate acts as a redox buffer preventing the reductive dissolution of Mn(III/IV)(hydr)oxides.
7. Mn(II) was mobilized, whereas Fe(II) was not mobilized in absence of oxygen and nitrate, but Fe(III)-reduction cannot be excluded at actual riverbank filtration systems under these conditions.

## Acknowledgements

This study was accomplished within the National Research Program “Sustainable Water Management” (NRP61) and funded by the Swiss National Science Foundation (SNF, Project No. 406140-125856). We would like to thank the AuA Laboratory, Elisabeth Salhi, Irene Brunner, Thomas Fleischmann and Stefan Koetzsch for the analytical support and Peter Gäumann and his workshop-team for constructing the columns. Moreover, we would like to express our gratitude to Samuel Diem, Fabian Soltermann, Sabrina Bahn Müller, Eduard Hoehn and Jacqueline Taber for helpful discussions.

### 3.5 References

- Acuna, V., Wolf, A., Uehlinger, U., Tockner, K., 2008. Temperature dependence of stream benthic respiration in an Alpine river network under global warming. *Freshwater Biol.* 53 (10), 2076-2088.
- Alexander, M., 1999. Biodegradation and bioremediation. Academic Press, San Diego.
- Bourg, A.C.M., Bertin, C., 1993. Biogeochemical processes during the infiltration of river water into an alluvial aquifer. *Environ. Sci. Technol.* 27 (4), 661-666.
- Brugger, A., Wett, B., Kolar, I., Reitner, B., Herndl, G.J., 2001. Immobilization and bacterial utilization of dissolved organic carbon entering the riparian zone of the alpine Enns River, Austria. *Aquat. Microb. Ecol.* 24 (2), 129-142.
- Burdige, D.J., 2011. Temperature dependence of organic matter remineralization in deeply-buried marine sediments. *Earth Planet. Sc. Lett.* 311 (3-4), 396-410.
- CH2011, 2011. Swiss Climate Change Scenarios CH2011. C2SM, MeteoSwiss, ETH, NCCR Climate and OcCC, Zurich, pp. 88.
- Deborde, M., von Gunten, U., 2008. Reactions of chlorine with inorganic and organic compounds during water treatment-Kinetics and mechanisms: A critical review. *Water Res.* 42 (1-2), 13-51.
- Diem, S., Cirpka, O.A., Schirmer, M., 2013a. Modeling the dynamics of oxygen consumption upon riverbank filtration by a stochastic-convective approach. *J. Hydrol.* 505, 352-363.
- Diem, S., Rudolf von Rohr, M., Hering, J.G., Kohler, H.P.E., Schirmer, M., von Gunten, U., 2013b. NOM degradation during river infiltration: Effects of the climate variables temperature and discharge. *Water Res.* 47 (17), 6585-6595.
- DIN, 1983a. Deutsche Einheitsverfahren zur Wasser-, Abwasser- und Schlammuntersuchung, Bestimmung des Ammonium-Stickstoffs (E5), Teil 5, DIN 38406. Deutsches Institut für Normung DIN, pp. 1-6.
- DIN, 1983b. Deutsche Einheitsverfahren zur Wasser-, Abwasser- und Schlammuntersuchung, Bestimmung von Mangan (E2), Teil 2, DIN 38406. Deutsches Institut für Normung DIN, pp. 1-8.
- DIN, 1993. Deutsche Norm zur Bestimmung von Nitrit, EN 26777. Deutsches Institut für Normung DIN, pp. 1-11.
- Doussan, C., Poitevin, G., Ledoux, E., Delay, M., 1997. River bank filtration: Modelling of the changes in water chemistry with emphasis on nitrogen species. *J. Contam. Hydrol.* 25 (1-2), 129-156.

- Egli, T., 1995. The ecological and physiological significance of the growth of heterotrophic microorganisms with mixtures of substrates. In: Jones, G.N. (Ed.), *Advances in Microbial Ecology*. Plenum Press, New York, pp. 305-386.
- EU, 1998. European Union (EU) Council Directive 98/83/EC of 3 November 1998 on the quality of water intended for human consumption.
- FOEN, 2012. Effects of Climate Change on Water Resources and Watercourses. Synthesis Report on the "Climate Change and Hydrology in Switzerland" (CCHydro) Project. Federal Office for the Environment FOEN, Bern, pp. 76.
- Green, T.R., Taniguchi, M., Kooi, H., Gurdak, J.J., Allen, D.M., Hiscock, K.M., Treidel, H., Aureli, A., 2011. Beneath the surface of global change: Impacts of climate change on groundwater. *J. Hydrol.* 405 (3-4), 532-560.
- Greskowiak, J., Prommer, H., Massmann, G., Nützmann, G., 2006. Modeling seasonal redox dynamics and the corresponding fate of the pharmaceutical residue phenazone during artificial recharge of groundwater. *Environ. Sci. Technol.* 40 (21), 6615-6621.
- Grischek, T., Hiscock, K.M., Metschies, T., Dennis, P.F., Nestler, W., 1998. Factors affecting denitrification during infiltration of river water into a sand and gravel aquifer in Saxony, Germany. *Water Res.* 32 (2), 450-460.
- Grünheid, S., Amy, G., Jekel, M., 2005. Removal of bulk dissolved organic carbon (DOC) and trace organic compounds by bank filtration and artificial recharge. *Water Res.* 39 (14), 3219-3228.
- Grünheid, S., Huebner, U., Jekel, M., 2008. Impact of temperature on biodegradation of bulk and trace organics during soil passage in an indirect reuse system. *Water Science and Technology* 57, 987-994.
- Hannappel, S., Scheibler, F., Huber, A., Sprenger, C., 2014. Characterization of European managed aquifer recharge (MAR) sites - Analysis. EU project Demeau, M11.1, pp 51.
- Henze, M., Gujer, W., Mino, T., Matsuo, T., Wentzel, M.C., Marais, G.V.R., Van Loosdrecht, M.C.M., 1999. Activated Sludge Model No.2d, ASM2d. *Water Sci. Technol.* 39 (1), 165-182.
- Herbert, D., Phipps, P.J., Strange, R.E., 1971. Chemical Analysis of Microbial Cells (Chapter III). In: *Methods In Microbiology*, Volume 5, Part B. Edited by J.R. Norris and D.W. Ribbons. Academic Press. .
- Hoehn, E., Scholtis, A., 2011. Exchange between a river and groundwater, assessed with hydrochemical data. *Hydrol. Earth Syst. Sc.* 15 (3), 983-988.

- Huntscha, S., Rodriguez Velosa, D.M., Schroth, M.H., Hollender, J., 2013. Degradation of Polar Organic Micropollutants during Riverbank Filtration: Complementary Results from Spatiotemporal Sampling and Push–Pull Tests. *Environ. Sci. Technol.* 47 (20), 11512-11521.
- Hyacinthe, C., Bonneville, S., Van Cappellen, P., 2006. Reactive iron(III) in sediments: Chemical versus microbial extractions. *Geochim. Cosmochim. Acta* 70 (16), 4166-4180.
- Jacobs, L.A., von Gunten, H.R., Keil, R., Kuslys, M., 1988. Geochemical changes along a river-groundwater infiltration flow path: Glattfelden, Switzerland. *Geochim. Cosmochim. Acta* 52 (11), 2693-2706.
- Joss, A., Siegrist, H., Ternes, T.A., 2008. Are we about to upgrade wastewater treatment for removing organic micropollutants? *Water Sci. Technol.* 57 (2), 251-255.
- Kedziorek, M.A.M., Geoffriau, S., Bourg, A.C.M., 2008. Organic matter and modeling redox reactions during river bank filtration in an alluvial aquifer of the Lot River, France. *Environ. Sci. Technol.* 42 (8), 2793-2798.
- Kuehn, W., Mueller, U., 2000. Riverbank filtration: An overview. *J. Am. Water Works Ass.* 92 (12), 60-69.
- Kunz, Y., von Gunten, U., Maurer, M., 2009. Wasserversorgung 2025 - Vorprojekt. Eawag, pp. 198.
- Maeng, S.K., Sharma, S.K., Magic-Knezev, A., Amy, G., 2008. Fate of effluent organic matter (EfOM) and natural organic matter (NOM) through riverbank filtration. *Water Sci. Technol.* 57 (12), 1999-2007.
- Massmann, G., Greskowiak, J., Dunnbier, U., Zuehlke, S., Knappe, A., Pekdeger, A., 2006. The impact of variable temperatures on the redox conditions and the behaviour of pharmaceutical residues during artificial recharge. *J. Hydrol.* 328 (1-2), 141-156.
- Matsunaga, T., Karametaxas, G., von Gunten, H.R., Lichtner, P.C., 1993. Redox chemistry of iron and manganese minerals in river-recharged aquifers: A model interpretation of a column experiment. *Geochim. Cosmochim. Acta* 57 (8), 1691-1704.
- Middelburg, J.J., Klaver, G., Nieuwenhuize, J., Wielemaker, A., De Haas, W., Vlug, T., Van Der Nat, J.F.W.A., 1996. Organic matter mineralization in intertidal sediments along an estuarine gradient. *Mar. Ecol.-Prog. Ser.* 132 (1-3), 157-168.
- Mouchet, P., 1992. From conventional to biological removal of iron and manganese in France. *J. Am. Water Works Ass.* 84 (4), 158-167.
- Mueller, B., 2004. ChemEQL, V.3.0, a program to calculate chemical speciation and chemical equilibria, Eawag.

- Müller, R., Widemann, O., 1955. Die Bestimmung des Nitrat-Ions im Wasser. *Vom Wasser* 22, 247-271.
- Nowotny, N., Epp, B., von Sonntag, C., Fahlenkamp, H., 2007. Quantification and modeling of the elimination behavior of ecologically problematic wastewater micropollutants by adsorption on powdered and granulated activated carbon. *Environ. Sci. Technol.* 41 (6), 2050-2055.
- O'Connell, A.M., 1990. Microbial decomposition (respiration) of litter in eucalypt forests of South-Western Australia: An empirical model based on laboratory incubations. *Soil Biol. Biochem.* 22 (2), 153-160.
- OECD, 1992. OECD Guideline for Testing of Chemicals, Guideline 301 D. Organisation for Economic Co-operation and Development OECD pp. 62.
- Peter, S., Koetzsch, S., Traber, J., Bernasconi, S.M., Wehrli, B., Durisch-Kaiser, E., 2012. Intensified organic carbon dynamics in the ground water of a restored riparian zone. *Freshwater Biol.* 57 (8), 1603-1616.
- Pusch, M., Fiebig, I., Brettar, H., Eisenmann, H., Ellis, B.K., Kaplan, L.A., Lock, M.A., Naegeli, M.W., Traunspurger, W., 1998. The role of micro-organisms in the ecological connectivity of running waters. *Freshwater Biol.* 40 (3), 453-495.
- Scheurer, M., Michel, A., Brauch, H.J., Ruck, W., Sacher, F., 2012. Occurrence and fate of the antidiabetic drug metformin and its metabolite guanylurea in the environment and during drinking water treatment. *Water Res.* 46 (15), 4790-4802.
- Schmidt, C.K., Lange, F.T., Brauch, H.J., 2007. Characteristics and evaluation of natural attenuation processes for organic micropollutant removal during riverbank filtration. *Wat. Sci. Technol.* 7 (3), 1-7.
- Schoenheinz, D., Grischek, T., 2011. Behavior of dissolved organic Carbon during bank filtration under extreme climate conditions. *NATO Science for Peace and Security Series C: Environmental Security* 103, 51-67.
- Smith, P.K., Krohn, R.I., Hermanson, G.T., 1985. Measurement of protein using bicinchoninic acid. *Anal. Biochem.* 150 (1), 76-85.
- Sobczak, W.V., Findlay, S., 2002. Variation in bioavailability of dissolved organic carbon among stream hyporheic flowpaths. *Ecology* 83 (11), 3194-3209.
- Sprenger, C., Lorenzen, G., Hulshoff, I., Grutzmacher, G., Ronghang, M., Pekdeger, A., 2011. Vulnerability of bank filtration systems to climate change. *Sci. Total Environ.* 409 (4), 655-663.



- Storck, F.R., Schmidt, C.K., Wülser, R., Brauch, H.J., 2012. Effects of boundary conditions on the cleaning efficiency of riverbank filtration and artificial groundwater recharge systems regarding bulk parameters and trace pollutants. *Water Sci. Technol.* 66 (1), 138-144.
- Stumm, W., Morgan, J.J., 1996. *Aquatic Chemistry. Chemical Equilibria and Rates in Natural Waters*, Third Edition. Wiley-interscience, New York.
- Toride, N., Leij, F.J., van Genuchten, M.T., 1995. The CXTFIT Code for Estimating Transport Parameters from Laboratory or Field Tracer Experiments, Version 2.0, Research Report No. 137. US Salinity Laboratory, Riverside, CA, pp. 131.
- Tufenkji, N., Ryan, J.N., Elimelech, M., 2002. Bank filtration. *Environ. Sci. Technol.* 36 (21), 423-428.
- Valentini, A., Garuti, G., Rozzi, A., Tilche, A., 1997. Anaerobic degradation kinetics of particulate organic matter: A new approach. *Water Sci. Technol.* 36 (6-7), 239-246.
- Vavilin, V.A., Fernandez, B., Palatsi, J., Flotats, X., 2008. Hydrolysis kinetics in anaerobic degradation of particulate organic material: An overview. *Waste Management* 28 (6), 939-951.
- Vogler, P., 1965. Beiträge zur Phosphatanalytik in der Limnologie. II. Die Bestimmung des gelösten Ortophosphates. *Fortschritte der Wasserchemie und ihrer Grenzgebiete* 2, 109-119.
- von Gunten, H.R., Karametaxas, G., Krähenbühl, U., Kuslys, M., Giovanoli, R., Hoehn, E., Keil, R., 1991. Seasonal biogeochemical cycles in riverborne groundwater. *Geochim. Cosmochim. Acta* 55 (12), 3597-3609.
- von Gunten, U., Zobrist, J., 1993. Biogeochemical changes in groundwater-infiltration systems: Column studies. *Geochim. Cosmochim. Acta* 57 (16), 3895-3906.
- Weston, N.B., Joye, S.B., 2005. Temperature-driven decoupling of key phases of organic matter degradation in marine sediments. *P. Natl. Acad. Sci. USA* 102 (47), 17036-17040.
- WHO, 2011. *Guidelines for Drinking-water Quality*, Fourth Edition. World Health Organization WHO, pp. 541.
- Worch, E., 2010. Competitive adsorption of micropollutants and NOM onto activated carbon: Comparison of different model approaches. *J. Water Supply Res. T.* 59 (5), 285-297.
- Zimmermann, S.G., Wittenwiler, M., Hollender, J., Krauss, M., Ort, C., Siegrist, H., von Gunten, U., 2011. Kinetic assessment and modeling of an ozonation step for full-scale

municipal wastewater treatment: Micropollutant oxidation, by-product formation and disinfection. *Water Res.* 45 (2), 605-617.

# **Supporting Information for Chapter 3**

## **Column studies to assess the effects of climate variables on redox processes during riverbank filtration**

2 figures and 5 tables

Reprinted from *Water Research* 61, Rudolf von Rohr, M.; Hering, J. G.; Kohler, H.-P. E.; von Gunten, U., Column studies to assess the effects of climate variables on redox processes during riverbank filtration, 263-275. Copyright 2014, with permission from Elsevier.

<http://dx.doi.org/10.1016/j.watres.2014.05.018>

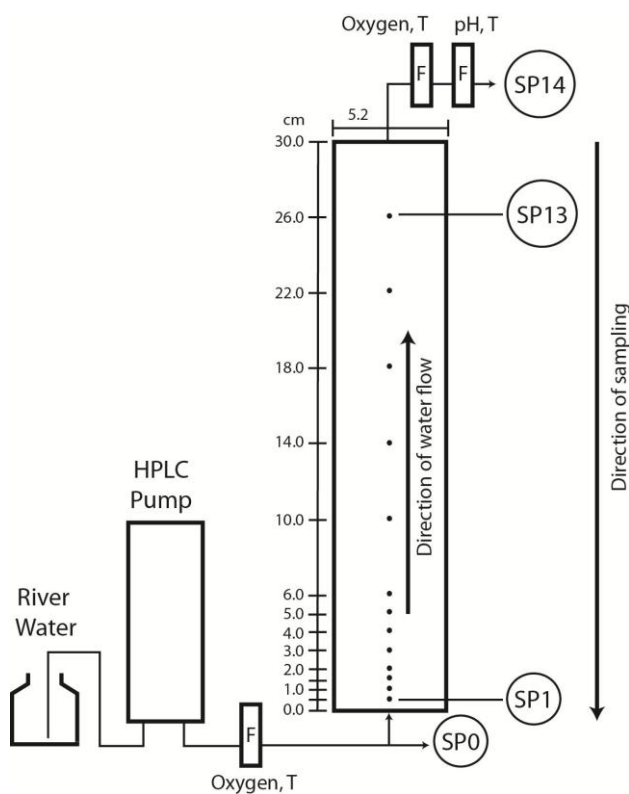


Fig. S3.1. Set-up of the column system, in which river water was pumped by a HPLC-pump from the bottom to the top of the column. The column was equipped with 13 sampling ports (SP1-13), one sampling port was installed before (SP0) and one after (SP14) the column. Oxygen, temperature (T) and pH were measured in flow-through cells (F). Samples were taken in counter current mode from top to bottom during sampling events. Modified from Diem et al., 2013.

Table S3.1. Composition of feed waters used for the column experiments. Thur River waters were collected at the Thur River field site (Diem et al., 2013). Treated wastewater effluent (called effluent) was collected at the wastewater treatment plant Dübendorf Neugut.

Experiment	Feed water and sampling date (day/month/year)	DOC mg C/L	Alkalinity mM	pH	NO <sub>2</sub> <sup>-</sup> μg N/L	NH <sub>4</sub> <sup>+</sup> μg N/L	NO <sub>3</sub> <sup>-</sup> mg N/L	Cl <sup>-</sup> mg/L	SO <sub>4</sub> <sup>2-</sup> mg/L	Na <sup>+</sup> mg/L	K <sup>+</sup> mg/L	Ca <sup>2+</sup> mg/L	Mg <sup>2+</sup> mg/L	PO <sub>4</sub> <sup>3-</sup> μg P/L
(1.1) Thur River water/effluent mixtures (%%)	Thur River water/effluent mixtures													
90/10	10.08.2011/11.07.2011	2.6	4.3	8.0	3.8	5.2	1.4	9.6	9.6	11.5	2.0	67.5	11.2	42.1
80/20	10.08.2011/29.08.2011	3.0	4.1	8.0	3.6	5.2	1.3	9.3	14.2	17.2	2.2	59.8	9.9	40.4
70/30	10.08.2011/29.08.2011	3.5	3.9	8.0	3.5	3.3	1.2	8.7	20.0	25.8	2.6	52.3	8.7	55.5
60/40	10.08.2011/13.09.2011	3.9	3.7	8.0	3.2	2.8	1.0	8.2	24.2	32.0	2.9	44.8	7.4	61.5
(1.2) Variation of flow rate	Thur River water													
1.0	16.02.2011	2.1	4.8	8.0	29.4	85.0	3.4	26.0	13.1	16.5	3.1	78.9	16.8	18.8
	24.03.2011	2.2	4.6	8.0	12.5	56.2	2.6	18.2	10.4	11.8	2.5	73.7	13.9	26.1
	20.04.2011	2.0	4.2	8.0	32.0	14.3	2.9	24.5	12.5	16.9	3.0	72.9	14.3	32.5
0.33	08.11.2011	2.4	5.0	8.0	3.7	<5.0	3.6	38.0	17.5	27.3	4.9	80.5	16.6	32.2
0.1, 0.2	06.02.2012	1.7	5.5	8.0	43.0	54.4	3.6	39.0	13.0	18.4	3.1	94.4	18.2	38.6
(2.1) Variation of temperature	Thur River water													
	13.08.2012	2.3	3.8	8.6	9.1	19.0	2.1	25.2	14.0	18.2	3.6	58.9	13.7	14.3
(2.2) Thur River water	Thur River water													
	26.09.2012	2.5	4.6	8.4	2.9	5.5	1.7	11.8	8.0	8.1	2.3	71.2	12.3	26.0
(2.3) Addition of "DOM-free" Thur River water	Treated Thur River water													
	26.09.2012	0.1	4.2	8.3	3.6	6.8	1.4	11.7	7.9	8.2	2.4	66.0	13.0	30.3
(2.4) Addition of acetate	Thur River water													
	07.02.2013	4.2	4.9	8.5	11.0	38.2	2.6	30.2	8.0	20.0	1.8	78.0	13.7	30.7
(2.5) Addition of oxygen- and nitrate-free Thur River water	Treated Thur River water													
	08.03.2013	2.1	4.5	8.4			0.1	138.1	7.0	98.2	<1.0	63.9	10.9	

Table S3.2. Composition of effluent before and after treatment with electrodialysis.

<b>Effluent treatment with electrodialysis</b>	<b>DOC</b> mg C/L	<b>Alkalinity</b> mM	<b>NO<sub>2</sub><sup>-</sup></b> µg N/L	<b>NH<sub>4</sub><sup>+</sup></b> µg N/L	<b>NO<sub>3</sub><sup>-</sup></b> mg N/L	<b>Cl<sup>-</sup></b> mg/L	<b>SO<sub>4</sub><sup>2-</sup></b> mg/L	<b>Na<sup>+</sup></b> mg/L	<b>K<sup>+</sup></b> mg/L	<b>Ca<sup>2+</sup></b> mg/L	<b>Mg<sup>2+</sup></b> mg/L	<b>PO<sub>4</sub><sup>3-</sup></b> µg P/L
Effluent 11.07.2011	4.9	4.4	4.8	14.8	7.2	68.9	31.6	68.1	9.7	69.8	10.6	88.0
After electrodialysis	4.9	1.7	<1.0	9.6	0.3	4.0	30.8	47.9	2.1	3.0	0.8	83.0
Effluent 29.08.2011	5.4	5.4	18.0	22.8	7.7	94.4	42.3	79.2	12.8	91.3	15.0	54.6
After electrodialysis	5.5	2.0	1.1	7.0	0.3	5.5	41.7	56.6	2.8	<5.0	<2.5	51.9
Effluent 13.09.2011	6.4	6.5	16.6	13.2	9.8	129.5	51.0	111.6	17.7	96.5	17.0	103.0
After electrodialysis	6.2	2.4	1.7	<5.0	0.3	5.2	50.0	68.8	4.1	<5.0	<2.5	98.0

Table S3.3. Composition of Thur River water collected on 26.09.2012 before and after treatment with 500 mg/L powdered activated carbon (PAC) (Norit W15 powdered activated carbon, NORIT Deutschland GmbH, Riesbürg, Germany).

<b>River water treatment with PAC</b>	<b>DOC</b> mg C/L	<b>Alkalinity</b> mM	<b>NO<sub>2</sub><sup>-</sup></b> µg N/L	<b>NH<sub>4</sub><sup>+</sup></b> µg N/L	<b>NO<sub>3</sub><sup>-</sup></b> mg N/L	<b>Cl<sup>-</sup></b> mg/L	<b>SO<sub>4</sub><sup>2-</sup></b> mg/L	<b>Na<sup>+</sup></b> mg/L	<b>K<sup>+</sup></b> mg/L	<b>Ca<sup>2+</sup></b> mg/L	<b>Mg<sup>2+</sup></b> mg/L	<b>PO<sub>4</sub><sup>3-</sup></b> µg P/L
River water	2.5	4.6	2.9	5.5	1.7	11.8	8.0	8.1	2.3	71.2	12.3	26.0
After treatment with PAC	0.1	4.2	3.6	6.8	1.4	11.7	7.9	8.2	2.4	66.0	13.0	30.3

Table S3.4. Composition of Thur River water collected on 08.03.2013 before and after treatment with electrodialysis and re-mineralization by addition of NaHCO<sub>3</sub> (300 mg/L final concentration), CaCl<sub>2</sub> x 6 H<sub>2</sub>O (350 mg/L final concentration) and MgCl<sub>2</sub> x 6 H<sub>2</sub>O (85 mg/L final concentration).

<b>River water treatment with electrodialysis</b>	<b>DOC</b> mg C/L	<b>Alkalinity</b> mM	<b>NO<sub>2</sub><sup>-</sup></b> µg N/L	<b>NH<sub>4</sub><sup>+</sup></b> µg N/L	<b>NO<sub>3</sub><sup>-</sup></b> mg N/L	<b>Cl<sup>-</sup></b> mg/L	<b>SO<sub>4</sub><sup>2-</sup></b> mg/L	<b>Na<sup>+</sup></b> mg/L	<b>K<sup>+</sup></b> mg/L	<b>Ca<sup>2+</sup></b> mg/L	<b>Mg<sup>2+</sup></b> mg/L	<b>PO<sub>4</sub><sup>3-</sup></b> µg P/L
River water	2.2	4.0	9.5	8.2	2.3	14.1	7.0	8.4	1.8	63.7	11.3	14.0
After electrodialysis	2.1	1.0			0.1	1.1	7.0	16.8	<1.0	<5.0	<2.5	
After electrodialysis and re-mineralization	2.1	4.5			0.1	138.1	7.0	98.2	<1.0	63.9	10.9	

Table S3.5. Mn(II) speciation in the column calculated by the chemical equilibrium modeling program ChemEQL V3.0 (Mueller, 2004). The initial  $\text{Mn}^{2+}$  concentration was calculated by the solubility product of rhodochrosite ( $\text{MnCO}_3$ ) ( $\text{Mn}^{2+} + \text{CO}_3^{2-} = \text{MnCO}_3$ ;  $\log K = -10.39$ , (Stumm and Morgan, 1996)) at pH 8.2 (for calculations, see Section 3.2.4). The main Mn(II) species are  $\text{Mn}^{2+}$  and  $\text{MnCO}_3$  (aq) (highlighted in rectangles).

Species	Concentration [M]
$\text{Ca}^{2+}$	$1.60 \times 10^{-3}$
$\text{CaOH}^+$	$4.21 \times 10^{-8}$
$\text{CaCO}_3$ (aq)	$8.86 \times 10^{-5}$
$\text{CaHCO}_3^+$	$9.28 \times 10^{-5}$
$\text{Mn}^{2+}$	$1.22 \times 10^{-6}$
$\text{MnOH}^+$	$4.86 \times 10^{-9}$
$\text{Mn}(\text{OH})_2$ (aq)	$1.93 \times 10^{-12}$
$\text{Mn}(\text{OH})_3^-$	$7.70 \times 10^{-17}$
$\text{Mn}(\text{OH})_4^{2-}$	$3.86 \times 10^{-22}$
$\text{Mn}_2\text{OH}^{3+}$	$5.93 \times 10^{-15}$
$\text{Mn}_2(\text{OH})_3^+$	$7.46 \times 10^{-12}$
$\text{MnCO}_3$ (aq)	$3.23 \times 10^{-6}$
$\text{MnHCO}_3^+$	$4.89 \times 10^{-7}$
$\text{H}_2\text{CO}_3$ (aq)	$6.36 \times 10^{-5}$
$\text{HCO}_3^-$	$4.50 \times 10^{-3}$
$\text{CO}_3^{2-}$	$3.34 \times 10^{-5}$
$\text{OH}^-$	$1.59 \times 10^{-6}$
$\text{H}^+$	$6.31 \times 10^{-9}$
Species	Initial Concentration [M]
$\text{Ca}^{2+}$	$1.60 \times 10^{-3}$
$\text{Mn}^{2+}$	$1.22 \times 10^{-6}$
$\text{HCO}_3^-$	$4.50 \times 10^{-3}$
$\text{H}^+$	$6.31 \times 10^{-9}$

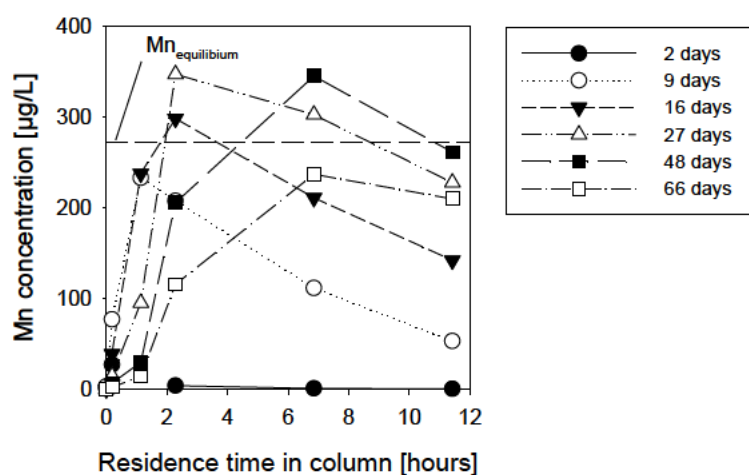


Fig. S3.2. Profiles of Mn(II) concentration as a function of residence time after 2, 9, 16, 27, 48 and 66 days of the experiment at 20°C and at a flow rate of 0.3 mL/min. Data points refer to SP0, SP1, SP5, SP8, SP11 and SP14. The Mn(II) concentration in equilibrium with rhodochrosite ( $\text{MnCO}_3$ ) is shown with the dashed line (for calculations, see Section 3.2.4).



# **Chapter 4**

## **Characterization and source identification of particulate organic matter by preparative thermochemolysis-GC-MS**

Rudolf von Rohr, M.; Hering, J. G.; Kohler, H.-P. E.; Grasset, L.; von Gunten, U.,  
Characterization and source identification of particulate organic matter by preparative  
thermochemolysis-GC-MS. In preparation for submission.

**Abstract**

Particulate organic matter (POM) associated with riverbed sediments can be an important driver for the microbial respiration during riverbank filtration. In this study, we characterized the molecular composition of POM by preparative thermochemolysis coupled to gas chromatography-mass spectrometry to elucidate its potential origins. POM samples from various sources relevant to a river-infiltration system in NE-Switzerland including sand from a gravel bar, riverbed sediment, macrophytes, periphyton, soil and sludge from a wastewater treatment plant (WWTP) as well as solids collected by filtering river water and a WWTP effluent were investigated. The main biomolecules detected were fatty acid methyl esters (FAMES) derived from lipids, permethylated deoxy aldonic acids from carbohydrates and methylated lignin monomers from lignins. Bacterial, vascular plant and aquatic macrophytes contributions to POM were assessed on the basis of various ratios (e.g., branched/C<sub>16</sub> for FAMES, fucose/glucose for carbohydrates, syringyl/guaiacyl for lignins). Data from the FAMES and carbohydrates showed a bacterial signature for riverbed sediment POM and a macrophytes signature for the river water POM. The POM signatures of sand collected from a gravel bar and subsequently used in a laboratory column experiment were compared with the POM signatures of the other samples for all of the biological markers examined. Although no single predominant source for the sand POM could be identified, a shift in the carbohydrate and lignin signatures in the column sand (which was run for ~2 years with river water) as compared with the original sand indicated that the POM composition was altered by bacterial processes that were observed in the column experiments under aerobic and anaerobic conditions.

Keywords: pyrolysis-GC-MS, TMAH, tracer molecule, particulate organic matter, soil organic matter, biogeochemical processes

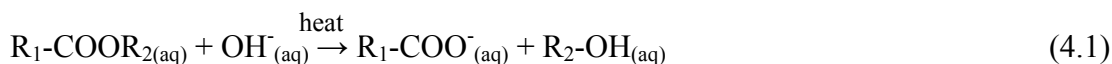
## 4.1 Introduction

During the infiltration of river water into an aquifer, natural organic matter (NOM) is retained in riverbed sediments, acting as a substrate for bacterial growth (Pusch et al., 1998). The origin of the retained NOM can either be autochthonous, i.e. produced in the river by primary production (e.g., algae, aquatic macrophytes or benthic phytoplankton) or allochthonous, i.e. coming from the terrestrial environment (e.g., soil) or a mix thereof (Pusch et al., 1998). Another source of NOM in riverbed sediments can be anthropogenic, for instance from discharge of wastewater effluents. The quality of the drinking water derived from river infiltration depends on the filtration efficiency for particles and microorganisms and on the biogeochemical processes (i.e., aerobic respiration, denitrification, Mn(III/IV)/Fe(III) reduction, etc.) occurring at the river-sediment interface. It has been demonstrated that particulate organic matter (POM) associated with riverbed sediments is the major electron donor for the biogeochemical processes in field studies (Grischek et al., 1998; Brugger et al., 2001; Massmann et al., 2006; Diem et al., 2013) and in column studies (Rudolf von Rohr et al., 2014). Since POM is an important driver for redox processes occurring during riverbank filtration, knowledge about its composition and source is of interest.

Pyrolysis techniques have been applied to gain qualitative information on the molecular composition of NOM in soils (Vancampenhout et al., 2008; Grasset et al., 2009), river and lake sediments (Carrie et al., 2009; Steinberg et al., 2009; Micić et al., 2011) and rivers (Frazier et al., 2005; Berwick et al., 2010). Among the pyrolysis techniques, thermochemolysis has been frequently used because it is more selective in breaking specific ester and ether bonds than conventional pyrolysis techniques (Shadkami and Helleur, 2010). Moreover, another advantage of thermochemolysis is that most acidic functional groups can be derivatized and less fragments are formed due to lower temperatures (~400°C) (Shadkami and Helleur, 2010).

During preparative (or off-line) thermochemolysis, samples are subjected to a stepwise treatment, which is conducted manually, as opposed to on-line thermochemolysis, in which samples are injected into an automatic pyrolysis-GC-MS device. With preparative thermochemolysis, it is possible to treat a large sample mass (>1 g) without pre-treatment, which is advantageous for samples with a low organic carbon content (Grasset and Amblès, 1998). Tetramethylammonium hydroxide (TMAH) is generally applied as thermochemolysis reagent because of its strong alkylating properties and because it produces only minor secondary reactions avoiding decarboxylation (Del Rio et al., 1998; Shadkami and Helleur, 2010). Joll et al. (2004) provide a comparative study to assess various thermochemolysis reagents suited for different purposes.

The reaction mechanism of TMAH-thermochemolysis involves hydrolysis of specific ester or ether bonds present in NOM by  $\text{OH}^-$  originating from TMAH ( $(\text{CH}_3)_4\text{N}^+\text{OH}^-$ ) (Eq. 4.1), (Challinor, 2001), followed by an alkylating reaction of the hydrolysis products by TMAH (Eq. 4.2) (Shadkami and Helleur, 2010).



In Eq. 4.1,  $\text{R}_1\text{-COOR}_{2(\text{aq})}$  represents a hydrolysable molecule with an ester bond (such as a lipid, see Fig. S4.1). Heat is used in both reactions (Eq. 4.1 and 4.2) to initiate the hydrolysis and the alkylating processes, respectively. As a result of TMAH-thermochemolysis, less polar and alkylated thermochemolysis products are formed, which can easily be analysed by GC-MS (Shadkami and Helleur, 2010).

Several classes of biomolecules can be identified through thermochemolysis followed by GC-MS, such as lipids, in the form of fatty acid methyl esters (Frazier et al., 2003; Frazier et al., 2005; Grasset et al., 2009), carbohydrates, in the form of permethylated deoxy aldonic acids (Fabbri and Helleur, 1999; Grasset et al., 2009; Estournel-Pelardy et al., 2011), lignin monomers, in the form of methyl esters of aromatic carboxylic acids (Challinor, 1995; Filley et al., 1999; Wysocki et al., 2008; Steinberg et al., 2009), amino acids (Zang et al., 2001; Riboulleau et al., 2002) and nucleic acids (Abbas-Hawks et al., 1996). Fig. S4.1, S4.2 and S4.3 show the reactions occurring during TMAH-thermochemolysis of lipids, carbohydrates and lignins, respectively.

Since thermochemolysis is a qualitative method for NOM characterization, different indicators and ratios are commonly used to gain more information about the molecular composition and origin of each class of biomolecules. For lipids, the presence of short-chain and branched fatty acids (as methyl esters) suggests a bacterial origin (Zelles, 1999; Drenovsky et al., 2004), while long-chain fatty acids indicate a vascular plant origin (higher plants, including angiosperms, i.e. flowering plants, such as grasses and gymnosperms, i.e., woody plants, such as conifers) (Kolattukudy et al., 1976).

For carbohydrates, ratios of xylose/glucose and fucose/glucose are commonly used to discriminate between vascular plant and bacterial origin, respectively (Rumpel and Dignac, 2006; Grasset et al., 2009). As lignins are decomposed very slowly in the environment, their degradation fragments and phenolic components can be preserved, thereby providing

information about their origin (Steinberg et al., 2009). Different ratios of lignin subunits are used to describe the vegetation type (syringyl/guaiacyl (Harris and Hartley, 1980)) and the contribution of woody and non-woody tissues (cinnamyl/guaiacyl (Hedges and Mann, 1979)). Moreover, the acid/aldehyde-ratio of guaiacyl lignin subunits (G6/G4) is used to estimate the degree of lignin degradation (Hedges and Mann, 1979).

The objectives of the present study are: (i) To assess the origin of POM associated with sand samples from a gravel bar in the infiltration zone of the Thur River (NE-Switzerland) and from a column experiment based on the molecular composition of various possible POM sources (riverbed sediment, river water, macrophytes, periphyton, soil and wastewater effluent) by preparative TMAH-thermochemolysis-GC-MS. (ii) To assess changes in the POM composition of sand samples from a column, which was operated with Thur River water for ~2 years under aerobic and anaerobic conditions.

## 4.2 Materials and Methods

### 4.2.1 Samples collection and preparation

Samples were collected at a selected site at the Thur River infiltration system in Niederneunforn (Diem et al., 2013) and at the wastewater treatment plant in Frauenfeld, both located in NE-Switzerland (Fig. 4.1a, Table 4.1). The peri-alpine Thur River features a very dynamic discharge regime, because of the absence of retention basins along the whole course of the river. The North-West side of the Thur River field site is characterized by a succession of four distinct zones, which are the result of restoration measures (Peter et al., 2012): gravel bar (rarely inundated), grass, willow bush and alluvial forest (Fig. 4.1b).

A sand sample taken from a gravel bar at the sampling location “Sa” (Fig. 4.1b) was used as reference material for POM associated with riverbed sediments and was air-dried prior to thermochemolysis. The same sand material has been used to study the biogeochemical processes occurring during river infiltration in laboratory column experiments (Rudolf von Rohr et al., 2014). In these column experiments conducted under aerobic and anaerobic conditions it could be shown that POM associated with the sand material acted as the main substrate and electron donor for biogeochemical processes (i.e., aerobic respiration, denitrification, Mn(III/IV) reduction) (Rudolf von Rohr et al., 2014). Sand samples (SP6-8, SP9, SP10 and SP11, see Table 4.1) from a column run under aerobic and anaerobic conditions were taken after an operation time of ~2 years (Rudolf von Rohr et al., 2014) and air-dried prior to thermochemolysis. To differentiate between the sand sample taken at the sampling location

“Sa” and the sand from the column experiment, the former sample is called pristine sand and the latter column sand.

Two riverbed sediment (RS1 and RS2) samples were collected from the top 1-5 cm of the sediment and two soil (S1 and S2) samples from the top 5-10 cm of the soil, air-dried in laboratory and sieved to achieve specific grain-size fractions (0.063-0.125 mm, 0.125-0.250 mm and 0.250-0.500 mm) prior to thermochemolysis. The sand, riverbed sediment and soil samples were mainly composed of sandy gravel with little silt and clay. Aquatic macrophytes of 3-4 cm in length were detached manually from the riverbed and periphyton samples were scratched away from submerged stones with a laboratory spatula. A wastewater sludge sample was taken from the digestion tower at the wastewater treatment plant in Frauenfeld (Fig. S4.4). These three samples were air-dried and ground in an agate mortar prior to thermochemolysis. For the liquid samples (Thur River water and treated wastewater effluent from the wastewater treatment plant in Frauenfeld), about 2 L were filtered through a 0.7  $\mu\text{m}$  GF/F Whatman microfiber glass filter, which was air-dried thereafter and cut into small stripes of 1-2 cm in length prior to thermochemolysis.

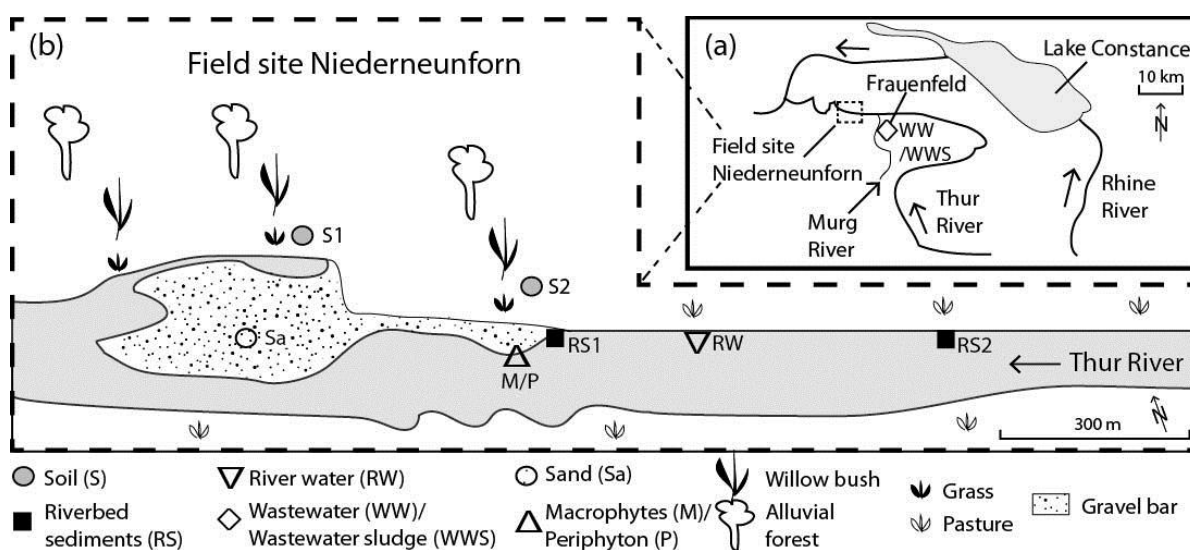


Fig. 4.1. (a) Field site at the Thur River in Niederneunforn and sampling location (◇) at the wastewater treatment plant in Frauenfeld, both in NE-Switzerland. (b) Enlargement of the field site in Niederneunforn with sampling locations. Adapted from Diem et al., 2013.

Table 4.1. Description of samples subjected to thermochemolysis including grain-size fraction, organic carbon and total nitrogen content.

Sample name	Sample description	Grain-size fraction [mm]	Organic C [% w/w]	Total N [% w/w]
Macrophytes (M)	Aquatic macrophytes (3-4 cm) on the riverbed (benthic zone)		~ 25-29*	n.d.
Periphyton (P)	“Biofilm” on stones in the benthic zone		1.9	0.2
River water (RW)	Glass fiber filter (0.7 µm) after filtration of 2 L Thur River water		n.d.	n.d.
Pristine sand (Sa)	Sediment from gravel bar	0.125-0.250	0.3	<0.1
Column sand	Sampling Port (SP) 6-8 (merging of SP6, SP7 and SP8)	0.125-0.250	0.2	<0.1
	SP9	0.125-0.250	n.d.	<0.1
	SP10	0.125-0.250	n.d.	<0.1
	SP11	0.125-0.250	0.1	<0.1
Riverbed sediment1 (RS1)	Sediment (first 1-5 cm) from riverbed near gravel bar	0.063-0.125	0.8	n.d.
		0.125-0.250	0.6	n.d.
Riverbed sediment2 (RS2)	Sediment (first 1-5 cm) from riverbed near pasture zone	0.063-0.125	0.2	n.d.
		0.125-0.250	0.1	n.d.
Soil1 (S1)	Soil (first 5-10 cm) from grass/willow bush zone	0.063-0.125	0.8	0.1
		0.125-0.250	0.8	0.1
		0.250-0.500	1.2	0.1
Soil2 (S2)	Soil (first 5-10 cm) from grass/willow bush zone, about 400 m upstream compared to Soil1 sample	0.063-0.125	1.2	0.1
		0.125-0.250	0.7	0.1
		0.250-0.500	1.3	0.1
Wastewater Frauenfeld (WW)	Glass fiber filter (0.7 µm) after filtration of 2 L treated wastewater effluent		n.d.	n.d.
Wastewater sludge Frauenfeld (WWS)	Wastewater sludge from digestion tower		~ 50**	n.d.

n.d.: not determined \* according to Richter and Gross (2013) \*\*according to Gujer (1999)

### 4.2.2 Wastewater treatment plant Frauenfeld

The wastewater treatment plant in Frauenfeld (NE-Switzerland) treats communal and industrial wastewater for about 100'000 population equivalents. The plant consists of a primary sedimentation process at the beginning (Fig. S4.4). One part of the wastewater effluent is then diverted into the trickling filters (nitrification), while the other is directly introduced into the activated sludge treatment (mixing and aeration). After secondary sedimentation, the treated wastewater effluent is discharged into the Murg River, which is a tributary to the Thur River (distance of < 1 km). A wastewater effluent sample (about 2 L) was taken after secondary sedimentation (Fig. S4.4).

Concerning the wastewater sludge flow, activated sludge mixes with excess sludge coming from the sedimentation after the trickling filters and is collected in the digestion tower (35°C) together with sludge from the primary sedimentation. Here it is digested anaerobically for about 25 days before disposal. A wastewater sludge sample was taken from the digestion tower after these 25 days (Fig. S4.4).

### 4.2.3 Analytical methods

The organic carbon content of the samples was determined by subtracting the inorganic carbon content, measured with a CO<sub>2</sub> Coulometer CM5015 (UIC Inc., Joilet, USA), from the total carbon, measured with a CNS analyzer Eurovector EA3000 (Hekatech GmbH, Wegberg, Germany). Total nitrogen was also measured with a CNS analyzer Eurovector EA3000 (Hekatech GmbH, Wegberg, Germany).

### 4.2.4 Preparative thermochemolysis

Preparative thermochemolysis was conducted according to the method developed by Grasset and Amblès (1998), allowing the treatment of a large sample mass (>1 g) without pre-treatment. One to seven grams of sample was thoroughly mixed with 2 mL of a 50% (w/w) methanol (gradient grade) solution of tetramethylammonium hydroxide pentahydrate (TMAH) (Acros organics) for 30 minutes in a ceramic boat. After that, the ceramic boat was transferred in a 60 x 3 cm (inner diameter) Pyrex<sup>®</sup> tube and heated in a tubular oven Thermolyne 21100 (Barnstead/Thermolyne, Dubuque, USA) at 400°C for 30 minutes (isothermal period). The tube was continuously flushed by nitrogen at a flow rate of 100 mL/min to collect the volatile thermochemolysis products in a glass flask containing chloroform cooled at 0°C. Chloroform was subsequently removed with a rotary evaporator (Büchi labor-technik AG, Flawil,



Switzerland) and the trapped thermochemolysis products recuperated in a vial by addition of a few millilitres of chloroform for GC-MS analysis.

#### 4.2.5 Gas chromatography – mass spectrometry (GC-MS)

The thermochemolysis products were measured by capillary GC on a Trace GC Thermo Finnigan (split injector at 250°C, flame ionization detector at 300°C) coupled to a Thermo Finnigan Automass. The Trace GC Thermo Finnigan featured a fused silica capillary column (SGE BPX 5%, 30 m length, 0.25 mm inner diameter, 0.25  $\mu\text{m}$  film thickness) with helium as carrier gas. The heating of the GC was programmed from 60 to 300°C at 5  $^{\circ}\text{C min}^{-1}$  (isothermally for final 20 min). The MS was operated in the electron impact mode with a 70 eV's ion source energy. Ion separation was conducted in a quadripolar mass filter. The specific thermochemolysis products were identified according to their GC retention times, their mass spectra and literature data. Peak integration was performed in the selected ion chromatogram at  $m/z$  74 for fatty acid methyl esters derived from fatty acids (see Fig. S4.1 for structure), at  $m/z$  129 for permethylated deoxy aldonic acids derived from carbohydrates (see Fig. S4.2 for structure) and in the total ion chromatogram for lignin monomers. Due to difficulties in the assignment and integration of the peaks for the G4 lignin monomer for the column sand samples (P6-8, P9, P10, P11), the analytical error was  $\sim 20\%$ , whereas it was  $< \sim 10\%$  for all other samples. For all other detected compounds, the analytical error was  $< \sim 10\%$ .

#### 4.2.6 Web charts

To assess the origin of POM associated with the pristine and column sand samples, web charts were used. The web charts were constructed based on the proximity of the sand samples to the POM source samples for each biological marker (FAMES, carbohydrates and lignins) according to the procedure shown in Fig. S4.7. Firstly, average values of the specific ratios (e.g.,  $(\text{C}_{12}\text{-C}_{20})/(\text{C}_{12}\text{-C}_{30})$ - and branched/ $\text{C}_{16}$ -ratios) were calculated for the riverbed sediment and soil samples. Then, vectors from the sand samples to the individual POM source samples were established and their lengths calculated. The lengths were expressed as relative distances by normalizing them to the maximum length. Finally, to assign a higher number for a close proximity of the sand samples to the POM source samples, the normalized values were subtracted from one. The web charts for the column sand were constructed by averaging the ratios of the corresponding biomarkers.

## **4.3 Results and Discussion**

### **4.3.1 Bulk organic parameters**

The organic carbon content of the pristine sand, column sand and riverbed sediment RS2 samples was  $\leq 0.3\%$  (w/w), whereas it was higher for the riverbed sediment RS1 (0.6-0.8% (w/w)), soil (0.7-1.3 % (w/w)) and periphyton samples (1.9% (w/w)) (Table 4.1). The values for the pristine sand and riverbed sediment samples were in a similar range as in a previous study conducted at the same field site (Diem et al., 2013). No clear correlation between the grain-size fractions and the organic carbon content could be observed for the riverbed sediment and the soil samples. For the macrophytes and wastewater sludge samples, organic carbon contents of ~25-29% and ~50% (dry weight), respectively, are assumed based on literature (Gujer, 1999; Richter and Gross, 2013).

### **4.3.2 Thermochemolysis products**

The chromatograms of the thermochemolysis products derived by GC-MS analysis for the pristine sand showed series of fatty acids, as fatty acid methyl esters (FAMES) (Fig. 4.2a), permethylated deoxy aldonic acids derived from carbohydrates (i.e., glucose (Glu), galactose (Gal), xylose (Xyl), rhamnose (Rha) and fucose (Fuc)) (Fig. 4.2b) and various ligneous subunits (e.g., G6, G7, G8, S7) (Fig. 4.2c). Based on the obtained results, we focus the analysis of the thermochemolysis products of all other samples on these biological markers (FAMES, carbohydrates and lignins).

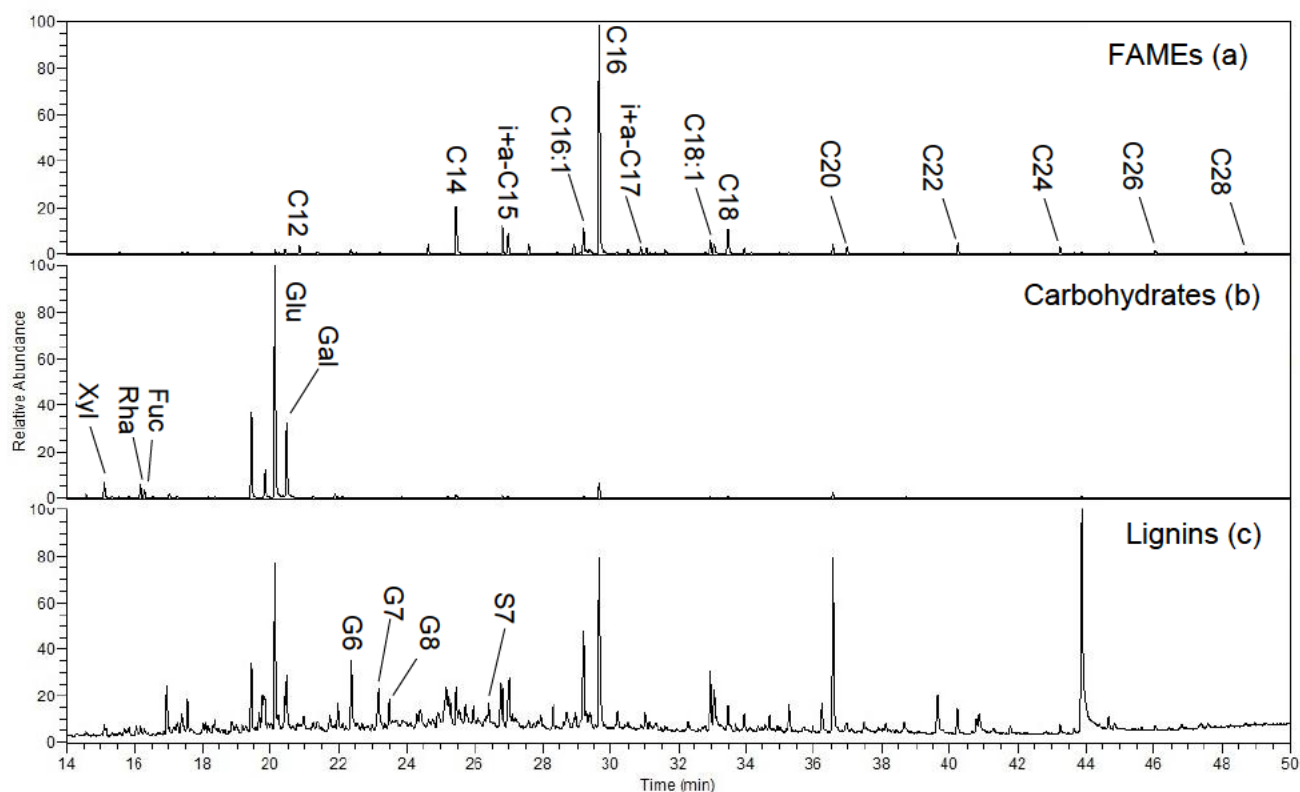


Fig. 4.2. Extracted ion chromatograms for fragments (a)  $m/z$  74 for fatty acid methyl esters (FAMES), (b)  $m/z$  129 for permethylated deoxy aldonic acids and (c) total ion chromatogram (TIC) for ligneous subunits of the thermochemolysis products of the pristine sand sample (“Sa” in Fig. 4.1b). C<sub>16:1</sub> refers to a C<sub>16</sub> FAME with one unsaturation, i+a-C<sub>15</sub> to C<sub>15</sub> FAMES containing a methyl group in iso and anteiso position, respectively (see Fig. S4.5 for structures). Glu: glucose, Gal: galactose, Xyl: xylose, Rha: rhamnose, Fuc: fucose. G6-8 represent guaiacyl-type and S7 syringyl-type lignins (see Fig. S4.6 for structures).

#### *Fatty acid methyl esters (FAMES)*

The distribution pattern of the FAMES showed a predominance of the saturated short-chain members (C<sub>12</sub>-C<sub>20</sub>) over the total FAMES (sum of short- and long-chain FAMES) (Fig. 4.3). A fraction of 1 means that all FAMES are present in a short-chain form (C<sub>12</sub>-C<sub>20</sub>) without any long-chain FAMES (C<sub>22</sub>-C<sub>30</sub>). A slightly higher contribution of long-chain FAMES was observed in the two coarsest grain-size fractions (0.125-0.250 and 0.250-0.500 mm) of the Soil2 samples (Fig. 4.3). Short-chain (C<sub>12</sub>-C<sub>20</sub>) FAMES are rather ubiquitous in the environment and long-chain FAMES ( $\geq$  C<sub>22</sub>) originate from vascular plants (Kolattukudy et al., 1976). Based on these results, it seems that the contribution from vascular plants in the two coarsest Soil2 samples was higher than in the other samples, possibly due to the proximity of these samples to the willow bush zone.

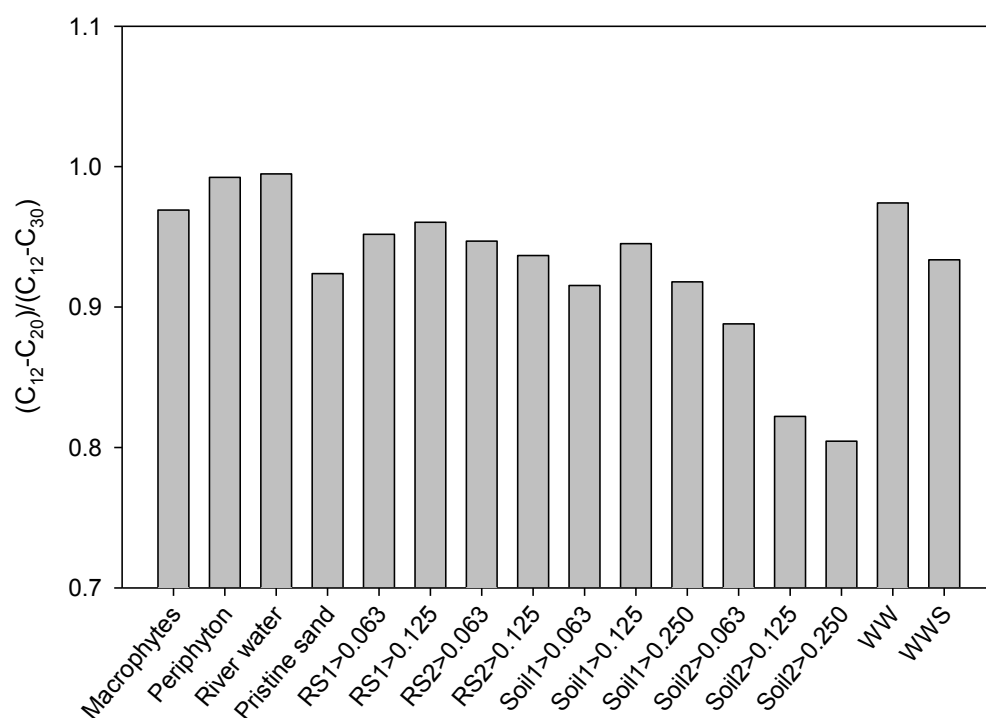


Fig. 4.3. Fraction of short-chain FAMES of selected samples calculated as the ratio of short ( $C_{12}-C_{20}$ ) to short- plus long-chain ( $C_{12}-C_{30}$ ) FAMES. Short-chain FAMES consist of the sum of  $C_{12}$ ,  $C_{14}$ ,  $C_{15}$ ,  $C_{16}$ ,  $C_{17}$ ,  $C_{18}$  and  $C_{20}$  FAMES, long-chain FAMES of the sum of  $C_{22}$ ,  $C_{24}$ ,  $C_{26}$ ,  $C_{28}$  and  $C_{30}$  FAMES. >0.063 denotes the grain-size fraction 0.063-0.125 mm, >0.125 the fraction 0.125-0.250 mm and >0.250 the fraction 0.250-0.500 mm.

The FAMES also showed a minor presence of unsaturated  $C_{16:1}$  and  $C_{18:1}$ , as well as branched iso- and anteiso- $C_{15}$  and iso- and anteiso- $C_{17}$  components (see Fig. 4.2a). Branched FAMES (iso- and anteiso- $C_{15}$  and iso- and anteiso- $C_{17}$  FAMES) are typically of bacterial origin since they can be largely found in Gram-positive and sulphate-reducing Gram-negative bacteria (Zelles, 1999) and their fraction can be expressed as ratio to the  $C_{16}$  FAME, which was the most ubiquitous FAME. Fig. 4.4 shows a plot of the fraction of the branched FAMES (Branched/ $C_{16}$ ) as a function of the fraction of the short-chain FAMES ( $(C_{12}-C_{20})/(C_{12}-C_{30})$ ).

A clustering of the samples can be observed, with the highest fraction of branched FAMES for the riverbed sediments and for the wastewater sludge samples (Fig. 4.4). This suggests that FAMES of these samples had a more pronounced bacterial origin than the other samples. For the wastewater sludge sample the high fraction of the branched FAMES is due to the bacterial origin of activated sludge, whereas for the riverbed sediment samples it could represent an enhanced bacterial activity in the river-groundwater infiltration zone.

The soil samples did not form a clear cluster, since they differed in the fraction of the short-chain FAMES (Fig. 4.4). The pristine sand and column sand samples represent another cluster, which was characterized by a similar fraction of the branched FAMES. This suggests that the sand material used during the column experiment did not change significantly with respect to the FAMES signature compared to the pristine sand. The wastewater sample showed a different FAMES signature (i.e., a lower branched/ $C_{16}$ -ratio) compared to the wastewater sludge sample, which might be related to anaerobic sludge digestion processes (e.g., bacterial hydrolysis and acetogenesis of POM) leading to a higher branched/ $C_{16}$ -ratio for the sludge sample. Finally, river water, macrophytes and periphyton, the latter two representing autochthonous POM, showed the lowest fraction of branched FAMES, indicating that the contribution of bacterial FAMES was low in these samples (Fig. 4.4). Even though periphyton is an assemblage of attached algae and bacteria (Pusch et al., 1998), our FAMES results point towards a rather non-bacterial composition, which shows similarities to the FAMES composition of the macrophytes. The FAMES composition of river water reflects a mixed origin derived from macrophytes and wastewater sources.

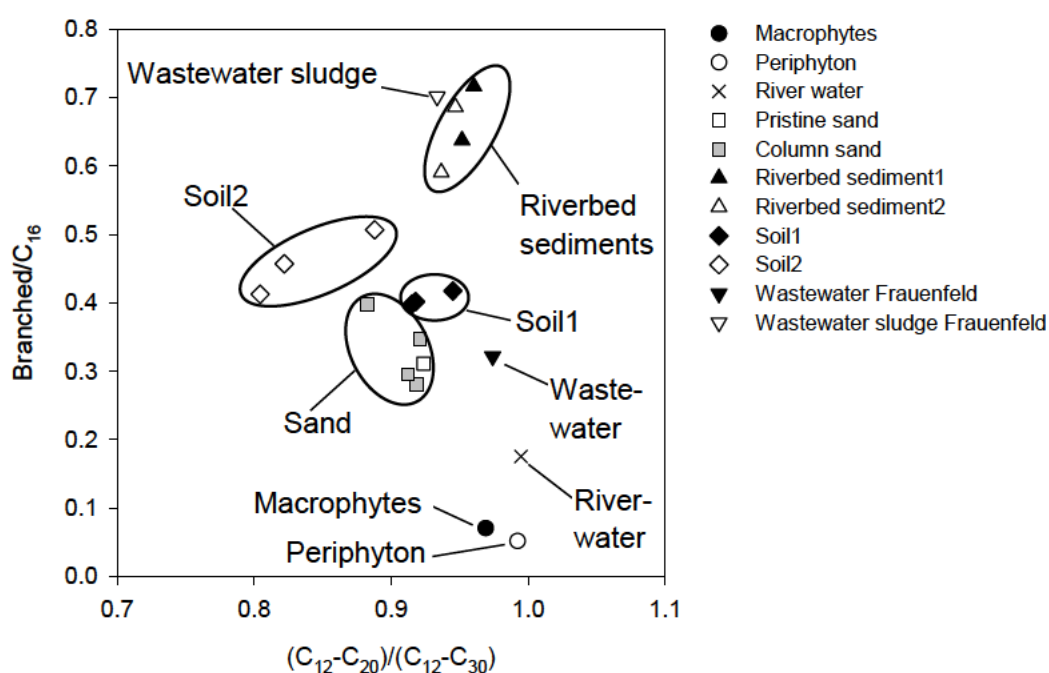


Fig. 4.4. Fraction of branched FAMES (calculated as the ratio of the sum of iso- and anteiso- $C_{15}$  and iso- and anteiso- $C_{17}$  FAMES to  $C_{16}$  FAMES) as a function of the fraction of short-chain FAMES ( $(C_{12}-C_{20})/(C_{12}-C_{30})$ ). Samples are grouped to show qualitative patterns.

*Permethylated deoxy aldonic acids derived from carbohydrates*

Carbohydrates were identified as permethylated deoxy aldonic acids, which are formed under strong alkaline conditions by methylation of mono- and polysaccharides (Fabbri and Helleur, 1999) (see Fig. S4.2). The main permethylated deoxy aldonic acids originated from the monosaccharides glucose (Glu) (most abundant), galactose (Gal), xylose (Xyl), rhamnose (Rha) and fucose (Fuc) (see Fig. 4.2b for ion chromatograms). Their thermochemolysis products give typical ion fragments at  $m/z$  129 in mass spectrometry (see Fig. S4.2), which can be easily identified (Fig. 4.2b). Glucose is present in all living organisms and also in vascular plants and xylose is mainly produced by vascular plants (Wicks et al., 1991). Conversely, fucose is rarely present in vascular plants, but has been found as a storage sugar in bacteria (Cowie and Hedges, 1984). By plotting the Fuc/Glu-ratios against the Xyl/Glu-ratios, a distinction between bacterial and vascular plant carbohydrates can be obtained (Rumpel and Dignac, 2006; Grasset et al., 2009). High Fuc/Glu-ratios suggest carbohydrates of bacterial origin and high Xyl/Glu-ratios indicate carbohydrates of vascular plant origin.

The riverbed sediment samples showed the highest Fuc/Glu- and Xyl/Glu-ratios, suggesting a relatively high bacterial contribution and also an important contribution of vascular plant carbohydrates (Fig. 4.5). The high Fuc/Glu-ratios are in line with the results obtained from the branched FAMES (Fig. 4.4), in which the highest fraction of branched FAMES was also observed for the riverbed sediments. No carbohydrates were observed for the wastewater sludge sample, presumably due to their complete degradation during the anaerobic sludge digestion processes. The soil samples form a cluster with a relatively important contribution of vascular plant carbohydrates (Fig. 4.5). This pattern is in contrast to the FAMES pattern (Fig. 4.4), in which the soil samples showed an important bacterial contribution.

The lowest Fuc/Glu- and Xyl/Glu-ratios were observed for the pristine sand sample, since very low levels of xylose and fucose were detected in this sample (see Fig. 4.2b for ion chromatograms). The pristine sand sample was taken from the surface of a gravel bar and was stored dry until thermochemolysis. Higher ratios could be seen for the column sand samples (Fig. 4.5), which indicates that the composition of the carbohydrates changed during the column operation time of ~2 years with Thur River water. The change in the carbohydrate signature may be attributed to the establishment of a bacterial community after the sand was exposed to aerobic and anaerobic conditions in the laboratory columns over 2 years (Rudolf von Rohr et al., 2014). In contrast, the pristine and the column sand showed similar ratios of branched FAMES and hence did not reflect any change in POM due to microbial activity (Fig. 4.4).

River water and macrophytes form another cluster of similar Fuc/Glu- and Xyl/Glu-ratios (Fig. 4.5), which supports the interpretation of the FAMEs signature (Fig. 4.4) that POM in river water has an important macrophytes contribution. The carbohydrate signature of periphyton indicates a bacterial origin and is quite different from the signature of the macrophytes and river water samples (Fig. 4.5), which is in contrast to the FAMEs results (Fig. 4.4). Overall, the carbohydrate signatures suggest a relatively important bacterial contribution of POM associated with the riverbed sediments and an important macrophytes contribution to river water POM, but no clear pattern can be seen for the soil, periphyton and wastewater samples with regard to their origin (bacterial or vascular plant).

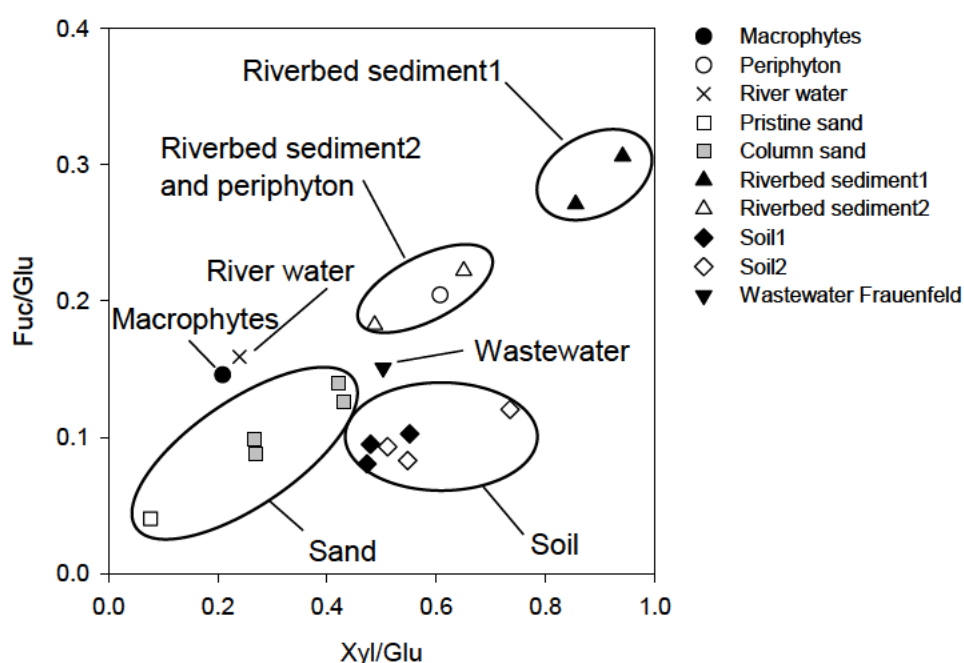


Fig. 4.5. Fraction of fucose (calculated as the ratio of fucose to glucose) as a function of the fraction of xylose (calculated as the ratio of xylose to glucose). High Fuc/Glu-ratios indicate carbohydrates of potentially bacterial origin, high Xyl/Glu-ratios suggest a potentially higher contribution of vascular plants.

*Lignin monomers*

Lignin monomers were identified as their methylated forms and included guaiacyl compounds (G-type), syringyl compounds (S-type) and cinnamyl compounds (C-type) (see Fig. S4.6 for structures), in accordance with previous studies (Challinor, 1995; Martín et al., 1995; McKinney et al., 1995; Hatcher and Minard, 1996; Hatcher et al., 1996; Klap et al., 1998). The most abundant lignin subunit was 3,4-dimethoxybenzoic acid methyl ester (G6), a G-type compound (see Fig. 4.2c for ion chromatograms and Fig. S4.6a for structure). Other detected G-type lignins were G4, G7 and G8 (see Fig. S4.6a for structures). These G-types lignins are present in all vascular (i.e. lignified) plants. The identified S-type lignins were S4, S6, S7 and S8, which can be primarily found in angiosperms, but not in gymnosperms (Steinberg et al., 2009). The main C-type lignins found were *p*-coumaric acid and ferulic acid (see Fig. S4.6c for structures). A plot of the S/G-ratio versus the C/G-ratio was used to describe the contribution of woody and non-woody tissues (C/G-ratio) and the contribution of the vegetation type (S/G-ratio) in plant tissues (Hedges and Mann, 1979). High S/G- and C/G-ratios are indicative of angiosperms and non-woody tissues, respectively, while low S/G- and C/G-ratios suggest a greater contribution of gymnosperms and woody tissues, respectively (Hedges and Mann, 1979).

The riverbed sediment, soil and pristine sand samples form a cluster with similar S/G- and C/G-ratios, suggesting a similar lignin composition and no relevant differences in the vegetation type (Fig. 4.6). The column sand and the river water showed C/G-ratios of zero, due to the absence of C-type lignins. This pattern does not allow the assessment of the woody and non-woody contribution of lignins. Therefore, these two samples were not considered for the assessment of the POM origin of the sand samples, which is discussed later (see Section 4.3.3). For the column sand, microbial degradation of C-type lignins in the column may have caused the shift in the C/G-ratios compared to the pristine sand.

For the macrophytes and periphyton samples, the S/G- and C/G-ratios were quite different compared to the cluster composed of riverbed sediment, soil and pristine sand. This shows that the contribution of POM from macrophytes and periphyton is not so dominant in the pristine sand for this biological marker. The wastewater and the wastewater sludge samples are not shown in Fig. 4.6, because we could not identify G-type lignins in them, which is in accordance with literature (Shon et al., 2006).



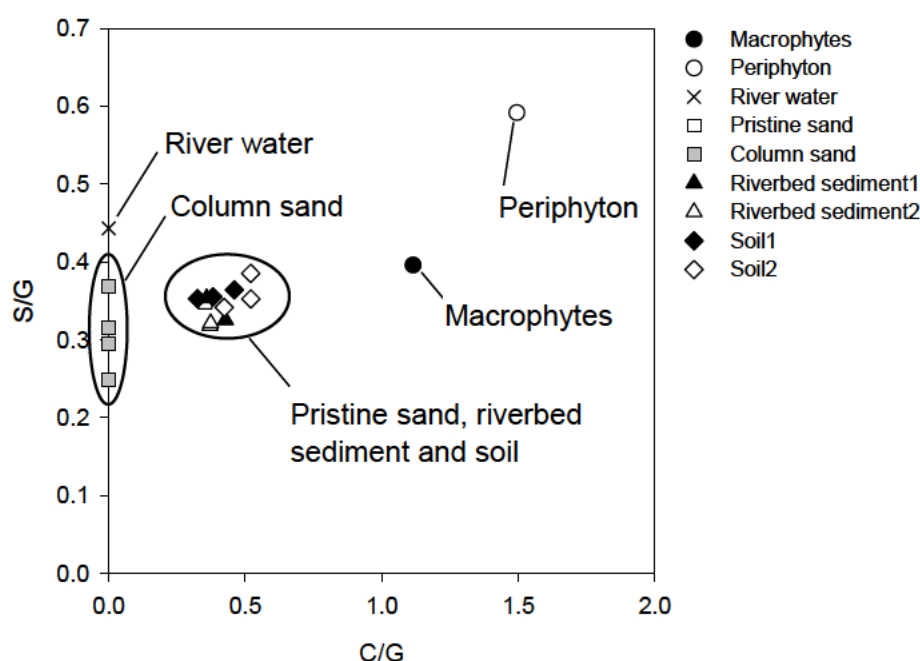


Fig. 4.6. Fraction of S-type lignins (calculated as the ratio of S-type to G-type lignins) as a function of the fraction of C-type lignins (calculated as the ratio of C-type to G-type lignins). High S/G- and C/G-ratios indicate a potentially higher contribution of angiosperms and non-woody tissues for terrestrial samples, respectively, whereas low S/G- and C/G-ratios are indicative of gymnosperms and woody tissues, respectively. S-type lignins were calculated as sum of S4, S6, S7 and S8; G-type lignins as sum of G4, G6, G7 and G8; C-type lignins as sum of *p*-coumaric acid and ferulic acid.

Another indicator commonly used for lignin characterization of terrestrial samples during TMAH-thermochemolysis is the acid/aldehyde ratio between 3,4-dimethoxy benzoic acid methyl ester (G6) and 3,4-dimethoxyl benzaldehyde (G4) (see Fig. S4.6a for structures) (Hedges and Mann, 1979; Frazier et al., 2005; Steinberg et al., 2009). This ratio is used to describe the degree of lignin degradation and either increases during lignin degradation as the aldehyde (G4) is oxidized to the acid (G6) (Hatcher et al., 1996), or decreases as the acid is metabolized (Frazier et al., 2005). Fig. 4.7 illustrates the G6/G4-ratios as a function of the fraction of the G6-type lignin (calculated as the ratio of G6-type lignins to the C<sub>16</sub> FAMES), which was the most abundant lignin subunit.

The riverbed sediment and pristine sand samples form a cluster with a similar degree of lignin degradation and fractions of the G6-type lignin (Fig. 4.7). The soil samples showed the highest G6/C<sub>16</sub>-ratios and a slightly higher degree of lignin degradation than the riverbed

sediment and the pristine sand samples (Fig. 4.7). These high G6/C<sub>16</sub>-ratios could be related to the contribution of vascular plants (e.g., grasses) present near the sampling location. For the column sand samples a high variation of the G6/G4-ratios can be observed, which indicates changes in the degree of lignin degradation during the column experiment (Fig. 4.7). The wastewater and wastewater sludge samples are not shown in Fig. 4.7 because they did not contain any G-type lignins and the river water sample is not shown because it did not contain G6-type lignins. The macrophytes and periphyton samples form a cluster with relatively low G6/C<sub>16</sub>-ratios, indicating a rather low contribution of this lignin subunit (Fig. 4.7).

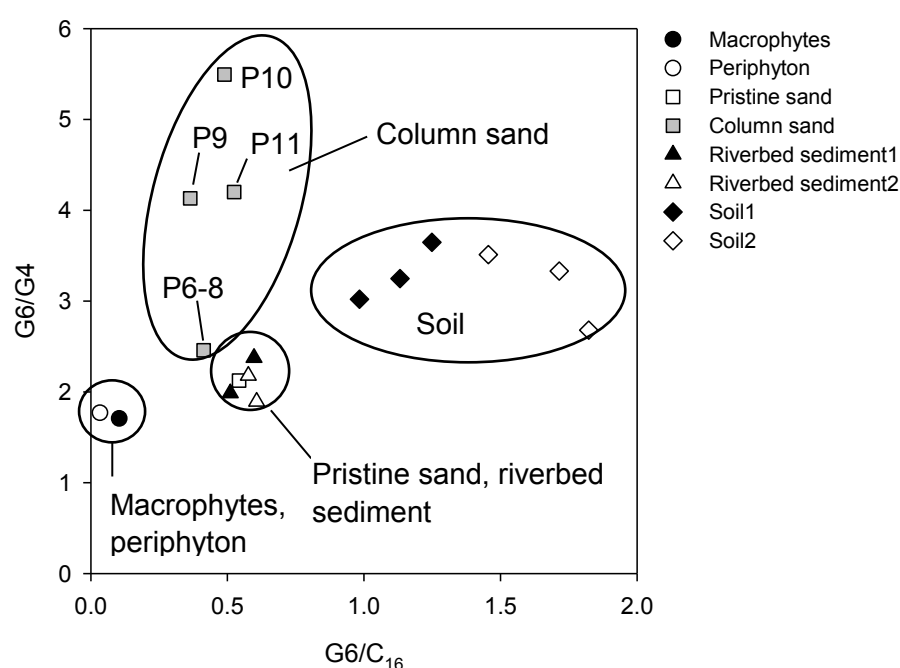


Fig. 4.7. Acid/aldehyde ratios of G-type lignin subunits (G6/G4) as a function of the fraction of the G6-type lignins (calculated as the ratio of G6-type lignins to the C<sub>16</sub> FAMES). High G6/G4-ratios indicate a higher degree of lignin degradation.

### 4.3.3 Origin of POM associated with the sand samples

To assess the origin of POM associated with the sand samples (pristine and column sand), we compared their molecular descriptors with those of the potential POM source samples (i.e., riverbed sediment, river water, macrophytes, periphyton, soil, wastewater) in web charts (see Section 4.2.6 and Fig. S4.7 for explanations).

For the FAMES, no clear trend towards a specific POM origin was observed for the pristine sand, with a relatively equal contribution of the soil, wastewater and river water samples (Fig. 4.8a). The pattern of the column sand did not differ significantly from that of the

pristine sand, suggesting that during the column operation time the composition of the FAMES did not change significantly.

The web chart for the carbohydrates did not reveal a distinct origin of the pristine sand, but prevalently pointed towards the POM source samples macrophytes and river water (Fig. 4.8b). This specific pattern could be related to occasional flooding of the pristine sand, leading to a POM input from the river (i.e., from macrophytes and river water). The column sand showed a shift in the carbohydrate composition as compared to the pristine sand, probably caused by bacterial growth during the column experiments (Rudolf von Rohr et al., 2014).

For the lignins, two web charts were assembled, one referring to Fig. 4.6 (Lignins1) and another to Fig. 4.7 (Lignins2). These web charts show a trend towards a common POM origin of the pristine sand and the riverbed sediments (Fig. 4.8c and 4.8d). In addition, an allochthonous origin (i.e., soil) of the pristine sand could be observed for the lignins1 (Fig. 4.8c), which was not found for the lignins2 (Fig. 4.8d), due to a different lignin signature (see Fig. 4.6 and 4.7). For the column sand web chart, a pronounced shift is observable for the lignins2 (Fig. 4.8d), which was associated with an altered degree of lignin degradation, possibly due to aerobic respiration processes during the column experiments. The web chart for the column sand for the lignins1 is not shown due to the absence of C-type lignins (see Fig. 4.6).

Previous studies have shown a higher contribution of terrestrial NOM (i.e., lignins) in river sediments compared to autochthonous NOM sources (Carrie et al., 2009; Micić et al., 2011). In another investigation, terrestrial runoff was found to largely influence the NOM composition of lake sediments, due to the presence of lignin subunits (Steinberg et al., 2009). To this end, the role of flood events as a driving force for POM replenishment in riverbed sediments was investigated at the Thur River-infiltration site (Diem et al., 2013). A significant correlation between river discharge and oxygen consumption associated with the degradation of POM could be shown in this study. It was concluded that flood events and hence surface runoff, containing soil organic matter, can substantially contribute to POM replenishment in riverbed sediments. Based on our results, we could identify a common POM origin of the pristine sand, riverbed sediment and soil samples, which supports the field-based observations that surface runoff of soil components can be an important source for POM replenishment in gravel bars or riverbed sediments.

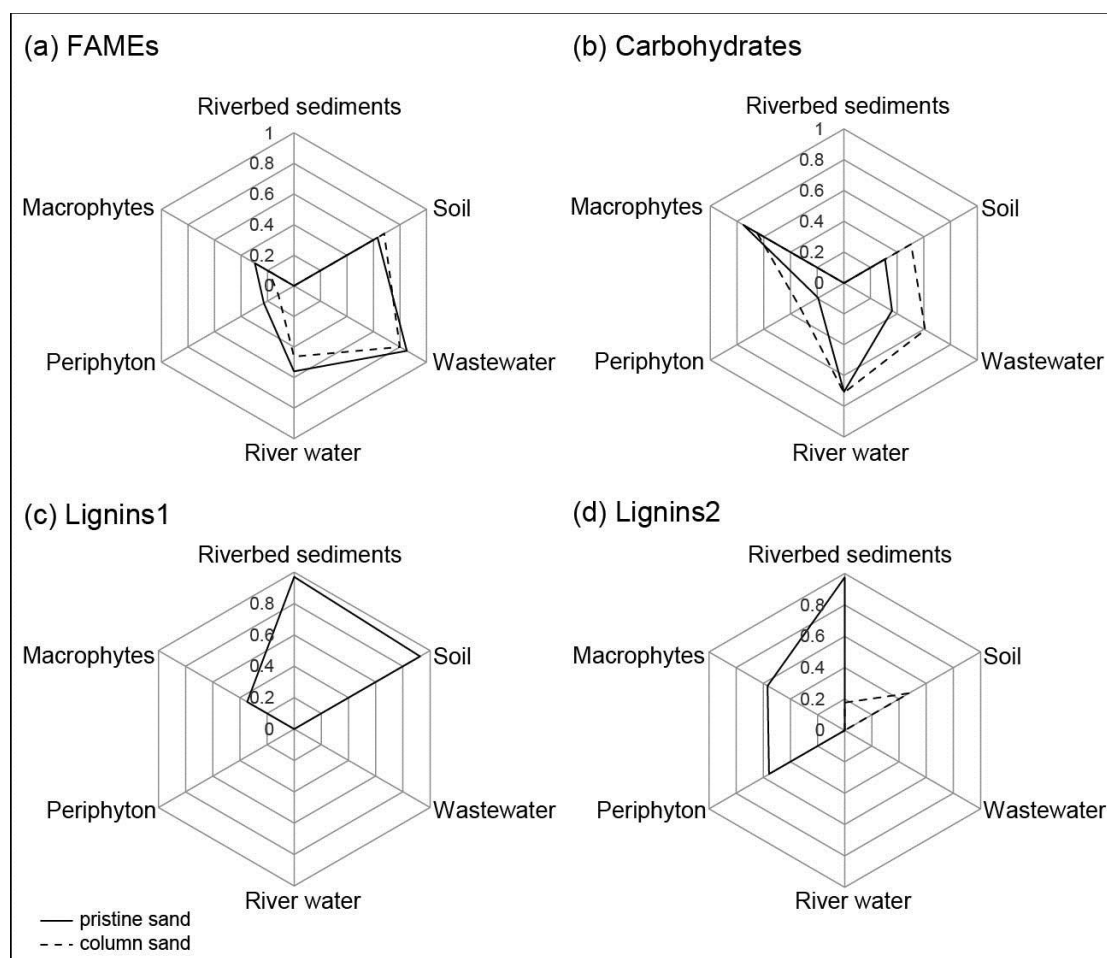


Fig. 4.8. Assessment of POM origin of the pristine (solid lines) and column (dashed lines) sand using web charts for (a) FAMEs, (b) carbohydrates and (c, d) lignins (Lignins1 refer to Fig. 4.6, Lignins2 to Fig. 4.7). Web charts were constructed based on the proximity of POM source samples to the pristine and column sand (see Section 4.2.6 and Fig. S4.7 for explanations). High values imply a close proximity of POM source samples to sand samples, potentially indicating a common origin. For the Lignins1 web chart, values for the column sand and river water samples are missing, due zero values of the C/G-ratios (see Fig. 4.6). Wastewater refers to the “Wastewater Frauenfeld” sample. Non-visible dashed lines mean overlapping with the solid lines.

## 4.4 Conclusion

Particulate organic matter (POM) associated with riverbed sediments and sand from a river-infiltration system has been shown in previous studies to be an important driver for redox processes during riverbank filtration. To gain information about the origin of POM associated with sand samples from a gravel bar and from a laboratory column experiment, we determined the molecular composition of these sand samples and various possible POM sources (riverbed sediment, river water, macrophytes, periphyton, soil and wastewater). To this end, we treated and analysed the samples by preparative TMAH-thermochemolysis-GC-MS and compared the results in web charts. The following conclusions can be drawn from our results:

- Samples with a low organic carbon content ( $< 1\%$  (w/w)) showed clear GC-MS chromatograms, allowing the identification of the thermochemolysis products.
- The main detected biomolecules in all samples were fatty acid methyl esters (FAMES) derived from lipids, permethylated deoxy aldonic acids from carbohydrates and methylated lignin monomers from lignins.
- Specific ratios, such as branched/ $C_{16}$ -, fucose/glucose- and syringyl/guaiacyl-ratios for the FAMES, carbohydrates and lignins were used to assign the samples to a more bacterial, vascular plant or aquatic macrophytes origin.
- Based on the signatures from the FAMES and carbohydrates, POM associated with riverbed sediments showed a predominant bacterial origin, whereas river water POM showed an important contribution of aquatic macrophytes. For all other samples no clear pattern of the POM origin (bacterial, vascular plant, aquatic macrophytes) could be observed.
- Based on the results from the web charts, the POM origin of the sand samples could not be attributed to a specific POM source.
- The most relevant changes in the POM composition of sand samples used in a laboratory column experiment were identified for the carbohydrates and lignins, possibly due to bacterial growth and aerobic respiration processes during the laboratory column experiments, respectively.

## **Acknowledgements**

This study was accomplished within the National Research Program “Sustainable Water Management” (NRP61) and funded by the Swiss National Science Foundation (SNF, Project No. 406140-125856). All thermochemolysis GC-MS experiments were conducted at the Institute of Chemistry, Materials and Natural Resources (IC2MP) of the University of Poitiers. We also would like to thank Irene Brunner for the analytical support for the determination of the bulk organic carbon content of the samples and Marc Boehler for helpful discussions.

## 4.5 References

- Abbas-Hawks, C., Voorhees, K.J., Hadfield, T.L., 1996. In situ methylation of nucleic acids using pyrolysis/mass spectrometry. *Rapid Communications in Mass Spectrometry* 10 (14), 1802-1806.
- Berwick, L., Greenwood, P.F., Smernik, R.J., 2010. The use of MSSV pyrolysis to assist the molecular characterisation of aquatic natural organic matter. *Water Research* 44 (10), 3039-3054.
- Brugger, A., Wett, B., Kolar, I., Reitner, B., Herndl, G.J., 2001. Immobilization and bacterial utilization of dissolved organic carbon entering the riparian zone of the alpine Enns River, Austria. *Aquatic Microbial Ecology* 24 (2), 129-142.
- Carrie, J., Sanei, H., Goodarzi, F., Stern, G., Wang, F., 2009. Characterization of organic matter in surface sediments of the Mackenzie River Basin, Canada. *International Journal of Coal Geology* 77 (3-4), 416-423.
- Challinor, J.M., 1995. Characterisation of wood by pyrolysis derivatisation-gas chromatography/mass spectrometry. *Journal of Analytical and Applied Pyrolysis* 35 (1), 93-107.
- Challinor, J.M., 2001. Review: The development and applications of thermally assisted hydrolysis and methylation reactions. *Journal of Analytical and Applied Pyrolysis* 61 (1-2), 3-34.
- Cowie, G.L., Hedges, J.I., 1984. Carbohydrate sources in a coastal marine environment. *Geochimica et Cosmochimica Acta* 48 (10), 2075-2087.
- Del Rio, J.C., McKinney, D.E., Knicker, H., Nanny, M.A., Minard, R.D., Hatcher, P.G., 1998. Structural characterization of bio- and geo-macromolecules by off-line thermochemolysis with tetramethylammonium hydroxide. *Journal of Chromatography A* 823 (1-2), 433-448.
- Diem, S., Rudolf von Rohr, M., Hering, J.G., Kohler, H.P.E., Schirmer, M., von Gunten, U., 2013. NOM degradation during river infiltration: Effects of the climate variables temperature and discharge. *Water Research* 47 (17), 6585-6595.
- Drenovsky, R.E., Elliott, G.N., Graham, K.J., Scow, K.M., 2004. Comparison of phospholipid fatty acid (PLFA) and total soil fatty acid methyl esters (TSFAME) for characterizing soil microbial communities. *Soil Biology and Biochemistry* 36 (11), 1793-1800.
- Estournel-Pelardy, C., Delarue, F., Grasset, L., Laggoun-Défarge, F., Amblès, A., 2011. Tetramethylammonium hydroxide thermochemolysis for the analysis of cellulose and

- free carbohydrates in a peat bog. *Journal of Analytical and Applied Pyrolysis* 92 (2), 401-406.
- Fabbri, D., Helleur, R., 1999. Characterization of the tetramethylammonium hydroxide thermochemolysis products of carbohydrates. *Journal of Analytical and Applied Pyrolysis* 49 (1), 277-293.
- Filley, T.R., Minard, R.D., Hatcher, P.G., 1999. Tetramethylammonium hydroxide (TMAH) thermochemolysis: proposed mechanisms based upon the application of  $^{13}\text{C}$ -labeled TMAH to a synthetic model lignin dimer. *Organic Geochemistry* 30 (7), 607-621.
- Frazier, S.W., Kaplan, L.A., Hatcher, P.G., 2005. Molecular characterization of biodegradable dissolved organic matter using bioreactors and  $[^{12}\text{C}/^{13}\text{C}]$  tetramethylammonium hydroxide thermochemolysis GC-MS. *Environmental Science and Technology* 39 (6), 1479-1491.
- Frazier, S.W., Nowack, K.O., Goins, K.M., Cannon, F.S., Kaplan, L.A., Hatcher, P.G., 2003. Characterization of organic matter from natural waters using tetramethylammonium hydroxide thermochemolysis GC-MS. *Journal of Analytical and Applied Pyrolysis* 70 (1), 99-128.
- Grasset, L., Amblès, A., 1998. Structural study of soil humic acids and humin using a new preparative thermochemolysis technique. *Journal of Analytical and Applied Pyrolysis* 47 (1), 1-12.
- Grasset, L., Rovira, P., Amblès, A., 2009. TMAH-preparative thermochemolysis for the characterization of organic matter in densimetric fractions of a Mediterranean forest soil. *Journal of Analytical and Applied Pyrolysis* 85 (1-2), 435-441.
- Grischek, T., Hiscock, K.M., Metschies, T., Dennis, P.F., Nestler, W., 1998. Factors affecting denitrification during infiltration of river water into a sand and gravel aquifer in Saxony, Germany. *Water Research* 32 (2), 450-460.
- Gujer, W., 1999. *Siedlungswasserwirtschaft*, Springer Verlag Berlin, Heidelberg.
- Harris, P.J., Hartley, R.D., 1980. Phenolic constituents of the cell-walls of monocotyledons. *Biochemical Systematics and Ecology* 8 (2), 153-160.
- Hatcher, P.G., Minard, R.D., 1996. Comparison of dehydrogenase polymer (DHP) lignin with native lignin from gymnosperm wood by thermochemolysis using tetramethylammonium hydroxide (TMAH). *Organic Geochemistry* 24 (6-7), 593-600.
- Hatcher, P.G., Nanny, M.A., Minard, R.D., Dible, S.D., Carson, D.M., 1996. Comparison of two thermochemolytic methods for the analysis of lignin in decomposing gymnosperm



- wood: the CuO oxidation method and the method of thermochemolysis with tetramethylammonium hydroxide (TMAH). *Organic Geochemistry* 23 (10), 881-888.
- Hedges, J.I., Mann, D.C., 1979. Characterization of plant-tissues by their lignin oxidation-products. *Geochimica et Cosmochimica Acta* 43 (11), 1803-1807.
- Joll, C.A., Couton, D., Heitz, A., Kagi, R.I., 2004. Comparison of reagents for off-line thermochemolysis of natural organic matter. *Organic Geochemistry* 35 (1), 47-59.
- Klap, V.A., Boon, J.J., Hemminga, M.A., Van Soelen, J., 1998. Chemical characterization of lignin preparations of fresh and decomposing *Spartina anglica* by pyrolysis mass spectrometry. *Organic Geochemistry* 28 (11), 707-727.
- Kolattukudy, P.E., Croteau, R., Buckner, J.S., 1976. *Chemistry and Biochemistry of Natural Waxes*, Elsevier, Amsterdam.
- Martín, F., del Río, J.C., González-Vila, F.J., Verdejo, T., 1995. Thermally assisted hydrolysis and alkylation of lignins in the presence of tetra-alkylammonium hydroxides. *Journal of Analytical and Applied Pyrolysis* 35 (1), 1-13.
- Massmann, G., Greskowiak, J., Dunnbier, U., Zuehlke, S., Knappe, A., Pekdeger, A., 2006. The impact of variable temperatures on the redox conditions and the behaviour of pharmaceutical residues during artificial recharge. *Journal of Hydrology* 328 (1-2), 141-156.
- McKinney, D.E., Carson, D.M., Clifford, D.J., Minard, R.D., Hatcher, P.G., 1995. Off-line thermochemolysis versus flash pyrolysis for the in situ methylation of lignin: Is pyrolysis necessary? *Journal of Analytical and Applied Pyrolysis* 34 (1), 41-46.
- Micić, V., Krüge, M.A., Köster, J., Hofmann, T., 2011. Natural, anthropogenic and fossil organic matter in river sediments and suspended particulate matter: A multi-molecular marker approach. *Science of the Total Environment* 409 (5), 905-919.
- Peter, S., Koetzsch, S., Traber, J., Bernasconi, S.M., Wehrli, B., Durisch-Kaiser, E., 2012. Intensified organic carbon dynamics in the ground water of a restored riparian zone. *Freshwater Biology* 57 (8), 1603-1616.
- Pusch, M., Fiebig, I., Brettar, H., Eisenmann, H., Ellis, B.K., Kaplan, L.A., Lock, M.A., Naegeli, M.W., Traunspurger, W., 1998. The role of micro-organisms in the ecological connectivity of running waters. *Freshwater Biology* 40 (3), 453-495.
- Riboulleau, A., Mongenot, T., Baudin, F., Derenne, S., Largeau, C., 2002. Factors controlling the survival of proteinaceous material in Late Tithonian kerogens (Kashpir Oil Shales, Russia). *Organic Geochemistry* 33 (9), 1127-1130.

- Richter, D., Gross, E.M., 2013. Chara can outcompete Myriophyllum under low phosphorus supply. *Aquatic Sciences* 75 (3), 457-467.
- Rudolf von Rohr, M., Hering, J.G., Kohler, H.P.E., von Gunten, U., 2014. Column studies to assess the effects of climate variables on redox processes during riverbank filtration. *Water Research* (submitted for publication).
- Rumpel, C., Dignac, M.F., 2006. Gas chromatographic analysis of monosaccharides in a forest soil profile: Analysis by gas chromatography after trifluoroacetic acid hydrolysis and reduction-acetylation. *Soil Biology and Biochemistry* 38 (6), 1478-1481.
- Shadkani, F., Helleur, R., 2010. Recent applications in analytical thermochemolysis. *Journal of Analytical and Applied Pyrolysis* 89 (1), 2-16.
- Shon, H.K., Vigneswaran, S., Snyder, S.A., 2006. Effluent organic matter (EfOM) in wastewater: Constituents, effects, and treatment. *Critical Reviews in Environmental Science and Technology* 36 (4), 327-374.
- Steinberg, S.M., Nemr, E.L., Rudin, M., 2009. Characterization of the lignin signature in Lake Mead, NV, sediment: Comparison of on-line flash chemopyrolysis (600°C) and off-line chemolysis (250°C). *Environmental Geochemistry and Health* 31 (3), 339-352.
- Vancampenhout, K., Wouters, K., Caus, A., Buurman, P., Swennen, R., Deckers, J., 2008. Fingerprinting of soil organic matter as a proxy for assessing climate and vegetation changes in last interglacial palaeosols (Veldwezelt, Belgium). *Quaternary Research* 69 (1), 145-162.
- Wicks, R.J., Moran, M.A., Pittman, L.J., Hodson, R.E., 1991. Carbohydrate signatures of aquatic macrophytes and their dissolved degradation products as determined by a sensitive high-performance ion chromatography method. *Applied and Environmental Microbiology* 57 (11), 3135-3143.
- Wysocki, L.A., Filley, T.R., Bianchi, T.S., 2008. Comparison of two methods for the analysis of lignin in marine sediments: CuO oxidation versus tetramethylammonium hydroxide (TMAH) thermochemolysis. *Organic Geochemistry* 39 (10), 1454-1461.
- Zang, X., Brown, J.C., Van Heemst, J.D.H., Palumbo, A., Hatcher, P.G., 2001. Characterization of amino acids and proteinaceous materials using online tetramethylammonium hydroxide (TMAH) thermochemolysis and gas chromatography-mass spectrometry technique. *Journal of Analytical and Applied Pyrolysis* 61 (1-2), 181-193.
- Zelles, L., 1999. Fatty acid patterns of phospholipids and lipopolysaccharides in the characterisation of microbial communities in soil: A review. *Biology and Fertility of Soils* 29 (2), 111-129.

# **Supporting Information for Chapter 4**

## **Characterization and source identification of particulate organic matter by preparative thermochemolysis-GC-MS**

7 figures

Rudolf von Rohr, M.; Hering, J. G.; Kohler, H.-P. E.; Grasset, L.; von Gunten, U.,  
Characterization and source identification of particulate organic matter by preparative  
thermochemolysis-GC-MS. In preparation for submission.

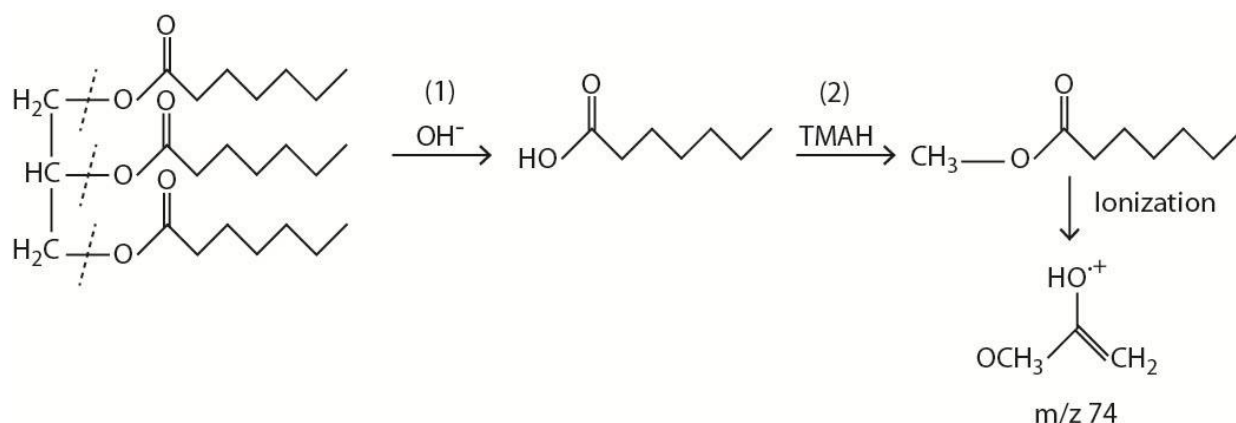


Fig. S4.1. TMAH-thermochemolysis for lipids (as an example, a saturated C7 triglyceride is shown). The first reaction (1) leads to the cleavage of the ester bonds (dashed lines) by hydrolysis reactions with  $\text{OH}^-$  generating three molecules of fatty acids (only one fatty acid is shown). In the second reaction (2), the carboxylic functional group of the fatty acid is alkylated by TMAH forming a fatty acid methyl ester (FAME). The ionization reaction during mass spectrometry leads to the formation of a main ion having  $m/z \ 74$ , which was used for peak integration.

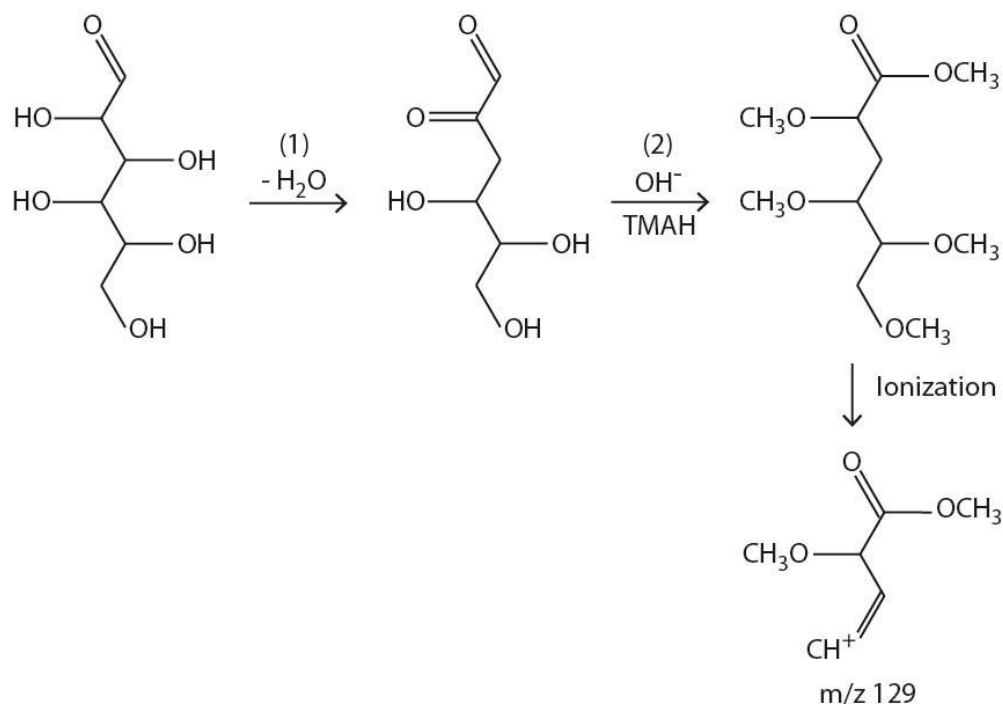


Fig. S4.2. Reaction mechanism of TMAH-thermochemolysis for carbohydrates (as an example, glucose is shown) according to Fabbri and Helleur 1999. In the first reaction (1), a molecule of water is eliminated under alkaline conditions. The second reaction (2) involves the addition of a hydroxyl group followed by alkylation, leading to the formation of a methylated deoxy aldonic

acid. The ionization reaction during mass spectrometry leads to the formation of a main ion having  $m/z$  129, which was used for peak integration.

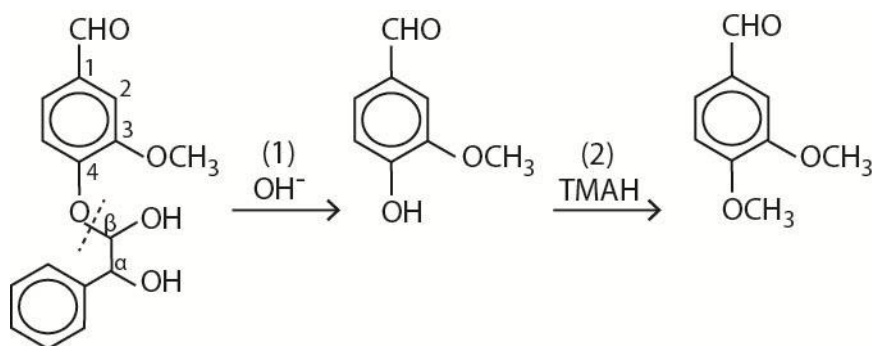


Fig. S4.3. TMAH-thermochemolysis for lignins (as an example, a model lignin compound is shown) according to Filley et al., 1999. The first reaction (1) leads to the cleavage of the  $\beta$ -O-4 ether bond (dashed line) by hydrolysis reaction with  $\text{OH}^-$ . In the second reaction (2) the hydroxyl group is alkylated by TMAH forming a methoxy aromatic compound (i.e., the lignin subunit G4).

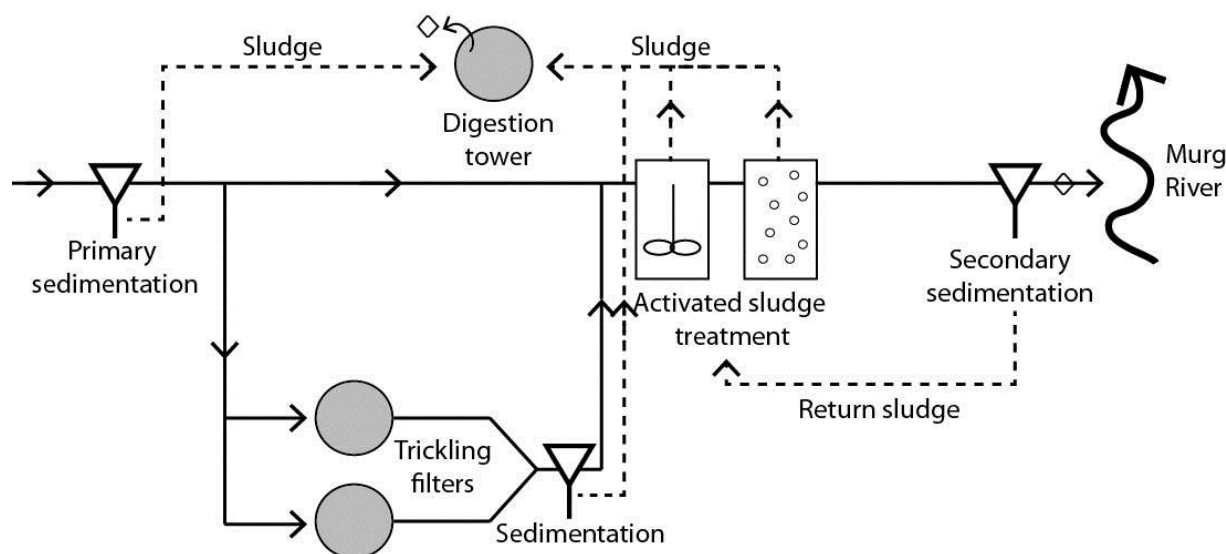


Fig. S4.4. Schematic representation of the wastewater treatment plant in Frauenfeld with sampling points ( $\diamond$ ). Solid arrows indicate wastewater flow, dashed arrows show wastewater sludge flow.

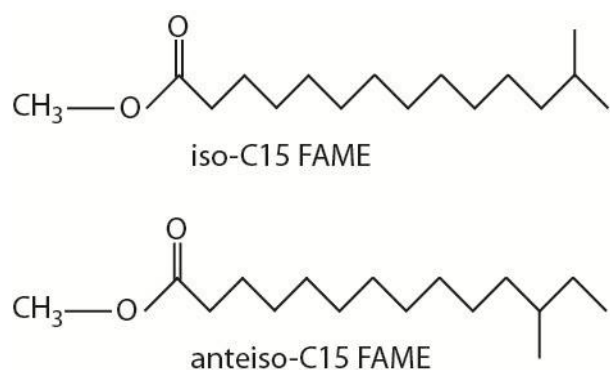


Fig. S4.5. Chemical structures of iso- and anteiso-C15 FAMES.

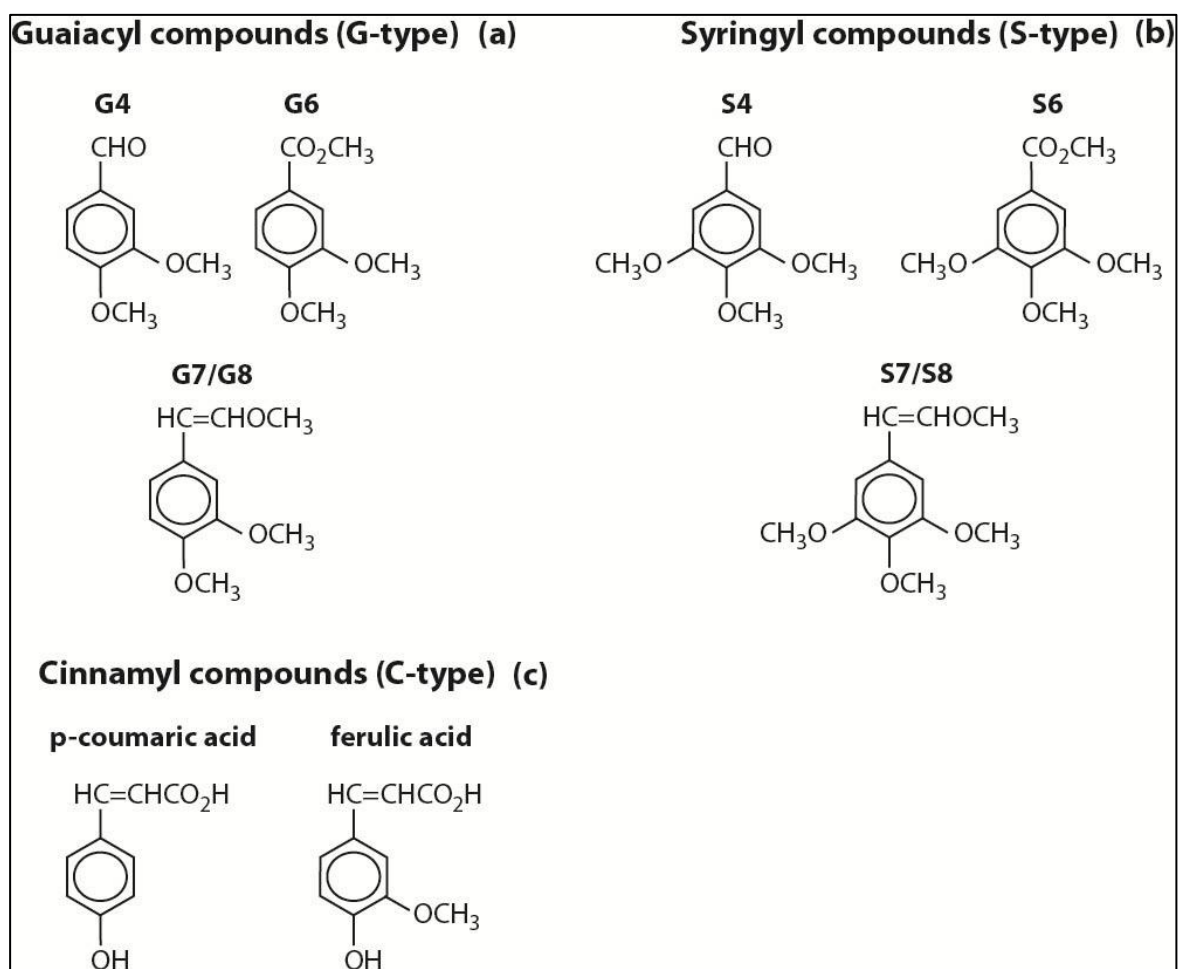


Fig. S4.6. Chemical structures of the lignin subunits (a) guaiacyl, (b) syringyl and (c) cinnamyl formed during TMAH-thermochemolysis of lignins (adapted from Wysocki et al., 2008).

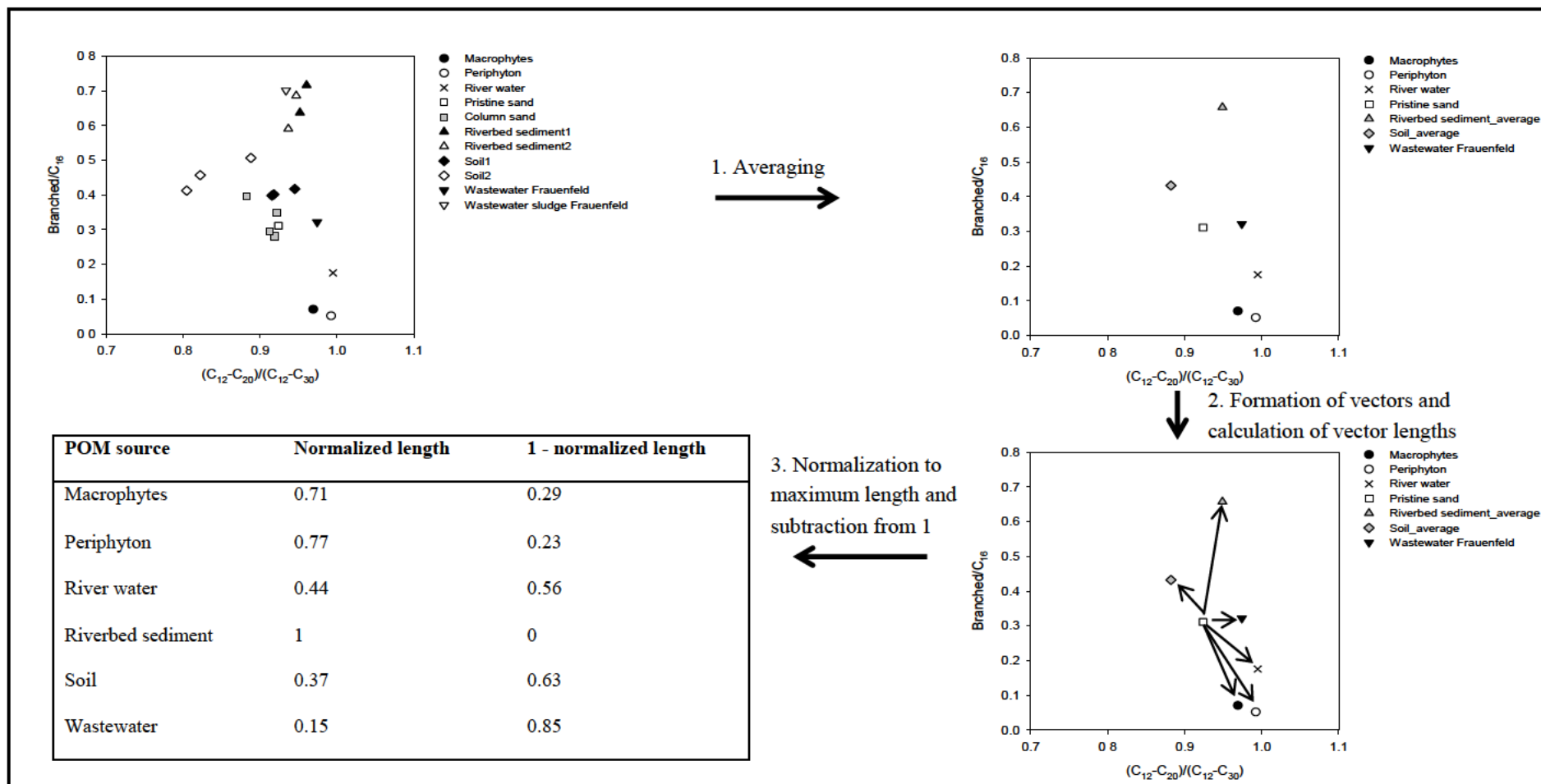


Fig. S4.7. Assessment of the proximity of the pristine sand to the POM source samples for the FAMES. The values for the soil and riverbed sediment samples were averaged (step 1), then vectors from the pristine sand to each POM source sample were established and their lengths calculated (step 2). After that, the lengths were normalized to the furthest distance, which in this case is represented by the distance to the riverbed sediment sample and finally the normalized values were subtracted from one to assign higher numbers for a close proximity of the sand samples to the POM source samples (step 3). These values were then used to construct the web charts shown in Fig. 4.8.





# **Chapter 5**

## **General Conclusions and Outlook**

Drinking water derived from riverbank filtration is generally of very good quality in Switzerland, due to prevalently oxic conditions in the aquifers and the natural attenuation processes removing particles, microorganisms and partially removing natural organic matter (NOM) and micropollutants. However, the occurrence of anoxic and Mn(III/IV)- and Fe(III)-reducing conditions at some riverbank filtration sites in Switzerland during past heat waves (e.g., in 2003) has shown that these systems are vulnerable to climate change. Prior to this dissertation, only a few studies have investigated the impact of climate change on the quality of drinking water derived from riverbank filtration. In the present thesis, the effects of climate-related variables (temperature, discharge, infiltration rate, proportion of wastewater effluent in river water) on redox processes and drinking water quality during riverbank filtration were systematically studied. To this end, field investigations carried out at a typical river-infiltration system in Niederneunforn (NE-Switzerland) and laboratory column experiments were conducted.

Field investigations have shown that oxygen was fully consumed under summer conditions (20-23°C), due to the temperature dependence of aerobic respiration. Denitrification was however not observed, so that nitrate still acted as a redox-buffer preventing the reductive dissolution of Mn(III/IV)- and Fe(III)(hydr)oxides. This situation is representative for most river-infiltration systems in Switzerland, meaning that under the actual summer conditions no additional water treatment measures (e.g., aeration, demanganation and deferrisation) are required. An electron balance for summer conditions between the consumption of dissolved organic matter (DOM) and oxygen revealed a strong discrepancy, suggesting that particulate organic matter (POM) associated with riverbed sediments was the main electron donor for aerobic respiration. Based on the findings of the field studies, two main driving forces affecting the redox conditions could be identified, i.e. temperature and POM.

The pronounced temperature dependence of aerobic respiration observed at the field site could be reproduced in laboratory column experiments, with the development of fully anoxic conditions at 30°C. Even at the highest temperature (30°C), only partial denitrification was observed, indicating that nitrate was still acting as a redox-buffer. POM was found to be the major electron donor for the biogeochemical processes, confirming the field-based observations. The infiltration rate was identified as another important driving force affecting the redox conditions, with low rates (i.e., implying high residence times) promoting the formation of anoxic conditions. At the same time, low infiltration rates are beneficial for the removal of microorganism and this needs to be considered especially at riverbank filtration sites exposed to microbial pollution from agriculture and wastewater effluents.

Future heat waves are characterized by long-lasting periods (1-3 months) of high river water temperatures ( $> 20^{\circ}\text{C}$ ) and low discharge conditions, which imply low infiltration rates. The results of the present study suggest that these two factors can potentially lead to transient anoxic conditions (complete oxygen consumption) in future with nitrate playing an important role as an ultimate barrier preventing the reductive dissolution of Mn(III/IV)- and Fe(III)(hydr)oxides. In the case of complete nitrate removal and release of Mn(II) and Fe(II) during future summer heat waves, removal of Mn(II) and Fe(II) has to be considered to prevent the temporary closure of groundwater pumping stations at riverbank filtration systems. The implications of the present findings on groundwater quality during future heat waves also depend on the hydrogeological properties of the river-infiltration system. A high vulnerability to climate change can be predicted for river-infiltration systems characterized by a gravelly riverbed with a direct hydraulic connection to the groundwater table and which are situated in catchments without retention basins. For those systems it will be important to conduct field observations on a routinely basis in future, especially during heat waves in order to monitor groundwater quality. Important drinking water quality parameters to be monitored in the groundwater are temperature, oxygen and nitrate.

Among the analytical techniques used for the molecular and structural characterization of POM, such as spectroscopic or mass spectrometric methods, preparative thermochemolysis-GC-MS is particularly useful because extraction and pre-concentration are not needed before analysis. Moreover, POM associated with different types of matrices (e.g., river water, wastewater, soil, macrophytes, etc.) can be treated and the derivatized volatile compounds identified and assigned by GC-MS. Preparative thermochemolysis-GC-MS has shown to be a useful technique for the molecular characterization of POM associated with different environmental samples from a river-infiltration site (sand, riverbed sediment, river water, macrophytes, periphyton, soil, wastewater) and a wastewater treatment plant. However, even though this technique has revealed a shift in the sand POM composition during the column experiments, the origin(s) of the sand POM could not be definitively identified. Therefore, alternative methods should be applied in combination with thermochemolysis-GC-MS to assess the origin(s) of POM, such as quantitative pyrolysis techniques (e.g., using internal standards), or selecting other specific biomarkers (e.g., alkanes, alkenes, phytols, amines, etc.). The application of quantitative pyrolysis techniques might be useful to assess the contribution of biomass to POM.

Regarding future research in the field of biogeochemical processes during riverbank filtration, more laboratory column studies are needed to confirm the role of POM as main electron donor. Such studies might include control experiments, in which the sand is heat-treated or washed to remove POM before being packed into the columns. Column experiments with unfiltered river water as feed water could also be conducted in future to investigate the contribution of river POM as electron donor. Moreover, as the dynamics of POM degradation (hydrolysis and mineralization processes) are still unclear, batch experiments using model POM compounds could be carried out and the oxygen concentration measured and modeled. During these batch experiments the bacterial communities responsible for the hydrolysis of POM and mineralization of DOM could be determined by molecular biology techniques. To further assess the origin(s) of POM associated with riverbed sediments, additional sampling of the possible POM sources followed by preparative thermochemolysis-GC-MS is a promising tool. Sampling after flood events might also allow a more comprehensive understanding of the processes (i.e., surface runoff) affecting POM replenishment in riverbed sediments. An important and emerging issue regarding the quality of bank-filtered water is the presence of micropollutants. Column and batch experiments should be conducted in future to investigate the biodegradation of emerging micropollutants (e.g., pesticides, industrial chemicals, pharmaceuticals) and the formation of transformation products. These studies should also be carried out under different redox conditions (i.e., aerobic, anoxic and anaerobic) to assess the effect of climate change on micropollutant degradation during riverbank filtration.





---

## Curriculum Vitae

### Matthias Rudolf von Rohr

Born on December 18, 1983 in Lugano, Switzerland

Citizen of Kestenholz, Switzerland

2003	Maturità liceale, Liceo Cantonale Lugano, Switzerland
2003-2008	Bachelor and Master studies in Environmental Sciences Swiss Federal Institute of Technology, Zurich, Switzerland Diploma thesis title: "Formation of hydrogen cyanide and mechanisms of mineral dissolution driven by <i>Pseudomonas fluorescens</i> "
2008	Scientific collaborator Institute for Forest, Snow and Landscape (WSL), Birmensdorf, Switzerland
2009	Scientific collaborator Institute for Forest, Snow and Landscape (WSL), Bellinzona, Switzerland
2010-2014	PhD student Eawag, Department of Water Resources and Drinking water, Switzerland

